UNIVERSIDADE DA BEIRA INTERIOR
Faculdade de Engenharia

Quantitative Analysis of Take-off Forces in Birds

Telmo José Anastácio da Silva

Tese para obtenção do Grau de Mestre em

Engenharia Aeronáutica

(2º ciclo de estudos)

Orientador: Prof. Doutor Jorge Manuel Martins Barata

Covilhã, Junho de 2016

Folha em branco

Dedication

Always I feel grateful to my parents for bringing me in to the world, take care of me and educate me.

Folha em branco

Acknowledgements

This work was performed under the scope of the LAETA-Associated Laboratory on Energy, Transport and Aeronautics sponsored by the FCT-Foundation for Science and Technology.

I want to thank my Parents, Family, Prof. Doutor Jorge Barata, Doutor Fernando Neves, Sr. Rui, LAETA associates…

Telmo Silva

Covilhã, 2016

Folha em branco

Resumo

O interesse crescente nos Veículos Aéreos não Tripulados "Unmanned Air Vehicles (UAV's)" e suas diversas utilidades em conjunto com a necessidade de seu fácil transporte e furtividade, levaram à necessidade de criar o conceito dos Micro Veículos Aéreos "Micro Air Vehicles (MAV's)" e os Nano Veículos Aéreos "Nano Air Vehicles (NAV's)". Este tipo de veículos tem como fonte inspiradora os insetos e aves devido à necessária produção simultânea de sustentação e propulsão. Tal como no voo convencional, também no voo animal podem ser identificadas as fases de levantamento (descolagem) e aterragem como diferenciadas do voo longe de uma superfície de apoio. Este trabalho é dedicado ao estudo da fase de levantamento de voo de uma ave *columba livia*. Foram realizadas experiências para medir a força inicial produzida pela ave para iniciar o voo e a respetiva trajetória na zona próxima do ponto de apoio inicial. Estas medidas foram efetuadas com um sensor de força dotado de elevada velocidade de aquisição de dados e uma camara de alta velocidade. As principais conclusões obtidas com a realização deste trabalho é o facto de que a ave consegue produzir movimentos, que aumentar o momento total quando a ave estica o pescoço para a frente e movendo a cabeça para baixo seguido por continuação de esticamento do pescoço e movimento da cabeça para cima impelindo-se para o ar, resultando num papel principal relativamente às forças mecânicas (contra o poleiro) para o momento linear actuante nos primeiros momentos. Columba livia consegue gerar cerca de 4 vezes o seu peso em força mecânica e acima de 8 vezes o seu peso durante o 2º downstroke.

Palavras-chave

Biomimética, *columba livia*.

Folha em branco

Abstract

The increasing interest on Unmanned Air Vehicles (UAV's) and their several utilities blended with the need of easy carrying and also the stealth, lead to the need to create the concept of Micro Air Vehicles (MAV's) and the Nano Air Vehicles (NAV's). Due to the current interest and the present lack of knowledge on the insect's and bird's flight, this study was intended to interpret the forces involved on the moment of the take-off of a bird, recurring to an experiment involving a fast data acquisition force sensor and high speed camera, in addition known facts from earlier studies. In order to do that a bibliographic revision was done, to know what was already studied and to find what could yet be studied. That way could be formed a link on the factors involved on the propulsion of a bird at the moment of take-off. The main conclusions obtained by this work is that the bird can produce movements that will enhance the total moment when the bird stretches its neck forward and moving head down followed by stretching even more its neck and moving head up impelling himself into the air, resulting in a main role on the mechanical forces (against perch) for the bird first moments momentum. Columba livia can generate about 4 times its weight worth mechanic force (against perch) and above 8 times its weight during the 2nd downstroke.

Keywords

Biomimetics, *columba livia*.

Folha em branco

Table of contents

Folha em branco

List of Figures

Folha em branco

List of Tables

Folha em branco

List of Symbols

U	horizontal velocity component
V	vertical velocity component
W	transverse velocity component
X	horizontal coordinate
t	time instant
Y	vertical coordinate
Z	transverse coordinate
Re	ratio between inertial and viscous forces
TO_{angle}	angle described at take-off
U_{∞}	forward undisturbed flow

Greek symbols

α	angle of trajectory
ψ	pitch
ϕ	roll
θ	yaw
Δx	size of the vision field pixel in meters
λ	wavelength

Subscripts

i	initial value

Folha em branco

Chapter 1

Introduction

1.1 Biomimetics

Humankind has looked at nature (living organisms) in search for answers to solve problems throughout their own existence. The term biomimetic derive from Ancient Greek and means (***bios*** ⇒ life; ***mimesis*** ⇒ imitation); **biomimetic** ⇒ **life imitation**, and has given rise to new technologies inspired by biological solutions at macro and nanoscales. In its fullness meaning, biomimetic refers to all human-made processes, substances, devices, or systems that imitate nature; i.e., refers to the imitation of the models, systems, and elements of nature with the purpose of solving complex human problems. Biomimetic studies belong to a highly multidisciplinary area, encapsulating several branches of science: chemistry, physics, computers, textile, mathematics and electronics. In Nature there are millions of species of which less than two million have been cataloged so far. Just to mention insects (they are among the most diverse groups of animals on the planet, including over a 1,000,000 described species and representing more than a half of all living organisms) According to National Museum of Natural History, most authorities agree on a conservative estimation of insect's species number of 2,000,000 and could be extended to up 30,000,000 – an gigantic base inspired solutions data in biological systems to solve engineering problems and other fields of technology. One of the early examples of biomimetic was the study of birds to enable human flight. Although never successful in creating a "*flying machine*", Leonardo da Vinci (1452–1519) was a keen observer of the anatomy and flight of birds, and made numerous notes and sketches on his observations as well as sketches of "*flying machines*"[1].The Wright Brothers, who succeeded in flying the first heavier-than-air aircraft in 1903, derived inspiration from observations of pigeons in flight[2].

---

[1] Romei, Francesca (2008). Leonardo Da Vinci. The Oliver Press. p. 56. https://en.wikipedia.org/wiki/International_Standard_Book_Number ISBN 978-1-934545-00-3.

[2] Howard, Fred (1998). Wilbur and Orville: A Biography of the Wright Brothers. Dober Publications. p. 33. https://en.wikipedia.org/wiki/International_Standard_Book_Number ISBN 978-0-486-40297-0.

1.2 Flight Stages

Barata *et al.*, 2015, performed a bibliographic review concerning Comparative Study of Wing's Motion Patterns on Various Types of Insects on Resemblant Flight Stages, revealing that the behavioral flight capacitance, maneuverability and ability of insect's flight in recent years has become an active research that provided biological adaptive inspirations for the design and control of man-made MAVs and NAVs, essentially by identifying, exploiting and understanding the basic principles of performance in-flight displayed, essentially due to a main reason: their maneuverability is remarkable and by far superior to every maneuverability of any man-made flying vehicle and has captured the humans attention in a way to achieve such knowledge. Although the authors have addressed this work to insect´s flight, there are parameters that are common to the study of the flight of birds.

The behavioral flight capacitance and ability of each animal (insect, bird, bat) is determined by the functional capabilities of their wing's muscles to produce force and to work at a certain response speed and depends as well of their efficiency in transforming chemical to mechanical energy – wing's muscles from different sources could vary widely in their performances. The power product of these muscles is subsequently transmitted to the wings, which unlike an aircraft wings are neither streamlined nor smooth: the shape, corrugation and performance of the wings and the complex flapping motion during the stroke cycles will determine the ability of an animal to fulfil successfully every stunning maneuver.

The aerodynamics between flapping and gliding flight differ substantially in two important ways: in a gliding wing, the air tends to remain attached and flowing smoothly over the surface of any airfoil; by contrast, the air over a flapping wing tends to become entrained in a swirling vortex bound to the upper surface of the wing - separated flow. And whereas the attached flow over a gliding wing look approximately similar from one moment to next, the separate flow over a flapping wing varies constantly - unsteady flow. Nowadays it is widely accepted that the insects make an extensive use of unsteady separated flow mechanisms in order to generate far greater aerodynamic forces that for them, would be impossible to achieve with steady, or quasi-steady, attached flow.

Birds change the angle of attack continuously within a flap as well as with speed. When a bird flaps its wings the lift force is rotated forward in order to provide thrust that counteracts drag and increases the bird speed and also increase lift to counteract its weight (allowing the bird to maintain height or to climb). Flapping involves two translational phases: the downstroke (providing the majority of the thrust), and the upstroke (depending on the bird's wings can or provide some to none thrust). During upstroke the wing is slightly folded inwards to reduce the energetic cost of flight. Flapping involves also two rotational phases: pronation

(associated with downstroke-forward movement), and supination (associated with upstroke-backward movement).

The ability of flight is a metabolically expensive way to move about, since gravity and drag has to be overcome. Mostly often the cross section a bird's wing reminds a teardrop with a flatter lower surface than the top, like an airfoil. On its forward trajectory, this airfoil passes through an air stream forcing it to split in two separate streams: over the top and bottom of the wing. Air is forced to travel over the top curved surface and creates an area of lower pressure over the wing. Air under the wing is not deflected as much and creates a relatively higher pressure than over the top of the wing. By consequence, this pressure difference effectively pushes the wing upwards and generates lift. By altering the shape and angle of the wings and feathers independently (twist, rotation speed, morphing, flapping angle and elastic deformation of feathers during a wing beat) some birds are able and naturally supplied to perform extremely acrobatic manoeuvers at their will.

1.3 Motivation

Since every animal needs to generate enough force to enable sufficient airflow across the wings in order to generate sufficient lift to ascend, the take-off is one of the most energetically demanding aspects to resume the flight. An important aspect is also the demand of knowledge related to take-off, since most MAVs created are designed without fully autonomous take-off technology; instead, they are hand-launched; in fact, many rely on a controlled crude crash-landing, contrasting the elegance precision landing of a perching bird. Regarding the take-off, a recent research dimension has focused on development of bird like perching mechanisms; not only the ground mobility as well as the perching mechanism inspired from bird claws. Beyond the difficulties on developing MAVs, only few designs adequately address the required control issues and almost only quite few ones are able to complete a flight cycle (including take-off and precision smooth landing); regarding this, the main objective of this work concerns in the search of Quantitative Analysis of Take-off Forces in Birds, thus, for future fully autonomous MAVs take-off improvements.

1.4 Literature Review

Tanaka *et al.,* 2011, conducted an experimental work concerning on the effect of wing flexibility in hoverflies using an at-scale polymer wing and an at-scale rigid wing carbon fiber model, both mimicking a natural wing of a hoverfly. The polymer artificial wing venation, corrugation and measured flexural stiffness are comparable to that of the natural wing. The experience consisted on the 5 levels of hinge stiffness variation: very soft; soft; intermediate; rigid; and very rigid. The artificial wings and hinges were tested with an at-scale tethered flapping mechanism driven by a piezoelectric actuator. It was tested single wings, independent of flow induced from the collateral wings, head, chest, abdomen or legs. The used wingbeat cadence and angles are identical to natural wings and were assayed appropriate trajectories for the flight of hoverflies. It was found that maximum lift was achieved when the stiffness of the hinge was similar to that of a hoverfly natural articulation in both wing cases and as well, as the magnitude of measured lift is sufficient for hovering; for identical wingbeat movements it was also found that the rigid wing proved to be most suitable for the production of greater lift. Their results also suggest the authors that hoverflies could exploit intrinsic compliances to generate desired motions of the wing [1].

Ang HaiSong *et al.*, 2009, elaborated a numerical investigation including the studies of low Reynolds number (*Re*) aerodynamics, unsteady computational fluid dynamics and flight control for fixed-wing MAVs, bird-like MAVs, dragonfly-like MAVs and bee-like MAVs. The authors found that characteristics between natural flight (Re 100-30,000) and conventional aircraft flight (*Re* > 500,000) have a notable difference relating to the Reynolds number that easily led to flow separation on the MAV's surfaces. Authors found that CFD methods of the steady flow and the unsteady flow with small amplitude were not suitable for the strongly unsteady characteristics of the flow field of flapping-wing and developed an effective solution method to perform simulations for unsteady flows with moving boundaries using N-S equations of compressible fluids, a method based on a dual time stepping scheme in conjunction with low Mach number preconditioning to solve the unsteady N-S equations. Characteristic boundary conditions were also developed to accommodate to the preconditioned characteristic system. Their test results indicated that the algorithm could provide satisfactory accuracy and convergence for a large range of unsteady flow problems. A dynamic unstructured overset grid method was developed for moving boundary problems with large relative movements. Their obtained results revealed that for fixed wing with low Aspect Ratio (AR) and low Re, the wing presents an involving 3D quite complex structure and that tip vortex not only affects the lift and drag, but also introduces unsteadiness in aerodynamic performance at high angles of attack. The CFD method for flapping wing demonstrated the unsteady vortex flow and the thrust generation mechanism of the flapping-wing flyers. By comparison of the aerodynamic forces of the flexible flapping-wing with those of rigid

flapping-wings, it was found that if the wing structure was controlled with suitable flexibility, and that the lift and thrust could be effectively raised. For the dragonfly tests, the results indicated that the wake of the flapping fore-wing exerts great influence on the aerodynamic performance of the hind-wing. For the bee tests, the results of flapping-wing with compound motion could produce higher lift and thrust; the motion parameters that have influence on lift and thrust of flapping-wing included plunging amplitude, plunging frequency, sliding amplitude, pitching mean angle and pitching amplitude. Their results for the bee-like MAV revealed also that the increase of pitching mean angle reduced the thrust [2].

Zhang & Yu, 2014, presented a numerical and experimental work proposing a new flapping wing type inspired by superior flight performance of natural flight masters like birds and insects and based on the ventilating flaps that can be opened and closed by the changing air pressure around the wing. For this, they created ventilated wings provided with a series of slots managed with the ability to be opened and closed either through active or passive control mechanisms during the flapping cycle. During the downstroke, the slots remain fully closed to represent the full wing area and thus, to generate maximum positive lift; as the upstroke begins, the slots open out and allow ventilation to occur within the wings by reducing the exposed wing area, drag, and hence negative lift generated in the process. These slots areas serve as a variable in which, a correlation with the decrease in negative lift can be generated. Related to materials, was used a corrugated Polypropylene Sheets; the wingbeats cycle varied from 30 degrees above to and 40 degrees below horizontal; the wings were reinforced with carbon rods at the leading edge, trailing edge and along chord. They tested wings with 0, 2 and 4 slots. The primary components of the experimental procedure were a brushless engine and a lithium battery, a gear mechanism for reducing the rotational speed, a crankshaft, a rack and a pinion to convert linear motion into rotational and a wing support; The authors stated their main challenge were to build such mechanism and to study their lift capacity. The numerical work was developed with the use of 2D and 3D CFD: ANSYS/FLUENT V.6.3.26 with a 120 X 56 X 60 mesh simulating velocity, U_∞ = 1.4 m/s. By opening slots during upward wing movement the downforce reduction was considerable; all support results were positive, which immediately justify the use of this type of ventilation. The use of ventilation, allowed identifying a clear trend of increased lift capacity with increasing frequency. Vortex formed in the leading edge exhibit the same general trend, including the formation and stroke (shedding), but due to the presence of the slots, the flow pattern becomes more complex [3].

Ha *et al.*, 2012, developed a work with the main objective of presenting a complete analysis of the artificial wings of an allomyrina dichotoma, investigating its static and dynamic characteristics and the relations between them, for posterior application to flapping wings on micro-airplane. The fabrication of the wings was based on the standards of the specie and the

complex structure was simplified with only the main veins system (carbon fiber – 0.1 mm thick) and wing membrane (Kapton film - 7.7 μm) [4].

Tanaka & Wood, 2010, presented a work about the fabrication of syrphidae artificial wings, micro molded in thermoset resin. The topology of the wing was generated by micro tomography x-ray (tainted with iodine) and posteriorly exported to a 3D CAD model; the patterns of the semi-circular veins sections were produced by four different size laser rays; 125, 100, 75, 50 μm; the wing has 11.7 mm of length and 100 μm undulation. The solid part of the veins and membrane was simultaneously formed and integrated by a simple molding process. The 3D mold was created by ablation of laser layers (laser Nd: YV04 – λ = 355 nm; 2W; pulsing radiation 15 ns a 20 KHz) with 6 μm height resolution, engraved on a silicon wafer [5].

Lehmann *et al.*, 2005, using a digital particle image velocimetry (DPIV) and a dynamically scaled mechanical model of the small fruit fly drosophila melanogaster, studied the "clap-and-fling" movement (force enhancement due to contralateral wing interactions during stroke reversal). They modeled the clap and-fling using two computer-controlled, dynamically scaled Plexiglas wings (left and right wing) programmed to flap back and forth in prescribed kinematic patterns; their model was equipped with a force transducer for measure perpendicular and parallel forces. Using software routines in MATLAB (MathWorks, Inc., Natick, MA, USA), they managed to reconstruct the lift and drag force based on the results of the measured forces and based on the angular position of the wing throughout the stroke cycle; the model was flapped at (50 <Re <200) and had an aspect ratio of ~1.9, with the experience being made at an immersed onto a 2 m^3 tank of mineral oil (wings length = 25 cm; oil density = $0.88x10^3$ $kg{\cdot}m^{-3}$; kinematic viscosity = 115 cSt). Their experimental work consisted on: varying the distance between the wings; the Reynolds number; the rotational time and angular velocity at the ventral and dorsal stroke reversal. To perform DPIV, they used a TSI dual mini-Nd:YAG laser to create two identically positioned light sheets through the wing at five equally spaced distances from the wing base and perform pairs of images of $\sim 185x185{\cdot}mm^2$ captured at 12 different phases of the stroke cycle. To visualize wake structure during clap-and-fling, the oil was seeded with bubbles by pumping room air through a ceramic water purification filter. Their results confirm previous research on the clap-and-fling mechanism and show that dorsal wing–wing interaction modestly enhances total normal flight force and lift production among insects flying at an intermediate Reynolds number. For wing kinematics modeled on tethered flying fruit fly, the magnitude and orientation of the mean force vector produced by wings during clap-and-fling generates a lift increase of 8.2% (mean lift: single wing = 0.222 N; two wings = 0.243 N). This enhancement occurs when the two wings are still in close proximity and the angular separation between them is less than about 10°, but vanishes at greater angular separations. They also found that besides a role for total lift enhancement, a concomitant 10% lift augmentation due to clap-and-fling

beneficially counterbalances pitch moments on the animal body produced by the increase in ventral stroke amplitude [6].

Lehmann & Pick, 2007, made an improvement of the previous study (Lehmann et al, 2005), using the same dynamically scaled mechanical model of the small drosophila melanogaster wing, in the "clap-and-fling" movement. Their experience was made in an immersed 2 m3 tank of mineral oil (wings length = 25 cm; oil density = 0.88×10^3 kg·m^{-3}; kinematic viscosity = 115 cSt). The authors do not made references to the used technics, so, it might be considered that they used the same DPIV, TSI dual mini-Nd:YAG and seeding systems. They used two computer-controlled dynamically scaled Plexiglas wings (left and right wing) programmed to flap back and forth in prescribed kinematic patterns. One wing was equipped with a 2-DoF force transducer that measured forces perpendicular and parallel to the wing in the spanwise direction. Using software routines in MATLAB (MathWorks, Inc., Natick, MA, USA), they managed to reconstruct the lift and drag force based on the results of the measured forces and based on the angular position of the wing throughout the stroke cycle; the model was flapped at (Re ~134) and had an aspect ratio of ~1.9. All the 17 bio-inspired kinematic patterns experiments were conducted using a horizontal stroke plane of 160° stroke amplitude, 0.17 Hz stroke frequency and 50° angle of attack with respect to the horizontal; the heaving motion was changed. Although none of the patterns used in this study exactly matched any of those found in flying insects, the various wing trajectories covered various categories of stroke shapes used by flying insects, such as oval or figure-eight shapes. They found that the clap-and-fling movement induced vertical force augmentation significantly decreased with increasing vertical force production averaged over the entire stroke cycle, whereas total force augmentation was independent from changes in force produced by a single wing. They obtained maximum (17.4%) and minimum (1.4%) vertical force augmentation in two types of figure-eight stroke kinematics whereby rate and direction of heaving motion during fling may explain 58% of the variance in vertical force augmentation. This finding suggested the authors that vertical wing motion distinctly alters the flow regime at the beginning of the downstroke. Their data revealed that pitching moments were largely independent from mean vertical force; however, clap-and-fling reinforces mean pitching moments by approximately 21%, compared to the moments produced by a single flapping wing. Pitching moments due to clap-and-fling significantly increased with increasing vertical force augmentation and produced nose-down moments in most of the tested patterns [7].

Miller & Peskin, 2009, presented 2D numerical simulations of flight constructed to be similar to the physical experiments of previous investigators. They solved the Navier–Stokes equations on a 1230×1230 Cartesian grid computational domain, and each wing was discretized on a Lagrangian array of 120 points (flexible and rigid models). They calculated the Lift and drag forces as functions of time by summing the forces that each immersed boundary point of the model wing applied to the fluid at each time step and taking the

opposite sign of that value; the angles of attack were defined using a set of equations describing the angular velocity during the rotational phase of the stroke. The Re was set to 10, corresponding to the case of some of the smallest flying insects, and the non-dimensional bending stiffness was varied from about 0.25 to 4. Related to some limitations of their model, the authors concluded from this work that the drag forces generated from wing–wing interactions could be an order of magnitude larger than a single wing, and that the addition of flexibility could reduce the drag but the maximum and average drag forces were still substantially larger than the single wing case. Related to clap and fling, the authors found that the drag forces generated during fling with rigid wings could be up to 10 times larger than what would be produced without the effects of wing–wing interaction. They concluded also that the horizontal components of the forces generated during the end of the upstroke and beginning of the downstroke cancel as a result of the motion of the two wings, and could not be used to generate thrust. As a result, clap and fling appears to be rather inefficient for the smallest flying insects. Authors also add flexibility to the wings and found that the maximum drag force generated during the fling could be reduced by about 50%. In some instances, the net lift forces generated were also improved relative to the rigid wing case [8].

Ramamurti & Sandberg, 2007, presented 3D Computer simulations of unsteady flow past a *drosophila* under hovering and free flight conditions. The governing equations were the incompressible Navier–Stokes equations in Arbitrary Lagrangian-Eulerian (ALE) and they managed the computations by using a time-accurate flow solver that was discretized in space using a Galerkin procedure with linear tetrahedral elements (a feflo incompressible flow solver). They studied both the hovering and the yaw axis directions for a maneuvering, by considering that the unsteady forces and moments were produced by both flapping wings and including the body of the *drosophila* as it hovers and then executes a saccade maneuver. All kinematics of the wings and the body of the *drosophila* were prescribed from experimental observations and were used in a XYZ experimental coordinates system consisted of the coordinates of the head, the tail, the wing hinges and tips and the unit vector normal to the wings. In order to convert this data to rigid body translation and rotation, first the *drosophila* body was placed in the computation coordinate system (xyz) with the head to tail aligned along the x-axis, the two wings placed flat on the (y-z) plane. The body was rotated along the x-axis through a roll angle ϕ, followed by a yaw rotation of θ about the y-axis, and the by a pitch rotation of ψ about the z-axis. This set of rotations was equivalent to the Euler angle systems commonly used in aeronautical engineering. After, the kinematics of the wings was converted to 6-DOF motion for the body and the wings. The results revealed that the differences in the kinematics between the right and the left wings show that subtle change in the stroke angle and deviation angle could result in the yaw moment for the turning maneuver. The origin of the yaw moment was investigated by computing the center of pressures on each wing and the individual moment arms and had led to the conclusion that it was the forward force and a component of the lift force that combined to produce the

turning moment while the side force alone produced the restoring torque during the maneuver [9].

Fontaine *et al*., 2009, In order to quantify flight kinematics during different types of maneuvers, developed a visual tracking system that estimates the posture of the fly from multiple calibrated cameras. An accurate geometric fly model was posteriorly designed using unit quaternions to capture complex body and wing rotations, automatically fitted to the images in each time frame. Their video subjects consisted of 3 day old female *drosophila melanogaster* filmed at 6000 fps with a shutter speed of 50 μs. The video sequence was filmed in a previous study that analyzed flight initiation using high-speed cameras (Photron Ultima APX) to capture orthogonal views at a resolution of 512 pixels by 512 pixels. With the video sequences the model-based image tracking was quantified; the body and wing kinematics of *drosophila* were recorded in multiple synchronized cameras, and first built a geometric model of the *drosophila*, assuming a rigid flying body. After, they used a polygonal model to construct a parameterized generative model of the *drosophila* that contains three primitive shapes: the body, head and wings. The primitive shapes were assembled into an articulated model that each wing joint was modeled as a spherical joint (permitting arbitrary rotations about all three coordinate axes); the shapes were constructed by applying continuous transformations to a B-spline curve. To parameterize the rotations of the *drosophila* body and wings relative to a fixed global frame, they utilize unit quaternions because their global representation does not suffer from the singularities inherent in Euler angle schemes: a 4×4 matrix defined the position of a body-fixed reference. To assess the accuracy of the proposed method, they compared body pose estimates in six video sequences with those reported by previous researchers. Their visual tracking system algorithm was written in MATLAB and had an average computation time of 45±3 s per frame on a 3.0 GHz Intel® Xeon processor and for each video sequence the geometric model was manually initialized to the first frame according to “Coordinate transformations”. The database of training samples consisted of 380 samples from a voluntary take-off and 111 samples from an escape take-off; the orientation measurements were smoothed with a zero phase lag fourth order Butterworth filter with a cut-off frequency of 1000 Hz and 250 Hz for the wings and body, respectively. This tracking system was able to measure stroke amplitude, geometric angle of attack and other parameters important to a mechanistic understanding of flapping flight. All sequences show that *drosophila melanogaster* do not utilize clap and fling during take-off and were able to modify their wing kinematics from one wingstroke to the next. Their approach should enable biomechanists and ethologists to process much larger datasets than possible at present and, therefore, accelerate insight into the mechanisms of free-flight maneuvers of flying insects [10].

Truong et al., 2012, investigated by visualization the aerodynamic characteristics of the beetles (mean body mass 5<gram<10); this insect has a pair of elytra wings (rigid

forewings→2.5 cm) and flexible hind wings→5 cm lengths. During the flapping motion, both elytra and hind wings flap on same frequency (37 - 40 Hz), however in different flapping angles: hind wing (160-180º) and for the elytra (34-38º). The beetles were kept on organic peat in the laboratory at a humidity of 50% and a temperature of 25ºC. They visualized free, tethered, hovering, forward and climbing flights experiments. The visualization of flow field around the beetle's wing was performed in a low speed, open-type wind. A small hook with a diameter of 0.5 mm was attached to the thorax of the beetle with cyanoacrylate glue. The hook was used to hang the beetle at the center of the test section (1 x 1 m) in a wind tunnel. After a few minutes of suspension, the beetle started to freely fly away. A vertical hot wire was used to generate a smoke sheet while paraffin was flowing through it. The quality of the smoke sheet was adjusted for the best resolution in the image processing. To generate the dense stroke streamlines, an array of knots with diameter of 0.2 mm was made along a 0.1 mm tungsten wire. A high-speed camera (Photron APX) was located outsider the test section, and 1 kW halogen lamps were placed at appropriate positions to illuminate the focus region. The beetle's wing motion was captured at 2000 fps at a pixel resolution of 1024×1024 and exposure time of 1/4000 s. The camera lens was connected to an image processor to a PC, while PHOTRON FASTCAM VIEWER software was used to capture images and control the high speed camera set-up. The incoming flow velocity was 1 ms^{-1} for free flight and 1.5 ms^{-1} for tethered flight. Leading edge, trailing edge and tip vortices on both wings were clearly observed by the authors. They observed that the leading edge vortex was stable and remained on the top surface of the elytron for a wide interval during the downstroke of free forward flight. They stated that the elytron wings may have a considerable role in lift force generation of the beetle. They found a suction phenomenon between the gaps of the hind wing and the elytron in upstroke that may improve the positive lift force on the hind wing. It was also found a reverse clap-fling mechanism while in hovering flight. The hind wings touch together at the beginning of the upstroke [11].

The aerodynamic theory of bird flight evolve continuously changing on motion of wing planform (a mixing of twist, rotation speed, morphing, flapping angle and elastic deformation of feathers during a wing beat) and differs abysmally from steady forward airplane´s flight; scientific evidences show that in a gliding wing the air tends to remain attached and flowing smoothly over the surface of any airfoil; by contrast, the air over a flapping wing tends to become entrained in a swirling vortex bound to the upper surface of the wing - separated flow. And whereas the attached flow over a gliding wing look approximately similar from one moment to next, the separate flow over a flapping wing varies constantly - unsteady flow. Nowadays it is widely accepted that animals (birds, insects and bats) make an extensive use of unsteady separated flow mechanisms in order to generate far greater aerodynamic forces that for them, would be impossible to achieve with steady, or quasi-steady, attached flow [12]; consequently, the state of art for calculation concerning instantaneous forces is still virtually impossible; however it is possible to consider two main approaches for modelling the

aerodynamics of such flight: by estimating the local force acting on a wing-strip (or blade element) and to integrate (or sum) the result over the wingspan, considering that the instantaneous forces on a wing in unsteady motion are equal to those in steady flow at the same local speed and angle of attack; or by taking advantage of the fact that flapping wings deform the fluid around them, and the aerodynamic force on the wing is associated with the impulse of the wake momentum change. Hence, from the topology and kinetic energy transferred in the vortex wake of the flying animal, lift and drag can be calculated although cannot offer instantaneous wing force resolution [13]. The mechanics of bird flight have been receiving an increasingly interest in the last decades. This interest was fostered by the need of MAVs – (Micro Air Vehicles) adequate and efficient to perform surveillance, communications relay links, ship decoys, and detection of biological, chemical, or nuclear materials. MAVs become even more challenging when DARPA launched in 1997 a pilot study into the design of portable (150 mm) flying vehicles to operate in D3 - dull, dirty and dangerous - environments [14]. More recently DARPA launched a Nano Air Vehicle (NAV) program with the objective of developing and demonstrating small (<100 mm) lightweight air vehicles (<10 g) with the potential to perform indoor and outdoor missions [15]. Figure 1 ranks NAV's and MAV's over a relation of mass and Reynolds number.

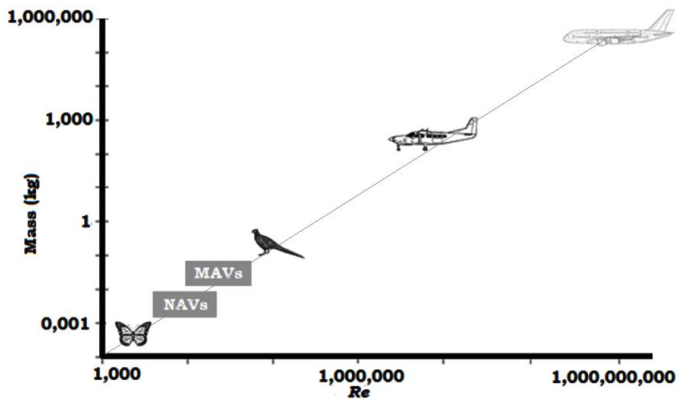

Figure 1. Classification of MAV's and NAV's over a relation of Mass and Reynolds Number.

All requirements of low altitude, long flight duration at low speeds (up to 100 km/h), small wing spans and masses, together with demanding capabilities of take-off, climb, loiter, hover, maneuver, cruise, stealth and gust response are further beyond today's fixed wing or rotorcraft vehicles. At the same time, MAVs fit in the general sizes, weights, and locomotion performance of natural flying animals [16].

Nevertheless, biomimetic engineered devices are still far from achieve similar performances of the living organisms, essentially due to a lack of a its total understanding and consequently more research is needed [17].

Although it can be found an extensive literature related to the understanding of aerodynamics on several flight stages on animals (insects, birds, bats) and some research related to the understanding of its flight control, there is a lack of research concerning to the initial flight stage on birds: the take-off procedure.
For a natural flyer, flight is never only to float and to move in the air. In addition to an instinctive and outstanding flight capability, a natural flyer excels in adopting appropriate pilot strategies to perfect the flight performance. One prominent flight strategy of a bird is to interact with the surrounding conditions, such as the environmental airflow and land forms. Kestrels and albatrosses are reported to be capable of exploiting a large-scale airflow to accomplish various skilled flight modes, for instance, flying against the wind at the velocity of the wind for wind hovering, and gaining energy by repeatedly crossing the boundary between air masses of significant velocity difference for dynamic soaring [18].

Passing to the take-off mechanisms, we know that the forces that most contribute during the take-off phase are generated by the bird's legs as studied with performed tests on a geopelia cuneate. Recent research has revealed that initial take-off velocity in birds is driven mostly by hindlimb forces. However, the contribution of the wings during the transition to air is unknown. Integrated measurements of both leg and wing forces during take-off and the first three wingbeats in zebra finch (*taeniopygia guttata*, body mass 15g) and diamond dove (*geopelia cuneata*, body mass 50g) were completed. Measured ground reaction forces produced by the hindlimbs using a perch mounted on a force plate, whole-body and wing kinematics using high-speed video, and aerodynamic forces using particle image velocimetry (PIV). Take-off performance was generally similar between species. When birds were perched, an acceleration peak produced by the legs contributed to 85±1% of the whole-body resultant acceleration in finch and 77±6% in dove. At lift-off, coincident with the start of the first downstroke, the percentage of hindlimb contribution to initial flight velocity was 93.6±0.6% in finch and 95.2±0.4% in dove. In finch, the first wingbeat produced 57.9±3.4% of the lift created during subsequent wingbeats compared with 62.5±2.2% in dove [19].

Consistent with Tobalske, *et. al.*, 2004, hummingbirds, with small body size and proportionally small hind limbs, fly differently compared with other birds. One important consequence of their unique method of take-off is that their initial flight velocity is comparatively slow. Due to their insect-like wingbeat style, thought to produce lift during upstroke and downstroke, hummingbirds appear particularly well suited for hovering flight. Their flight style results in a higher energetic cost of submaximal fast flight compared with hovering and slow flight. This may be unique among birds and may ultimately account for

their use of slow take-off velocity during autonomous take-off. Factors that may represent increased motivation to take-off quickly, for escape or aggression, results in increased velocity relative to autonomous take-off. However, take-off velocity in motivated hummingbirds is still less than mean take-off velocity in other species [20].

Wing and body movements of pigeons (*columba livia*) during short distance free-flights between two perches was observed and found that the greatest accelerations were observed during the second wingbeat of take-off [21].

Regarding to aerodynamic phenomena is known that the hummingbirds modulate the orientation and trajectory of their mechanical oscillator to accomplish a change in velocity [22].

The separating flow on the low pressure side of the wing reduces of aerodynamic performance. And giving as example in nature, the owl that is able to reduce and control the separation of flow on its wings. One of the special adaptations of the owl wing, that is, the velvet-like surface structure on the upper chamber, is assumed to strongly influence the flow field around the wing [23].

The *calypte* hummingbird uses its tail as a mean of deflecting the aerodynamic flux as mean to achieve stability during the hoovering flight [24].

Wing beat frequency much depends on birds mass, having the lowest value for bigger mass birds and the opposite for light birds [25].

Resuming works on biomimetics by Barata, et al. [26, 27, 28, 29, 30], much has been contributed.
It is known that the behavioral flight capacitance and ability of insects in flight in recent years, has been an active research that provided inspiration on their maneuverability and agile flight, for the design and control of man-made MAVs and NAVs, essentially by identifying and exploiting the basic principles of performance in-flight displayed by the insects. The current investigation focus is on the achieving of a greater perception of flight performances held by several types of insects on displaying their abilities on flight maneuvers on resemblant flight stages; thus regarding to a bio inspired flapping wings robustness for MAVs and/or NAVs applications.

On a more general perspective investigation has been performed focused on the mechanisms involved with natural locomotion (thrust and/or lift), known that biological systems with interesting applications to Micro Air-Vehicles (MAVs) are generally inspired on flying insects or birds; however, similarly to the aerodynamics of flight, powered swimming requires animals

to overcome drag by producing thrust. Commonalities between natural flying and swimming have an important role on flow control issues. Several researchers recognize that the perception of flight performances held by insects is not completely understood. All control surfaces present on flying animals (feet or wings) are not designed by nature as of rigid materials; instead, they are elastic materials. Insect's wings are morphological wonder (elastic material: every wing motion is a sum of horizontal, vertical and torsional movement), however, what really enables the wings to make enough force for the animal to stay in the air, is the way insects flap them: at a very high angle of attack, creating a structure at the leading edge of the wing, (tornado-like structure) called leading-edge vortex. Researchers investigated dimensionless numbers to study the flight, and their findings were disappointing since it became clear that different points of view exist in the biomechanics field on how to best define and use. So, successful biology-inspired or biomimetic concepts will depend on the understanding of the natural mechanisms especially when they do not agree with the present engineering design principles. An additional difficulty (and a very important one) is the fact that state of art on elastic materials with identical or similar elastic properties of natural insect's wing, does not exist yet.

The natural flight ability of animals has been an active research in recent years that provided inspiration on their maneuverability and agile flight, for the design and control of MAVs and NAVs. Nevertheless, biomimetic engineered devices are still far from the living organisms and more research is needed. There is a general agreement that an unsteady dynamics approach is required to capture the physical phenomena at this scale. Additionally, propulsion and lift should not be considered independently. Flapping wing systems appeared in animals such as insects, birds, and fishes, which are known to exhibit remarkable aerodynamic and propulsive efficiencies. Flapping wings induce angular, centripetal and Coriolis accelerations in the air near to the wing's surface, which diffuse into the boundary layer of the wing. Some results suggest that the flying animals could control the predictability of vortex-wake interactions, and the corresponding propulsive forces with their wings.

So, the main studies published so far have been dedicated to the aerodynamic effects during flight stages, wing structures. Nevertheless, the studies about the take-off stage are much more scarcer for both insects and birds. In the present study the take-off and initial stages of flight were studied using a *columba livia* specimen. For the accomplishment of this study, in order to interpret the forces involved on the moment of the take-off of a bird, it was recurred to an experiment involving a fast data acquisition force sensor and high speed camera. The remainder of this thesis is structured in 3 chapters. In the next chapter the experimental method is described in detail, and then the results are presented in Chapter 3. Then the main conclusions and findings of the present work are reported in the following chapter. The Appendixes include the software developed by the author as well as the main publications resulting from the present investigation.

Chapter 2

Experimental Method

2.1 Experimental setup

This chapter describes the experimental setup used in this work from which Figure 2 illustrate a general overview at a glance. The experimental set-up is described in detail, such as all used devices and components and how are they connected; it is also explained a used code and a specific code generated specially for this work as well as the visualization technique, the calibration of some components and the error estimation.

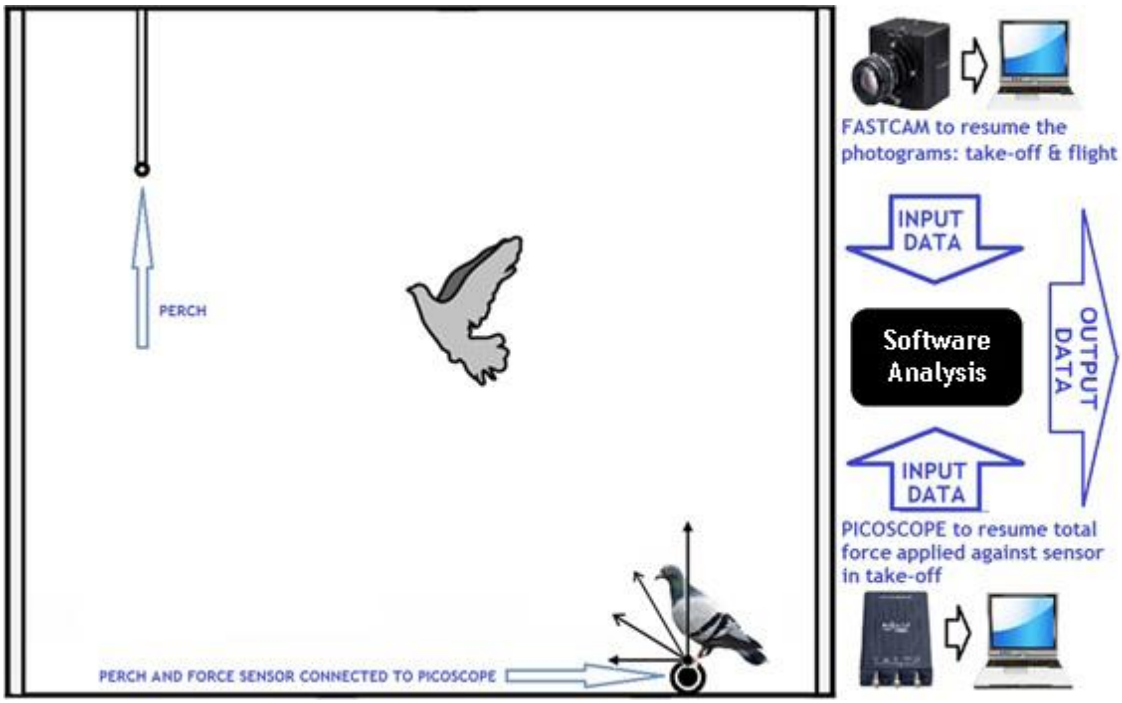

Figure 2. Experimental set-up.

The force produced by the bird during take-off is registered both by a FSS1500NSB Low Profile Force Sensor and a Photron FASTCAM Mini UX50. The perches are located at the middle section of the cage in order to allow a better focus of the images. A relation between real dimensions (rulers which measure the field of view dimensions with precision to 1 [mm]) and

the Photron FASTCAM Mini UX50 pixels (1280 x 1024 square proportion (1:1) pixels), resulting in the following relation:

$$\Delta x = \frac{86.5\,E{-}2}{1280}\ m \qquad (1)$$

Where 86.5E-2 m is the width of the horizontal axis of the field of view and 1280 the total number of pixels per line of the camera retina. So, equation (1) represents the dimension in meters of the field of view of each square pixel.

The measurements were made at an atmospheric pressure of 987.0 [kPa] and ambient temperatures from 17.8ºC up to 19.5ºC during March of 2016.

2.2 Measuring equipment

The experimental setup includes a bird cage with 1100 mm of height, 1300 mm of length and 1000 mm of depth. Inside the cage is a *columba livia* used as the subject of study for the take-off and flight tests. The distance between both perches is 962 mm. As illustrated in Figure 2, attached to the cage floor is a perch mounted on a base that supports the FSS1500NSB Low Profile Force sensor; this sensor records the vertical mechanical forces into analog signals (caused by the bird's legs). The sensor is connected by wires to a PicoScope 2204A that receives and reproduces the analog signals into digital signals in the form of plots. The PicoScope is connected to a computer that collects all information related to mechanical forces.

Another set of components is used in visualization technique: a FASTCAM Photron Mini-UX 50 using a TOKINA lens 100mm F 2.8 MACRO AT-X M100 PRO D, with its respective dedicated lens hood and a Manfrotto 190 tripod; this set is connected to another computer that collects all the video recorded information. In order to favor the analysis of frames (for both the code program and user), the image is saturated to a gain of 6.2 and illumination is compensated with the aid of a spotlight KAISER Videolight 6 1000 Watt. The cage has another perch in a higher position; all take-off and flight tests are carried out form the lowest to the highest perch. The video record footage is obtained at distance of ~ 7 meters in a parallel plane to trajectory performed by the bird.

2.2.1 FSS1500NSB Low Profile Force

After an extensive research for possible means of direct force measurements, it was concluded that a piezoresistive sensor would be the most adequate in order to measure force generated by the bird (*columba livia*). The measurements could be performed fast enough while maintaining equilibrium relative to the measurements precision.

The FSS1500NSB Low Profile Force Sensor was found to be adequate. It is capable of linear response in a range from 0 to 15 [N] forces and has a useful safe feature of overforce with a value of 45 [N], but most importantly its capability of very fast response with typical values of 0.1 [ms] while on a range of 10% to 90% of the full span signal.

In spite of these good characteristics it could not be used directly due to its reduced dimensions. So, a fixation device or platform was designed in order to accommodate this sensor which comprises an impressed circuit, a base structure, a jumping platform for the bird and the FSS1500NSB Low Profile Force Sensor (fig. 3).

Table 1. FSS1500NSB Low Profile Force Sensor characteristics.

FSS-SMT Series Caracteristics (At 10 ± 0.01 Vdc, 25°C [77°F]	Unit	FSS015WNGX		
		Min.	Typ.	Max.
Force sensing range	N	0 to 15		
Linearity (BFSL)	% Span	-	±0.5	-
Sensivity	mV/V/N	2.2	2.4	2.6
Sensivity shift (25°C to 0°C, 25°C to 50°C)	% Span	-	±5.0	-
Repeatability	% Span	-	±0.2	-
Response time (10% FS to 90% FS)	ms	-	0.1	0.5
Overforce	N	-	-	45

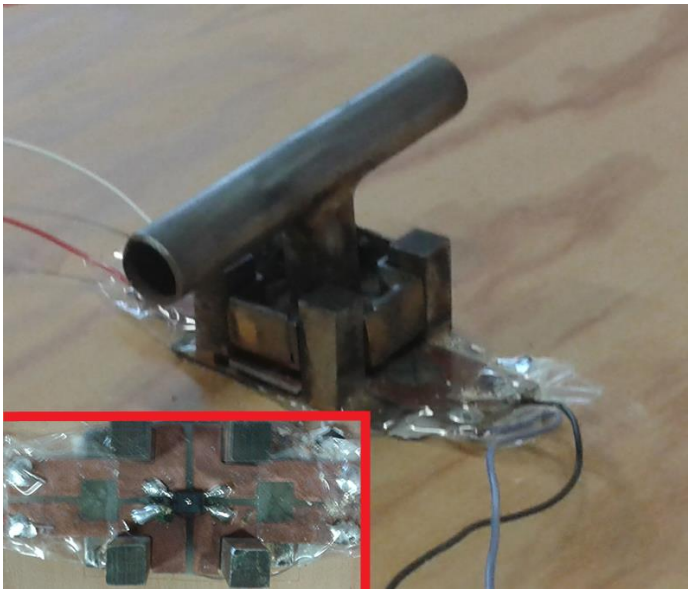

Figure 3. On top: detailed group of the perch the attachment base for both perch and sensor, left bottom corner: detail of FSS1500NSB Low Profile Force Sensor.

The structure or base was made of steel pieces welded with brass alloy, as was the jumping platform structure, the impress circuit was drawn with acid resistant and water resistant material so it would be ready to be submerged on 60% concentration nitric acid and relatively quickly removed from the acid meaning the impress circuits were well defined. Those 4 elements were assembled with the sensor glued with hot thermal glue to the impress circuit in a way that it would be positioned to connect each 4 terminals independently to a circuit on the IC, then each terminal was soldered with typical circuit solder (a mixture of tin and lead), after that was possible to perform 4 holes each on a terminal of the IC in order to be possible

to solder connecting wires on the IC, that wires would be able to facilitate the inter-connections. After that IC containing the sensor must be attached to the base structure by means of hot thermal glue. Then that base structure glued with hot thermal glue to cage floor providing a good fixation while the bird would perform the jump to the air from the jumping platform structure placed on top of the force sensor.

The force felt by the sensor is given by the following empirical relation:

$$F_{total} = \frac{span - 81.229}{11.645} \quad (2)$$

Where F_{total} is the total force impressed on the force sensor mechanism in Newton [N] as function of $span$ that is the electric tension in millivolt [mV] measured by the PicoScope 2204A described in the next section.

2.2.2 PicoScope 2204A (USB Oscilloscope)

This device is a PicoScope® 6 with a PC Oscilloscope software version 6.11.12.1692, which is the responsible part for the data acquisition from the FSS1500NSB Low Profile Force Sensor. It converts the electric potential difference into usable data taking advantage of its very fast acquisition capability, making possible to generate a very detailed plot of the potential difference as a function of time, posteriorly being traduced to a plot of F (force generated by the Columba Livia legs and its weight) as a function of time as mentioned before relating to equation (2).

Figure 4. PicoScope 2204A.

2.2.3 Photron Fastcam Mini-UX50

This device uses the Photron FASTCAM Viewer version 3610 (x64) and serves 2 main purposes. With it is possible to confirm and record the correct jump of the bird, defining a correct jump as a jump that the bird can take its claws of the perch at near the same time and without touching the ground at the moments of the entire record time post leaving contact with the perch, that conditions validate a correct jump. The other purpose is the most obvious for such kind of equipment, that is the recording of the moments of jump and flight that will allow a detailed visualization and post processment of images that will serve to calculate the force components, explained in detail on section 2.4.

The camera was set to operate at 250 [fps] (images per second), shutter speed of 1/2000 [s] (exposition time), trigger mode end (recording until pressed the trigger), resolution 1280 x 1024 pixels, 1000 [W] light source (to saturate the image irrelevant details such as wood knots) and a high gain of the camera signal.

Figure 5. Detailed set of equipment used for visualisation.

2.3 Measurements and dimensions of the bird

The columba livia was first described by Gmelin in 1789[3]. *Columba livia* (also known as rock dove or rock pigeon) is a member of the *Columbidae* bird family (doves and pigeons) often simply referred to as the "*pigeon*". Wild *Columba livia* are native to Europe, North Africa, and southwestern Asia; a large range with an estimated global extent of occurrence of 10,000,000 km^2. According to specialists, the rock pigeon's lifespan is anywhere from 3–5 years in the wild to 15 years in captivity, though longer-lived specimens have been reported[4]. Having in consideration the rank of main dimensions for an adult nominate *Columba livia*, their length, wingspan and weight will fall in ranges between 29 to 37cm; 62 to 72cm and 238 to 380g (fig. 6), respectively; for this work was used a specimen with such values of 27.2cm; 57.4cm; 298.89g (fig. 7).

Figure 6. Scientific classification of columba livia and the adult nominate dimensions.

[3] In J.F. Gmelin's https://en.wikipedia.org/wiki/Systema_Naturae appeared in Leipzig, 1788-93.

[4] BBC Science & Nature. http://www.bbc.co.uk/nature/wildfacts/factfiles/3030.shtml Retrieved 2008-02-19.

Figure 7. Precision scale used to obtain bird weight.

2.4 Data acquisition system and data processing

Just like illustrated (Figure 2) all data acquisition for this work was transferred from a Photron FASTCAM Mini UX50 and from a PicoScope 2204A with the help of two different PC's separately from each other: i.e, the first one collected all video recorded information and the second one collected all buffered data from PicoScope. As it was desired the crossing of all collected information it would be an imperative requirement for temporal synchronization, as a unique path for extrapolating of valid results concerning on the study of the contribution of muscular forces – before, during and after take-off; the contribution of these same forces to perform the take-off; the contribution of aerodynamic forces on the take-off; the total time of take-off manoeuvre, and as well as take-off angle measurements, required to obtain perch sensor force components. The temporal synchronization was achieved with the help of Matlab code entitled DLTdv5.m generated by Tyson Hedrick; such code served as a basis for obtainment of a consecutively positioning of the animal over time and was focusing on a reference point chosen accordingly to the ease of tracking on animal's body – and as all video recordings took place in a parallel plane related to the animal flight, the eye of the bird served as a graphical reference for easy recognition and consequent easy tracking. In fact, this way the DLTdv5.m code generated an output data file of coordinate points (pixels) corresponding to the alongside animal locomotion. This output data file was found to be insufficient for the present study, and a new code called T-BIRD was developed (Appendix A). Both codes were supposed to run exclusively on MATLAB®. The T-BIRD routines start to input the data obtained from DLTdv5.m, and performs a pixel to meter (m) conversion by multiplying Δx (eq. 1) on all values of positioning (with an estimated error below 5%). In order to calculate the aerodynamic forces for posterior plotting the results on this work, the

required derivatives were initially computed using first order equations (upward differences); since the results of such equations revealed unsatisfactory error values, the following step was the computation with 2nd order equations (central differences equations), that revealed a significantly error cutback; so, it was then decided to apply the discretization of central difference equations. Since velocity, V(t) is the derivative of position and acceleration, a(t), is the derivative of velocity, the second order discretized derivation (central differences) can be written as (eq. 3):

$$\boldsymbol{V} = {}^{d\boldsymbol{P}}/_{dt} = \frac{(\boldsymbol{P}_{t+1}+\boldsymbol{P}_{t-1}-4*\boldsymbol{P}_t)}{\Delta t} + O\,(h^2) \qquad (3)$$

Where:

$\Delta t = constant$;

$\boldsymbol{V}$ = velocity component [m/s];

$\boldsymbol{P}$ = bird eye position [m];

Δt = constant time step obtained by inverting the camera acquisition speed [s];

$O(h^2)$ = *higher order terms that correspond to the* 2nd order error.

(eq. 4) follows the derivation of $\boldsymbol{V(t)}$:

$$\boldsymbol{a} = {}^{d\boldsymbol{V}}/_{dt} = \frac{(\boldsymbol{V}_{t+1}+\boldsymbol{V}_{t-1}-4*\boldsymbol{V}_t)}{\Delta t} + O\,(h^2) \qquad (4)$$

Where $\boldsymbol{a}$ represents the acceleration component (a_x, a_y) [m/s^2].

Next is performed another calculus given by the next formula obtaining the force component (F_x, F_y) relative to the camera data (aerodynamic forces).

$$\boldsymbol{F} = m * \boldsymbol{a} \qquad (5)\ [31]$$

Where:

$\boldsymbol{F}$ = force components vector[N];

m = bird mass [kg].

Another important T-BIRD routine enables the user to evaluate by visualization, the specific frame number (N) on which the bird loses contact with the ground; once this is achieved, the user inputs the specific frame number (N) again on the code. The code than generate a position vector defined between frame numbers (N+1) – (N); this vector provides a direction that will enables the code to calculate the bi-dimensional angle of take-off, (TO_{angle} = arctg ((y_{N+1} – y_N) / (x_{N+1} – x_N)). This routine was mainly designed with the objective to allow the user

not only to obtain the take-off angle, as well as to compute the other component (horizontal) and the main vector of the mechanical forces on the sensor, resumed by (eq. 6 and 7):

$$\boldsymbol{F}_{total\,x} = F_{total} * cos\left(TO_{angle}\right) \quad (6)$$

$$\boldsymbol{F}_{total\,y} = F_{total} * sen\left(TO_{angle}\right) \quad (7)$$

Where:

F_{total} is given by (eq. 2);

By simplification the take-off angle was considered constant during the jump time.

The major contribution of code T-BIRD to this work is a routine especially designed to import the force sensor data and the FASTCAM data (input - offset in time) and processes all input information in order to make them match the temporal synchronization, as shown in Figure 8.

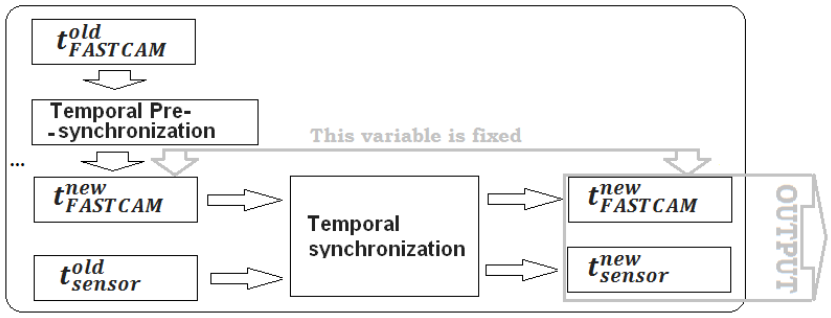

Figure 8. Resume of T-BIRD taking in account data temporal synchronization.

Explaining in detail, the algorithm processes the temporally pre-synchronized value, $t^{new}_{FASTCAM}$; this value remains unchanged and is processed to output as the reference time (t=0.000s) (fig. 9) and it is used by the code to adjust the t^{old}_{sensor} old variable in a new one t^{new}_{sensor} temporally synchronized with $t^{new}_{FASTCAM}$. Taking into account the last and the before last force value recorded on the sensor, it turns workable to perform a linearization in order to obtain the exact moment by which the force value on the sensor is F = 0 [N] – *i. e.*, the exact moment the bird loses contact with the ground (sensor). Force plots (graphics) show a negative value that the authors of this work attribute to the noise signal value. The temporal synchronizing point has become as the time reference (t = 0.000s).

- Case 1: t < 0.000s - the bird is on the ground yet (sensor);
- Case 2: t > 0.000s - bird has lost contact with the ground;
- Case 3: t = 0.000s - transition point of the two previous cases.

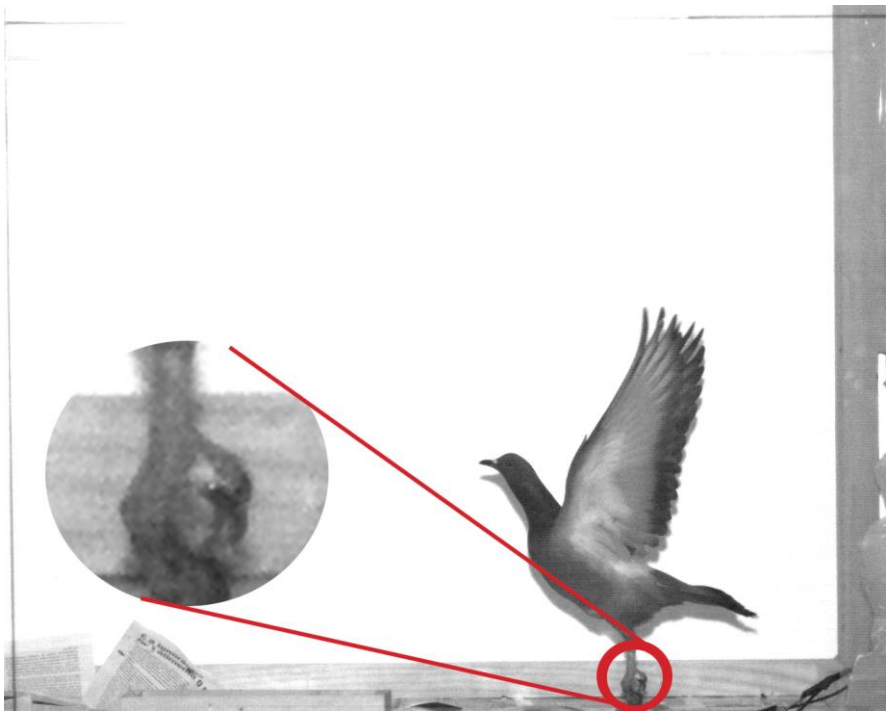

Figure 9. Take-off moment (t = 0.000s).

In this kind of sensor, the manufacturer manual does not mention mechanical or electronic damping. Although it might be possible to create an algorithm to perform damping or damping compensation, it was considered not advisable to change the input data, for several reasons: the sensor is not fitted with damping systems by the manufacturer; thus, it was also taken into account not to tamper (restrict or prevent its oscillations) and allow the greatest amount of data input. Although the force sensor consistently generates the same output for the same force, the applied sensor is excessively small and has little inertia; therefore, any linear vibration will act strongly, causing noise increase. In addition to the take-off, the raw data graph plots the forces measured (against the ground) by the sensor and read by the PicoScope for other moments prior to the bird intention to initialize the take-off maneuver; these moments before take-off, left recorded total force values in the sensor:

- Case 1: $F_{total} < W_{bird}$ - Bird does not intend to start the take-off maneuver;
- Case 2: $F_{total} \geq W_{bird}$ - Bird started the take-off maneuver (impulse).

Resuming the take-off time can be presented as the time period within first moment of no contact on the sensor (ground) F = 0 [N] and the moment of $F_{total} \geq W_{bird.}$

2.5 Calibration process and error estimation

The calibration process was achieved by making several measurements with different weights, until the possibility of estimating the maximum error produced by the FSS1500NSB Low Profile Force Sensor. After these tests was made a validation of the maximum error, achieving an error inferior to 5% and so turning to be proper for the direct force measurements at fast speed acquisition.

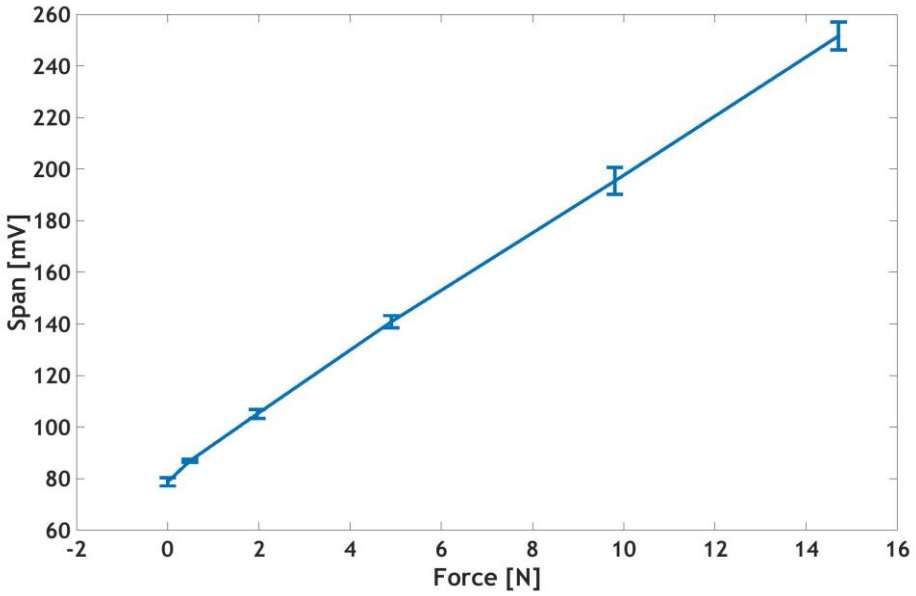

Figure 10. Span deviation [mV] as function of force [N].

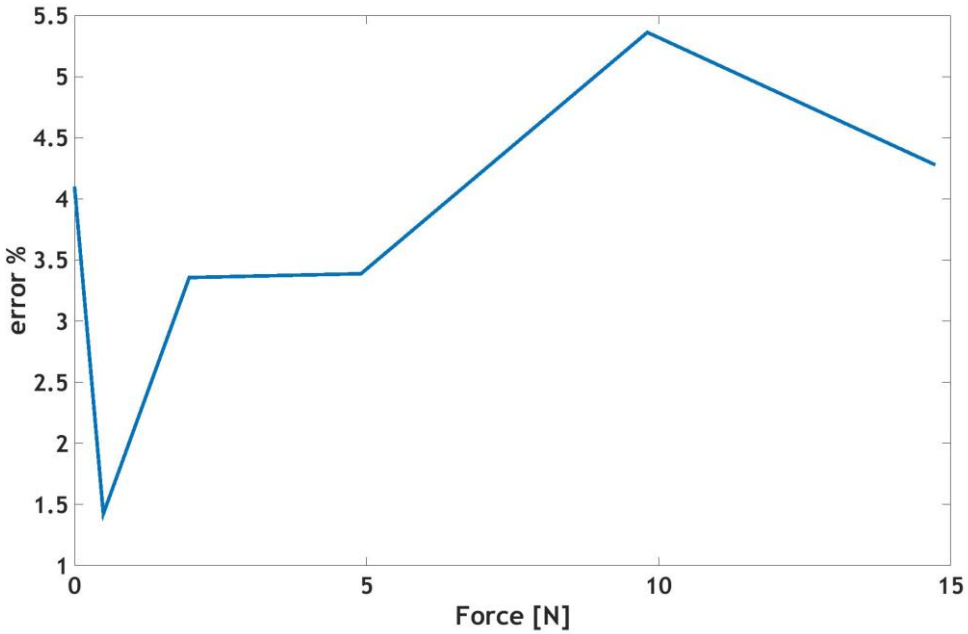

Figure 11. Relative error % as function of force [N].

2.6 Power source reliability

During the force sensor calibration, it was decided to implement the use of a Back UPS-400 Source (Emergency Battery Overvoltage Protection for Electronic and Computer Equipment) in order to guarantee the stability of DC voltage; however the noise values obtained with the inclusion of this equipment remained similar to those previously obtained, so it was decided to abandon the use of Back-UPC 400 source, since there was no explicit benefit on the results.

Figure 12. Back UPS-400 Source (Emergency Battery Overvoltage Protection for Electronic and Computer Equipment).

Chapter 3

Results and discussion

This chapter presents a summary of the 72 sequences of results obtained by direct visualization taken by FASTCAM Photron Mini-UX 50 and by reading the measurements of mechanical forces obtained by the set FSS1500NSB Low Profile Force Sensor and PicoScope 2204A. Of these 72 sequences were considered validated only 31, mainly due to two factors: 1 - incorrect bird postures on the sensor; all take-off tests were considered null when the bird jumped from the sensor to the ground; 2 – incorrect flight trajectory; all sequences were considered null when bird flight trajectory become not parallel, relative to the image acquisition plane. All the images and force plots presented in this chapter belong to a single sequence, representative of all remaining ones. This chapter is divided in six subchapters: 3.1: take-off angle of ascent on legs; 3.2: bending legs angle variation along take-off manoeuvre; 3.3: forward momentum simultaneously with take-off manoeuvre; 3.4: trajectory; 3.5: clap and fling (wing-wing interaction); and, 3.6: Comparison of force measurements.

3.1 Take-off angle of ascent on legs

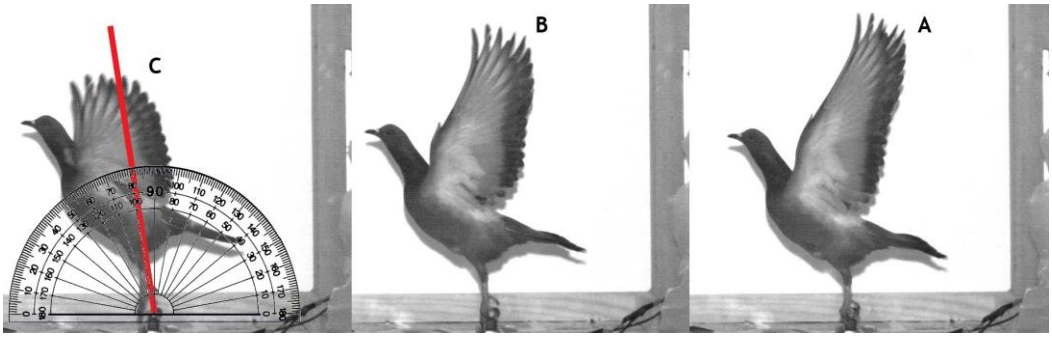

Figure 13. Take-off angle of ascent on legs.

As for initial information for this study, it was suggested to attain the measurement of the take-off angle; thus, it was intended to measure the angle within bird legs and the vertical of the sensor. Therefore, figure 13 shows three frames (58, 59 and 61), concerning to the positions immediately following the take-off, recorded on video. Figure 13.A refers to (t = 0.004s); Figure 13.B refers to (t = 0.008s); and Figure 13.C refers to (t = 0.016s) and are representative of early flight stage after take-off. As can be seen, in frame A, the bird is in the air, almost vertically to the sensor location; on frame C, was inserted an angular scale

which shows the predominance of vertical force; It can be seen that the angle of take-off (counting from the legs) is ~ 82°, very close to the vertical take-off.
Frame A reveals that the bird has its wings stretched-up vertically, meaning that downstroke wing movement is yet to start (bird is yet to achieve lift production). By taking in consideration that the animal has already lose all contact with the ground without any lift production of the wing downstroke, this analyses suggests that the animal practically started the flight by jumping in to the air.

3.2 Bending legs angle variation along take-off manoeuvre

Another import aspect related to the *columba livia* take-off maneuver is fact that they bend their legs over a wide angle, immediately before the take-off; such angle and its consequent use by the bird, suggests that they apparently benefit from the catapult effect (spring!?) force in a projected or desired direction. Figure 14 reveals the maximum amplitude of bending legs angle variation within frame A (31; t = -0.104s) and frame B (58; t = 0.004s). At frame B, the articulation of the leg shows an angle of ~180°; in frame A, the articulation of the leg, forms an angle of ~17°: therefore, the animal take advantage of an extra-impulse of a muscular "spring" of about ~163°, in order to gain velocity to resume flight.
This available evidence in conjunction with the evidence found in subchapter 3.1 of this work suggests and reinforces the idea that birds maximize their initial take-off flight velocity using leg thrust rather than wing downstroke.

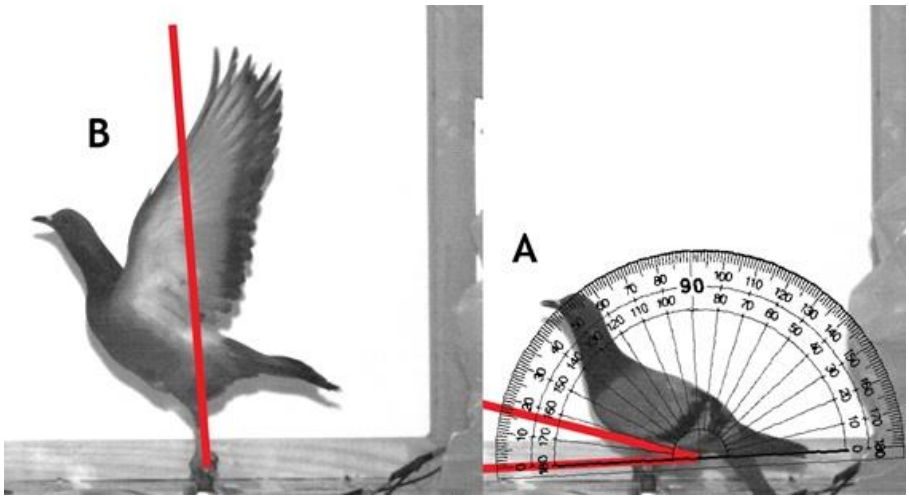

Figure 14. First take-off moments leg posture described angle.

3.3 Forward momentum simultaneously with take-off manoeuvre

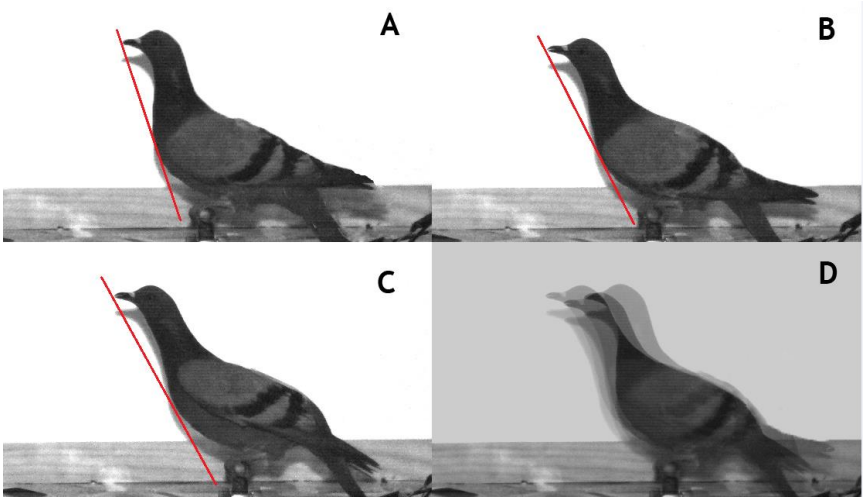

Figure 15. Forward momentum created by the bird during take-off manoeuvre.

Figure 15 illustrates the bird changing its center of mass, achieved by stretching of the body; frames A (1; t = -0.224s), B (29; t = -0.112s) and C (40; t = -0.068s), the red trace indicate small postural changes in the bird's head and neck in relation to the body. The frame D consists of an overlap of the three previous frames. In conjunction with what was observed in subchapters 3.1 and 3.2 of this work, it was also observed that during the maneuvers performed to better assist its take-off, the bird complemented its thrust with the help of moving its center of mass forward:

- extend the neck forward and the head moves down - frame A $\Rightarrow$ B;
- extend the neck forward again and the head moves up - frame B $\Rightarrow$ C.

In the plot (figure 16) the vertical and horizontal axis concerns a scale of horizontal force [N] and a time scale [s], respectively. The zero value at the center means the time synchronization reference – bird no longer has contact with the ground (sensor). The blue values were obtained by the sensor and the red values were processed data obtained by the FASTCAM video records. The obtained data suggest that the vertical momentum generated by the legs (mechanical force) is partially converted into horizontal momentum as the bird moves its center of mass forward; nearly everything of the remaining amount of momentum seems to be converted from mechanical vertical mechanism to horizontal aerodynamic mechanism. Region 1 on the plot, suggests a lack of lift force until the end of downstroke wing movement – B.

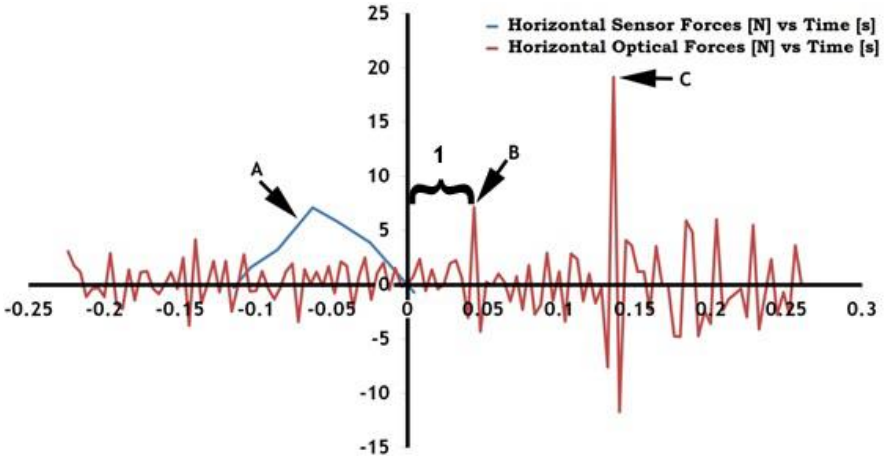

Figure 16. Plot of horizontal forces as function of time.

Plot (figure 17) concerns the case of vertical forces. Taking in consideration that the bird total weight is 298.89g (2.9311 N); the plot reveals a vertical force obtained ~12 N, (vertical force appeared to be nearly 4 times the total weight of the bird). This result obtained by the force sensor, is in accordance with the result obtained by the FASTCAM in sub-chapter 3.1 and verifies the possibility that the bird practically started the flight by jumping into the air (from a standing position); and is also in accordance with the resume in sub-chapter 3.2, were is suggested that the bird maximize their initial flight velocity (on take-off) using leg thrust rather than wing downstroke.

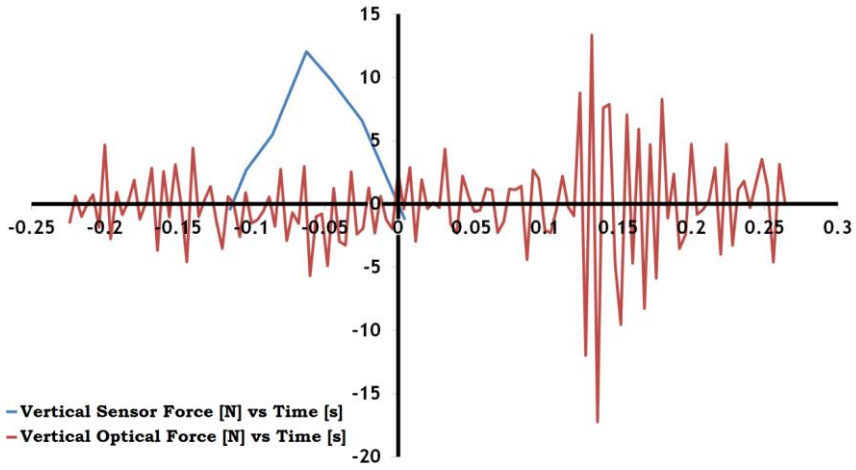

Figure 17. Plot of vertical forces as function of time.

3.4 Trajectory

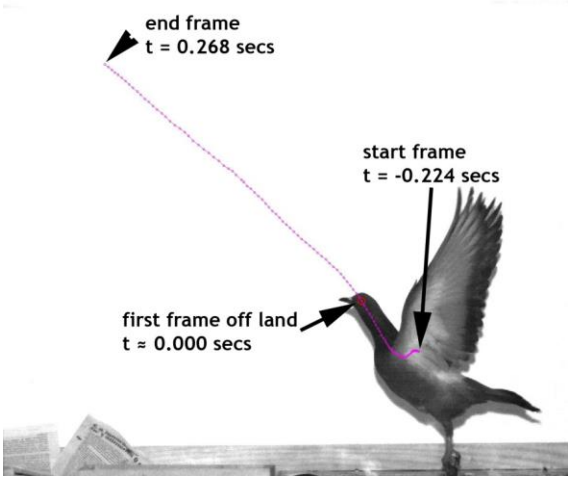

Figure 18. Path line.

This sub-chapter concerns the trajectory of the studied flight sequence. As referred before in this work, the code DLTdv5.m allow to perform the tracking of the bird, essentially by marking a point (eye of the bird); the code can track semi-automatically and may need adjustments in some points. Figure 18 illustrate the flight tracking of all sequence (t = 0.496 s), from the first frame (t = - 0.224s) to the last one (t = 0.268s). The pink dots spot the eye of the bird along the trajectory. It can be observed the eye position in first frame (t = - 0.224s); few frames ahead, the eye achieve the lowest position (as referred in previous sub-chapter related to forward momentum simultaneously with take-off maneuver). From the lowest eye position to the frame (t = 0.000s), bird reveal a higher take-off angle (TO_{angle} ~60º) than the rest of the angle of trajectory (~45º). All changing in bird´s body while moving its center of mass, leads to an interesting and intriguing result: this obtained take-off angles are distinct to the one obtained at sub-chapter 3.1 (take-off angle counting from the legs ~82º - almost vertical). Curiously, such angles difference may suggest and reinforce the idea of momentum conversion or transfer discussed on the resume of sub-chapter 3.3.

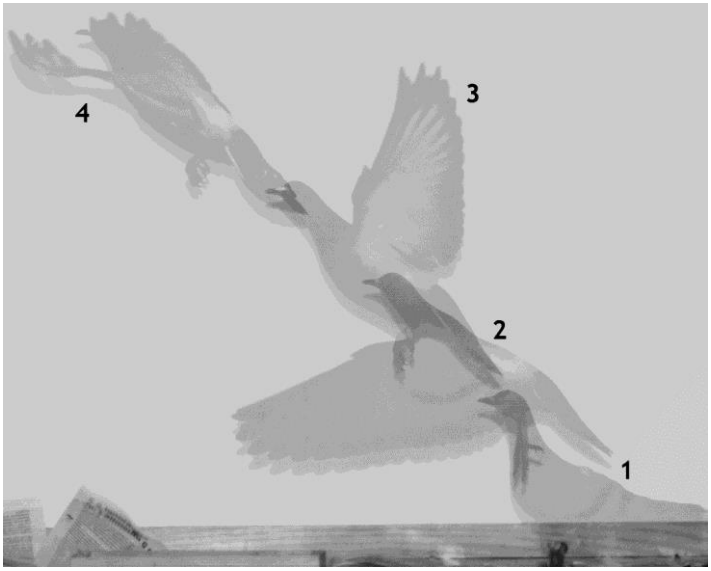

Figure 19. Wing beat.

Figure 19 illustrate wings and body positioning in four frames along trajectory followed: 1 - frame 11 (t = - 0.184s); 2 - frame 69 (t = 0.048s); 3 - frame 89 (t = 0.128s); 4 - frame 124 (t = 0.268s). The bird´s body posture is similar in the four moments; this verification may suggest that the behavior of the bird body behaves as a natural complex damper, since bird managed to dissipate his body movement from wingstrokes sudden movements and oscillations resulting this in a stabilized body trajectory along a straight path. The wingstroke is typically divided into two translational phases (upstroke and downstroke) and two rotational phases (pronation and supination). In the forward-downstroke movement (main power stroke) the wing initiate the downward loop with a high angle of attack until the leading edge tilts downwards, where the wing momentarily becomes horizontal in the middle of the stroke, minimizing the angle of attack; stalling is prevented due to the fastest moving of the wing at this point. During the recovery stroke, when the wing moves upwards and backwards, the leading edge tips backwards. The wing is rotated again at the top of the recovery stroke, restoring the maximum angle of attack immediately before the next downstroke movement initiation. According to data on figure 16 the first downstroke signal – B – is weak, because the bird does not yet need to generate more lift, essentially due to leg thrust forces until the moment after the peak in B need to compensate lift to resume flight.

3.5 Clap and fling (wing-wing interaction)

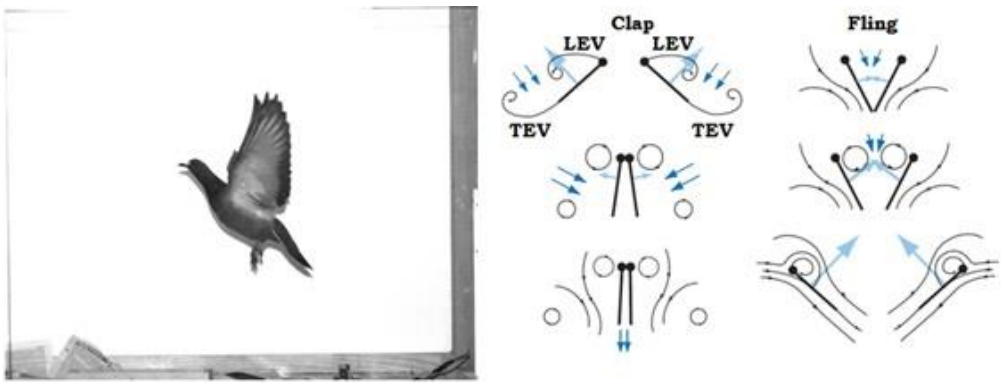

Figure 20. Clap and fling.

The *columba livia* can also takes benefits from an aerodynamic mechanisms called clap and fling. Such mechanism is used by some birds and insects as a way to augment the lift. Figure 20 (left) illustrates the bird at the end of the clap mechanism and at the beginning of the fling mechanism. The clap mechanism (figure 20 – right) consists on both wings clapping together above the animal on the upstroke; prior to the dorsal stroke reversal, as the wings come together and join, they carry with them leading edge vortices (LEV) and trailing edge vortices (TEV) and wakes which attenuate each other due to their mutually opposite sense. And as they clap together, they squeeze out a jet of air between them, which animals can use to augment thrust; some animals may enhance their manoeuvrability by redirecting this jet of air. The fling mechanism starts immediately when the wings peeled apart; this forces the vorticity to start on the wings; air flows around the leading edge of each wing which creates a bound vortex on each wing acting as the starting vortex for the opposite wing which allows a rapid buildup of circulation as well as a handy low-pressure zone above their body (expelling air from between them), with the consequent increase in total lift production (when the wings then separate, air is quickly drawn in to fill the void); and as the wings are flung apart, the lift is immediately generated because the air is already moving in the correct way.

Resuming, while flying at a ~45º inclined angle, the *columba livia* make use of aerodynamic clap and fling mechanism.

3.6 Comparison of force measurements

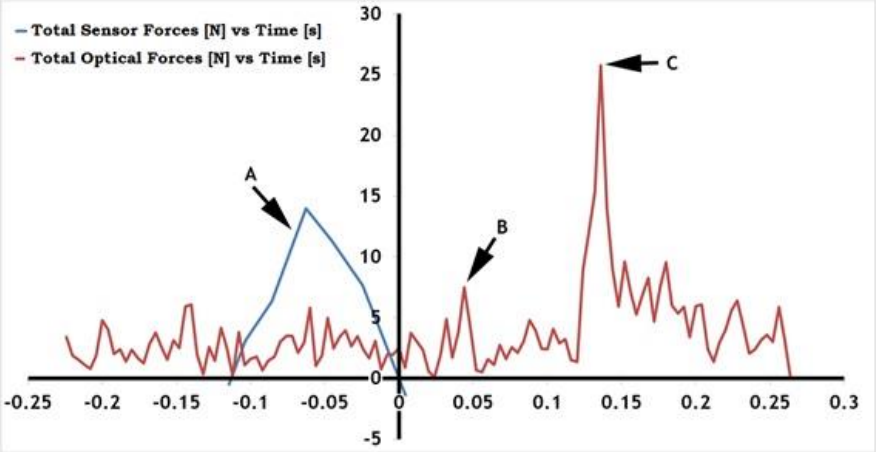

Figure 21. Plot of total forces as function of time.

In the plot (Figure 21) the vertical and horizontal axis concerns a scale of total force [N] and the time scale [s], respectively.

The plotted results reveal that the ratio between points C (2nd downstroke) and B (1st downstroke) is 330%. The ratio of the peak in the (sensor) and the weight of the bird is 477%; the ratio between peak C and the weight of the bird is 878%; the ratio between maximum aerodynamic and maximum mechanical forces is 185%. In general, the peaks of downstrokes are less intense than the peak of mechanical force, with exception of peak C. The take-off average time reveals a value of ~0.102s. Other authors ([19]) present data relating the forces produced by *diamond dove* and *zebra finch*, both quite smaller and lighter than *columba livia*. Their computed aerodynamic forces results differ from the obtained in the present work which can be explained by the huge difference of masses involved.

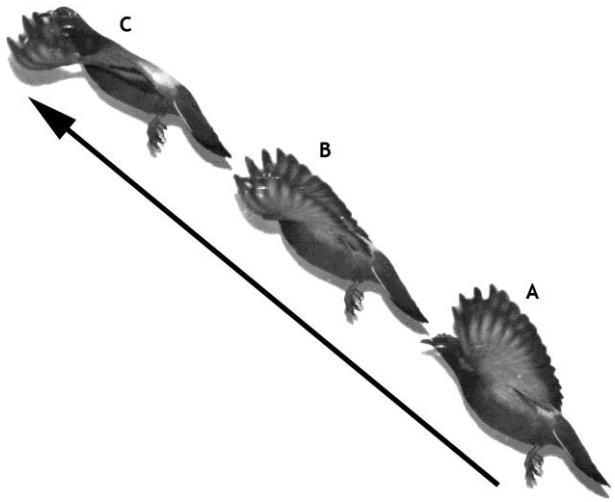

Figure 22. Animal during middle second downstroke.

Animal during the 2nd downstroke (phases A, B and C):

-From A to B: bird gathers the air to the undersurface of the wing and produces a flow directed downwards that generates lift but it also generates thrust while rotates and twists the wing (see phase B – figure 22);

-The 2nd downstroke initiates when wing is pronated on top of upstroke; as the wing moves downward and forward, (while at an almost parallel position in relation to the body) the bird has to compensate aerodynamically the lack of leg thrust that no longer exists; for this case, the obtained results revealed (at stage C – figure 21 which corresponds to figure 22B) a value above 8 times the total weight of the animal.

The reasons why the 1st downstroke in comparison with the 2nd downstroke produces considerable less lift is probably due to the fact that while during the 1st downstroke the bird is still fairly near the take-off phase and he is still under the influence of the leg thrust, which leads to a reinforcement of obtained results in this work.

Chapter 4
Conclusions

This chapter presents the main conclusion found in this work. As for initial information for this study, it was suggested to attain the measurement of the take-off angle measured on bird legs. Authors of this work observed that bird proceed to a near vertical take-off: at instant t = 0.016s the legs form a ~ 82° angle, very close to the vertical take-off. From sub-chapter 3.1 it was also observed that in time the range of t=0.000s to t=0.016s the bird has its wings stretched-up vertically, meaning that downstroke wing movement is yet to start (bird is yet to achieve lift production). By taking in consideration that the animal has already lose all contact with the ground without any lift production of the wing downstroke, this analyses suggests that the animal practically started the flight by jumping in to the air. From sub-chapter 3.2, the collected data revealed that bird bend their legs over a wide angle, immediately before the take-off; before take-off (t = -0.104s) bird has its legs bended at maximum value angle (loaded catapult); at instant t = 0.004s (without ground contact) all energy was released by the bird, suggesting that they apparently benefit from the catapult effect (spring!?) force in a projected or desired direction. This available evidence in conjunction with the evidence found in subchapter 3.1 of this work suggests and reinforces the idea that birds maximize their initial take-off flight velocity using leg thrust rather than wing downstroke. Sub-chapter 3.3 revealed that during the bird maneuvers performed to better assist its take-off, the animal improved and complemented its thrust by moving its center of mass forward essentially by a complex conjunction of movements: firstly, by extending the neck forward and moving the head down; followed by keep extending the neck forward and moving the head up – both movements happening when the animal is beginning to release the catapult effect on legs. The plot reveals a vertical force of ~12 N, nearly 4 times the total weight of the bird. This result obtained by the force sensor, is in accordance with the result obtained by the FASTCAM in sub-chapter 3.1 verifying the possibility that the bird practically started the flight by jumping into the air (from a standing position); and is also in accordance with the resume in sub-chapter 3.2, suggesting that the bird maximize their initial flight velocity (on take-off) using leg thrust rather than wing downstroke. Data collected suggests that due to leg thrust, the bird don't need to produce aerodynamic lift from t = 0.000s to peak B. Sub-chapter 3.4 concerns the trajectory of the studied flight sequence with the help of a tracking code marking the positioning of the bird's eye (pink dots spot the eye) along a flight sequence of t = 0.496s. Initially, the eye was spotted at instant t = - 0.224s; frames after, was observed that the eye achieve the lowest position (as referred in previous sub-chapter related to forward momentum simultaneously with take-off maneuver).

From the lowest eye position to t = 0.000s, bird reveal a take-off angle of TOangle ~60º; from t = 0.000s to t = 0.268s the trajectory angle of ~45º. All changing in bird´s body while moving its center of mass, leads to an interesting and intriguing result: this obtained angles are distinct to the one obtained at sub-chapter 3.1 (take-off angle counting from the legs ~82º - almost vertical). Curiously, such angles difference may suggest and reinforce the idea of momentum conversion or momentum transfer discussed on the resume of sub-chapter 3.3. Sub-chapter 3.5 reveled that while flying at a ~45º flight climb angle, the columba livia make use of aerodynamic clap and fling mechanism in order to obtain lift augmentation. The Comparison of force measurements obtained, reveals that the ratio between points C (2nd downstroke) and B (1st downstroke) is 330%; another ratio concerning the peak in the (sensor) and the weight of the bird is 477%; the ratio between peak C and the weight of the bird is 878%; and also that the ratio between maximum aerodynamic and maximum mechanical forces is 185%. In general, the peaks of downstrokes are less intense than the peak of mechanical force, with exception of peak C. The take-off average time reveals a value of ~0.102s. During the 2nd downstroke, bird gathers the air to the undersurface of the wing and produces a flow directed downwards that generates lift but it also generates thrust while rotates and twists the wing. The obtained results suggest that virtually all lift production is carried out along the downstroke movement, a full consistency result with all the authors who have studied the bird's flight, with exception for the hummingbird. The inflight bird´s body posture may suggest that the behavior of the bird body behaves as a natural complex damper, since bird managed to dissipate his body movement from wingstrokes sudden movements and oscillations resulting this in a stabilized body trajectory along a straight path. The reasons why the 1st downstroke in comparison with the 2nd downstroke produces considerable less lift is probably due to the fact that while during the 1st downstroke the bird is still fairly near the take-off phase and he is still under the influence of the leg thrust, which leads to a reinforcement of obtained results in this work. The 2nd downstroke initiates when wing is pronated on top of upstroke; as the wing moves downward and forward, (while at an almost parallel position in relation to the body) the bird has to compensate aerodynamically the lack of leg thrust that no longer exists; for this case, the obtained results revealed (at stage C – figure 21 which corresponds to figure 22B) a value above 8 times the total weight of the animal.

References

[1] Tanaka, H., Whitney, J. P., Wood, R. J., “Effect of Flexural and Torsional Wing Flexibility on Lift Generation in Hoverfly Flight”, *Integrative and Comparative Biology*, Vol. 51, No. 1, pp. 142-150, 2011.

[2] Ang H-S, Xiao T-H, Duan W-B, “Flight mechanism and design of biomimetic micro air vehicles”, *Science in China Series E-Technological Sciences*, Vol. 52, No. 12, pp. 3722-3728, 2009.

[3] Zhang, G. Q., Yu, S. C. M., “Aerodynamic Characteristics of the Ventilated Design for Flapping Wing Micro Air Vehicle”, *The Scientific World Journal*, Vol. 2014, pp. 1-11, 2014.

[4] Ha, N. S., Nguyen, Q. V., Goo, N. S., et al., “Static and Dynamic Characteristics of an Artificial Wing Mimicking an Allomyrina Dichotoma Beetle’s Hind Wing for Flapping-Wing Micro Air Vehicles”, *Experimental Mechanics*, Vol. 52, No. 9, pp. 1535-1549, 2012.

[5] Tanaka, H., Wood, R. J., “Fabrication of corrugated artificial insect wings using laser micromachined molds”, *Journal of Micromechanics and Microengineering*, Vol. 20, No. 7, pp. 1-8, 2010.

[6] Lehmann F-O, Sane, S. P., Dickinson, M., “The aerodynamic effects of wing–wing interaction in flapping insect wings”, *Journal of Experimental Biology*, Vol. 208, pp. 3075-3092, 2005.

[7] Lehmann F-O, Pick, S., “The aerodynamic benefit of wing–wing interaction depends on stroke trajectory in flapping insect wings”, *Journal of Experimental Biology*, Vol. 210, No. 8, pp. 1362-1377, 2007.

[8] Miller, L. A., Peskin, C. S., “Flexible clap and fling in tiny insect flight”, *Journal of Experimental Biology,* Vol. 212, No. 19, pp. 3076-3090, 2009.

[9] Ramamurti, R., Sandberg, W. C., "A computational investigation of the three-dimensional unsteady aerodynamics of Drosophila hovering and maneuvering", *Journal of Experimental Biology*, Vol. 210, No. 5, pp. 881-896, 2007.

[10] Fontaine, E. I., Zabala, F., Dickinson, M. H., et al., "Wing and body motion during flight initiation in Drosophila revealed by automated visual tracking", *Journal of Experimental Biology*, Vol. 212, No. 9, pp. 1307-1323, 2009.

[11] Tien V-T, Tuyen Q-L, Hieu T-T, et al., "Flow Visualization of Rhinoceros Beetle (Trypoxylus dichotomus) in Free Flight", *Journal of Bionic Engineering*, Vol. 9, No. 3, pp. 304-314, 2012.

[12] Barata, J. M. M., Neves, F. M. S. P., Manquinho, P. A. R., Silva, T. A. J., "Propulsion for Biological Inspired Micro-Air Vehicles (MAVs)", *Open Journal of Applied Sciences*, Vol. 6, No. 1, pp. 7-15, 2016.

[13] Hedenström, A., "Aerodynamics, evolution and ecology of avian flight", *In Trends in Ecology & Evolution*, Vol. 17, No. 9, pp. 415-422, 2012.

[14] McMichael, J.M., Francis, M.S., "Micro Air Vehicles - Toward a New Dimension in Flight", 1997. http://fas.org/irp/program/collect/docs/mav_auvsi.htm

[15] Hylton, T., Martin, C., Tun, R., Castelli, V. (2012) The DARPA Nano Air Vehicle Program. Proceedings of 50th AIAA Aerospace Sciences Meeting Including the New Horizons Forum and Aerospace Exposition, Nashville, Tennessee, 9-12 January 2012, Vol. 10, pp. 8549-8557.

[16] von Ellenrieder, K.D., Parker, K., Soria, J., "Fluid mechanics of flapping wings", *Experimental Thermal and Fluid Science*, Vol. 32, pp. 1578-1589, 2008.

[17] Evers, J.H., "Biological Inspiration for Agile Autonomous Air Vehicles", In Platform Innovations and System Integration for Unmanned Air, Land and Sea Vehicles (AVT-SCI Joint Symposium). Meeting Proceedings RTO-MPAVT- 146, Paper 15, RTO, Neuilly-sur-Seine, France, pp. 15-1-15-14, 2007.

[18] Su, J-Y, Tang, J-H, Wang, C-H, et al., "A numerical investigation on the ground effect of a flapping-flying bird", *Physics of Fluids*, Vol. 25, No. 9, 093101 , pp. 1-13, 2013.

[19] Provini, P., Tobalske, B. W., Crandell, K. E., et al., “Transition from leg to wing forces during take-off in birds”, *The Journal of Experimental Biology*, Vol. 215, No. 23, pp. 4115-4124, 2012.

[20] Tobalske, B. W., Altshuler, D. L., Powers, D. R., ” Take-off mechanics in hummingbirds (Trochilidae)”, *The Journal of Experimental Biology*, Vol. 207, No. 8, pp. 1345-1352, 2004.

[21] Berg, A. M., Biewener, A. A., “Wing and body kinematics of takeoff and landing flight in the pigeon (Columba livia)”, *The Journal of Experimental Biology*, Vol. 213, No. 10, pp. 1651-1658, 2010.

[22] Tobalske, B. W., Warrick, D. R., Clark, C. J., et al., “Three-dimensional kinematics of hummingbird flight”, *The Journal of Experimental Biology,* Vol. 210, No. 13, pp. 2368-2382, 2007.

[23] Winzen, A., Klaas, M., Schroeder, W., “High-speed PIV measurements of the near-wall flow field over hairy surfaces”, *Experiments in Fluids*, Vol. 54, No. 3, 1472, pp. 1-14, 2013.

[24] Altshuler, D. L., Princevac, M., Pan, H., et al., “Wake patterns of the wings and tail of hovering hummingbirds”, *Experiments in Fluids*, Vol. 46, No. 5, pp. 835-846, 2009.

[25] Pennycuick, C. J., ” Wingbeat frequency of birds in steady cruising flight: New data and improved predictions”, *The Journal of Experimental Biology,* Vol. 199, No. 7, pp. 1613-1618, 1996.

[26] Barata, J. M. M., Neves, F. M. S. P., Manquinho, P. A. R., Silva, T. A. J., “Biomimetics: Insect’s Wings Motion Patterns on Similar Flight Stages”, 3 EJIL - LAETA Young Researchers Meeting, ADAI, Coimbra, 7-8 May 2015

[27] Barata, J. M. M., Neves, F. M. S. P., Manquinho, P. A. R., “Comparative Study of Wing’s Motion Patterns on Various Types of Insects on Resemblant Flight Stages”, AIAA SciTech, 5-9 January 2015, Kissimmee, Florida, AIAA Atmospheric Flight Mechanics Conference, pp. 828-848.

[28] Barata, J. M. M., Neves, F. M. S. P., Manquinho, P. A. R., Silva, T.A.J., “Propulsion for Biological Inspired Micro-Air Vehicles (MAVs)”, *Open Journal of Applied Sciences*, Vol. 6, No. 1, pp. 7-15, 2016.

[29] Barata, J. M. M., Neves, F. M. S. P., Manquinho, P. A. R., Silva, T.A.J., “Propulsion for Biological Inspired Micro-Air Vehicles (MAVs)”, ICEUBI, International Conference on Engineering, Engineering for Society, University of Beira Interior, 2/4 December 2015.

[30] Barata, J. M. M., Neves, F. M. S. P., Manquinho, P. A. R., Silva, A. R. R., “Biological Inspired Propulsion of Micro-Air Vehicles”. 7th ECCOMAS, European Committee on Computational Methods in Applied Sciences, Thematic Conference on Smart Structures and Materials, SMART 2015, Ponta Delgada, S. Miguel, Azores, Portugal, 3-6 June 2015.

[31] Zabala, F. A., Card, G. M., Fontaine, E. I., et al., “Dynamics of Escaping Flight Initiations of Drosophila melanogaster”, Proceedings of the 2nd Biennial IEEE/RAS-EMBS International Conference on Biomedical Robotics and Biomechatronics, Scottsdale, AZ, USA, October 19-22, 2008.

[32] PicoScope 2200A Series (Data Sheet), Benchtop performance in a pocket-sized scope, MM051.en-7. Copyright © 2013–2016 Pico Technology Ltd. All rights reserved.

[33] PicoScope 2200A Series, PC Oscilloscopes (User's Guide), ps2200a.en r3., 20/04/2015. Copyright © 2014–2015 Pico Technology Limited. All rights reserved.

[34] PicoScope USB Oscilloscope (Quick Start Guide), DO115-17, Copyright © 2006–2014 Pico Technology Limited. All rights reserved.

[35] Honeywell FSS-SMT Series Low Profile Force Sensor (Data Sheet), 080281-3-EN, April 2014, © 2014 Honeywell International Inc. All rights reserved.

[36] Honeywell Force Sensors Line Guide, (User’s Guide), 008151-5-EN Il50, January 2016, Copyright © 2016 Honeywell International Inc. All rights reserved.

[37] Photron FASTCAM Viewer for High Speed Digital Imaging (User’s Manual), Ver. 3 revision 2.11E Operation Section, July 2015, PHOTRON LIMITED.

[38] FASTCAM Mini UX50/100 (Hardware Manual) Revision 1.06EN, June 2015, PHOTRON LIMITED.

[39] GigabitEthernet Interface (Connection Manual), revision 1.10E, July 2015, PHOTRON LIMITED.

[40] FASTCAM Mini Series, Stand-Alone Type HIGH-SPEED DIGITAL CAMERA, First-Step Guide Booklet for FASTCAM Cameras, July 2015, revision 1.10E, July 2015, PHOTRON LIMITED.

[41] How to use a bundled LAN Cable, Photron Pamphlet.

[42] Tokina Lenses, (Manual de Instrucciones), Kenko Tokina Co, Ltd. KT Nakano Building, 5-68-10, Nakano, Nakano-Ku, Tokyo 164-8616, Japan.

[43] Videoleuchte, Videolight 6 93304, Kaiser Phototechhnik GmbH & Co. KG, Im Krötenteich 2 – 74722 Buchen, Germany.

Appendix A – T-BIRD routines

```
%this script process experiment data
%add the 'sensor_data.xlsx' and 'videoxypts.xlsx'

clc
clear all

tic

%--------------------------------------------------------------------------
%---------------------- variables introduction ----------------------------
%--------------------------------------------------------------------------

fps = 250;                      %frame rate
delta_t = fps^(-1);             %frame period, or increments in time
to_frame = 57;                  %frame which bird take-off
delta_l = 86.5e-2/1280;         %length by pixel
mass = 298.89e-3;               %birds mass;
g = 9.80665;                    %gravity
weight = mass*g;
d_mode = 2;                     %discretization mode, '1' for 1st order,
%'2' for second order
clear tstart fps;

%--------------------------------------------------------------------------
%-------------------- end of variables introduction -----------------------
%--------------------------------------------------------------------------




%--------------------------------------------------------------------------
%------------------------ post initialization -----------------------------
%--------------------------------------------------------------------------

mc = xlsread('videoxypts.xlsx', 'Folha1');        %mass center initialization,
%1 = x coordinate, 2 = y coordinate
mc(:, 1) = mc(:, 1)*delta_l;
mc(:, 2) = mc(:, 2)*delta_l;
[sz, null] = size(mc);
clear null;
t = zeros(sz, 1);               %time initialization
istart = 1;
iend = sz;
range = iend - istart + 1;
time = -(to_frame - istart)*delta_t;

for i = 1:1:range
    t(i) = time;
    time = time + delta_t;
end
clear i time;

angle_to = atand((mc(to_frame + 1, 2) - mc(to_frame, 2))/((-1)*(mc(to_frame + 1, 1) - mc(to_frame, 1))));

%--------------------------------------------------------------------------
%--------------------- end of post initialization -------------------------
%--------------------------------------------------------------------------




%--------------------------------------------------------------------------
%------------------------------ processment -------------------------------
%--------------------------------------------------------------------------

%v = dx/dt
%a = d^2x/dt^2 = dv/dt

%1st order numeric derivation: dx_dt = (x_i - x_i-1)/dt
%2nd order numeric derivation:
%dx/dt = ((x_i+1 - x_i)/dt) + ((x_i - x_i-1)/dt)/2

v = zeros(range, 2);        %velocity initialization
```

```
a = zeros(range, 2);        %acceleration initialization

if d_mode == 1

    for i = 2:1:range
        v(i, 1) = (-1)*(mc(i, 1) - mc(i-1, 1))/delta_t;     %horizontal
        %component of velocity
        v(i, 2) = (-1)*(mc(i, 2) - mc(i-1, 2))/delta_t;     %vertical
        %component of velocity
    end
    clear i;

    for i = 1:1:range - 1
        a(i, 1) = (v(i+1, 1) - v(i, 1))/delta_t;        %horizontal
        %component of accelaration
        a(i, 2) = (v(i+1, 2) - v(i, 2))/delta_t;        %vertical
        %component of acceleration
    end
    clear i;
    a(range, 1) = a(range - 1, 1);
    a(range, 2) = a(range - 1, 2);

%-----------------------------------

elseif d_mode == 2

    for i = 2:1:range - 1
        v(i, 1) = (-1)*(((mc(i+1, 1) - mc(i, 1))/delta_t) + (mc(i, 1) - mc(i-1, 1)))/2;     %horizontal
        %component of velocity
        v(i, 2) = (-1)*(((mc(i+1, 2) - mc(i, 2))/delta_t) + (mc(i, 2) - mc(i-1, 2)))/2;     %vertical
        %component of velocity
    end
    clear i;

    a(1, 1) = (v(1+1, 1) - v(1, 1))/delta_t;        %horizontal
    %component of accelaration
    a(1, 2) = (v(1+1, 2) - v(1, 2))/delta_t;        %vertical
    %component of acceleration

    for i = 2:1:range - 2
        a(i, 1) = (((v(i+1, 1) - v(i, 1))/delta_t) + (v(i, 1) - v(i-1, 1)))/2;        %horizontal
        %component of accelaration
        a(i, 2) = (((v(i+1, 2) - v(i, 2))/delta_t) + (v(i, 2) - v(i-1, 2)))/2;        %vertical
        %component of acceleration
    end
    clear i;
    a(range, 1) = a(range - 1, 1);
    a(range, 2) = a(range - 1, 2);

end

f = zeros(range, 3);
f(:, 1) = mass*a(:, 1);
f(:, 2) = mass*a(:, 2);
f(:, 3) = ((f(:, 1)).^2 + (f(:, 2)).^2).^(1/2);



%-------------------------------------------------------------------------
%------------------------- end of processment ----------------------------
%-------------------------------------------------------------------------



%-------------------------------------------------------------------------
%---------------------------- post processment ---------------------------
%-------------------------------------------------------------------------

xlswrite('processed_data.xlsx', t, 'time')
xlswrite('processed_data.xlsx', f, 'force')

```

```
    %-------------------------------------------------------------------------
    %------------------------ end of post processment ------------------------
    %-------------------------------------------------------------------------



    %-------------------------------------------------------------------------
    %------------------------------ foot sensor ------------------------------
    %-------------------------------------------------------------------------

    mat = xlsread('sensor_data.xlsx');      %1st column is span[mV],
    %2nd collumn is time[s]
    [sz_s, null] = size(mat);
    clear null;
    f_s = zeros(sz_s, 3);                                   %3rd collumn is
    %absolute force, 1st is x component force and 2nd is y component force
    istart_s = 1;
    iend_s = sz_s;
    range_s = iend_s - istart_s + 1;
    f_s(:, 3) = (mat(:, 1) - 81.229)/11.645;
    f_s(:, 1) = f_s(:, 3)*cosd(angle_to);
    f_s(:, 2) = f_s(:, 3)*sind(angle_to);

    for i = 1:1:sz_s
        if f_s(i, 2) >= 0
            p = i;
        end
    end
    clear i;

    %take-off time
    m = (f_s(p+1, 2) - f_s(p, 2))/(mat(p+1, 2) - mat(p, 2));
    b = f_s(p, 2) - m*mat(p, 2);
    t_to = -b/m;
    t_s = mat(:, 2) - t_to;

    %take-off beggining
    for i = 1:1:range_s
        if f_s(i, 3) >= weight
            p_b = i;
            break;
        end
    end
    if p_b == 1
        t_tob = t_s(1);
    else
        m = (f_s(p_b+1, 2) - f_s(p_b, 2))/(mat(p_b+1, 2) - mat(p_b, 2));
        b = f_s(p_b, 2) - m*mat(p_b, 2);
        t_tob = (weight - b)/m;
    end
    delta_t_to = t_to - t_tob;                          %take off required time
    clear i;

    xlswrite('processed_data.xlsx', t_s, 'time_sensor')
    xlswrite('processed_data.xlsx', f_s, 'force_sensor')

    %-------------------------------------------------------------------------
    %---------------------------- end foot sensor ----------------------------
    %-------------------------------------------------------------------------

    toc
```

Appendix B – Scientific work publications

BIOMIMETICS: INSECT'S WINGS MOTION PATTERNS ON SIMILAR FLIGHT STAGES

J.M.M. Barata [a], F.M.S.P. Neves [a]*, P.A.R. Manquinho [a], F.C. Andrade[a], T.J.A. Silva[a]

a) LAETA-UBI/AeroG, UBI, Rua Marquês d'Ávila e Bolama 6201-001 Covilhã

***** e-mail: fernandomneves@gmail.com

Key words: flapping wings, insect flight, biomimetic MAV/NAV

Abstract. *The behavioral of insect´s flight performances has become an active research in recent years and has provided adaptive biological inspirations for design and control of man-made MAVs, essentially by identifying, exploiting and understanding the basic flight principles displayed by these animals. All insects flying skills rely on flight muscles, response speed and their mechanical power transmission to the wings: kinematics and deformations. This work details a summary consideration on a variety of flying insects and is focused on remarks of wings motion patterns along similar flight stages.*

1 BACKGROUND INTRODUCTION

The insects are among the most diverse groups of animals on the planet, including over a 1,000,000 described species and representing more than a half of all living organisms. According to Smithsonian Museum of Natural History, most authorities agree on a conservative estimation of 2,000,000 species and could be extended to up 30,000,000. By analyzing the History of the insect's development, the estimated number of described species and by verifying that they are found in about every single available habitat, the insects are far beyond the hugely successful specie in colonizing the Earth. They also proved to be very adaptable, once they survive changing conditions since even before the appearance of the dinosaurs 225 million years ago. The history of the insect's ability to fly has approximately 300 million years, which makes by far the first specie with such capacity on Earth (rather earlier than pterodactyls, birds and bats). Their wing structures and wing beat mechanisms are very complex, allowing them to hover for over extended time period and as well, suddenly change their direction at their will without any obstacle; this maneuverability is remarkable and by far, superior to every maneuverability of any man-made flying vehicle and has captured the humans attention in a way to achieve such knowledge [1]. When it comes to flight subjects, the insects Reynolds number range is within the interval $100 < Re < 10{,}000$ (housefly = 120; honeybee = 1,000; butterfly = 3,900), while in the aircrafts case could be of 1,600,000 for a simple glider, or up to 2,000,000,000 in the Boeing 747 case. However, such maneuverability capacity was to be firstly applied to smaller air vehicles. In 1997, DARPA started a "MAV-project", an initiative in order to seek, to develop and to test emerging technologies that could evolve into a mission capable system for military surveillance and reconnaissance applications [2]. The definition employed in DARPA's program limits these craft to a size less than 15 cm in length, width or height, with no

restrictions on its design or conception and a maximum total weight would be less than 100 gram [3]. In October 2005, DARPA launched a Nano Air Vehicle (NAV) program with the objective of developing and demonstrating small (< 10 cm wingspan), lightweight (< 10 gram) air vehicles systems with potential to perform challenging indoor and outdoor missions [4]. The physiological and biomechanical basis of flapping flight has been explored on the bird's flights, firstly by Giovanni Borelli [5], by Otto Lilienthal [6] and also by Étienne Jules Marey [7, 8, 9, 10] in more consistent studies; Marey also developed studies about the insects flapping flights [9, 11] and was the first to notice a complex wing motion pattern on its trajectory during the flight (a horizontal 8 shape). In 1874, Professor Pettigrew published a book [12] on which he drew attention to the fact that the birds while flying and during every cycle of wings beat, ran movements that could be represented with considerable accuracy with an 8-figure drawn vertically, while the insects ran the same figure drawn, but horizontally. The subject of the insect's flight acquaintance evolved and had been extensively explored on the last decades of the XX Century (Jensen [13]; Collett & Land [14]; Ellington [15, 16]; Ennos [17]; Dudley [18, 19]; Dudley & Ellington [20]). More recently, the knowledge of insects flight aerodynamics have advanced significantly, essentially due to the major scientific technological and methodological advances developed in several areas, such as high-speed imaging videography (Fry *et al* [21, 22];; Hedrick [23]); computational fluid dynamics simulations (Ramamurti & Sandberg [24]; Sun & Xiong [25]) and robotics wings used with dynamics forces scaling (Dickinson *et al* [26]; Sane Dickinson [27]). Tanaka *et al* 2011 [28], made an experimental visualization study on two artificial wing models with flexural and torsional wing flexibility replicated from the lift generation of the hoverfly wings: a polymer wing was compared with a rigid, flat, carbon-fiber wing using a flapping mechanism driven by a piezoelectric actuator. Both wing models presented venation and corrugation profiles mimicking a hoverfly wing and the flexural stiffness of the artificial wings are similar to the natural wing. Both models were tested in appropriate flight trajectories of the hoverfly. All tests were made single wing, independent of collateral induced wing flows by the head, thorax, abdomen or legs of the insect. Their main research consisted by varying the stiffness of the hinge by 5 levels and to observe the consequent relation to their generating results. The authors found that the maximum lift was achieved when the stiffness of the hinge was similar to that of a hoverfly in both wing cases and in this case, they also found that the magnitude of measured lift is sufficient for hovering. These results suggest that hoverflies could exploit intrinsic compliances to generate desired motions of the wing and that, for the same flapping motions, a rigid wing could be more suitable for producing large lift. Ang *et al* 2009 [29] conducted a numerical investigation based on studies of mechanisms of flight of birds and insects with its application on the design of flying MAVs. Their work include the studies of low Reynolds number aerodynamics, unsteady computational fluid dynamics and flight control for the fixed-wing and flapping-wing, flexible flapping-wing, the dragonfly-like and the bee-like MAVs. For the aerodynamics analysis, authors used a numerical solution of the Navier-Stokes equations, which at low Reynolds numbers tend to be inefficient in terms of convergence, stability and accuracy; due to this situation, they

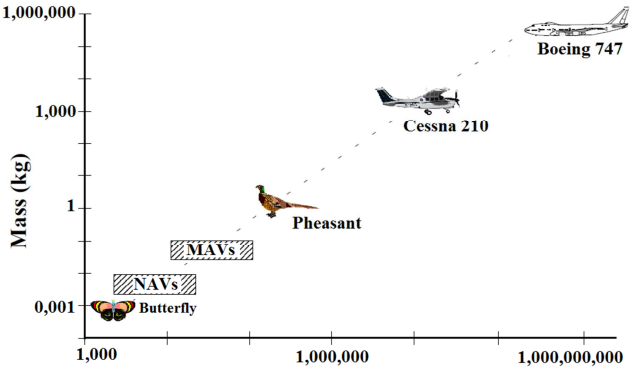

Figure 1: Classification of MAV's and NAV's over a relation of Mass and Reynolds Number.

used a numerical method to solve the equations of N-S with preconditions of dual-time stepping developed separately. For the case of unsteady flow characteristics of the flapping wings, their effective used method ($3D^2$MUFS N-S equation method) was based on the dual-stepping scheme in conjunction low Mach number preconditions running at an unstructured dynamic mesh built for dynamic boundary problems allowing large relative movements. The authors simulated that flexible wing deformation on their work, present a more accurate flapping motion and by their comparative results they found that the aerodynamic forces of the rigid-flapping and flexible-flapping wings with suitable flexibility both lift and thrust rose on the flexible-flapping case. By observing and studying all the obtaining data of earlier studies made by previous researchers concerning the flight of the insects, all analyzes suggest that the insects control their different flight stages at their will, without restrictions and ruled by the different wing motion trajectories; with such movements, they managed their high lift, high drag, gliding and the fast maneuverability and sudden course alteration. The main objective of this study is to collect data on the types of movement patterns of each insect wings observed for each type of flight taken and its comparative analysis with other insects at similar flight stages.

2 INTERPRETATION OF A BIOLOGICAL FLIGHT MACHINE

2.1 FLIGHT MUSCLES: POWER AND STEERING MUSCLES

Beyond a pair of dorsolongitudinal muscles (DLM), the direct flight muscles consists in two sets of muscles, which connections are directly from thoracic wall to individual sclerites located at the base of the wings. These two sets of muscles work in tandem, alternating their contractions to move the wing up and down. Their ligament attachments are composed by resilin, a highly elastic material that possesses ~100 times greater energy storage capabilities than the muscle itself [30]. In the indirect flight, two muscles beams (attached to the tergum instead of the wings) constrict the thoracic box that becomes distorted, thus transfer the energy to the wings. When the dorsoventral muscles (DVM) contract the DLM relaxes and when the DLM contract the DVM relaxes [31]. The neural control of such contractions is divided into synchronous and asynchronous muscles; synchronous muscles contracted once for each nerve impulse of the motor neuron and generally occurs in insects that beat their wings < 100 times per second; on the asynchronous muscles, a single nerve impulse causes a muscle fiber to contract multiple times, allowing frequency of wing beats to exceed the rate at which the nervous system can send impulses. Locusts possesses and made use of their anatomically bi-functional muscles to power their wings; such muscles are attached ventrally to proximal leg segments and their contraction could cause limb movements, especially if the wings are stationary, or wing movements, especially if the leg is held in a fixed position [32]. The steering muscles (< 3 % of the power muscle mass) are responsible for the control of the elements forming the hinge mechanism mean everything when it comes to making flight maneuvers.

2.2 WINGS-THORAX ARTICULATIONS: THE AXILLARY APPARATUS

The axillary mechanical components of the flight systems are located at the base of the wings. The blue colored region is known as the first axillary sclerite and forms the horizontal hinge allowing the wings to the flapping movements; the green colored region is known as the second axillary region and is the main mechanical axis for the wings and is responsible for the lagging motions of the wings - front and rear wings

movement; and the red colored region is known as the third axillary sclerite (Y-shaped) and is responsible for the vertical/torsional hinge. This hinge is responsible for a more complicated interactions because it permits also deformable folds; each of these hinges occurs at a vein-fold intersection and the wings motion can consider most part of their motion as a composition of the three hinges rotations: horizontal, vertical and torsional.

2.3 MEMBRANOUS WING: MEMBRANE, VEINS AND VENATION

Each wing is composed by a thin membrane supported by a convex-concave pattern system of veins running along the length of the wing and connected to each other by a variable number of cross-veins; this system enhance the mechanical rigidity of the wing. The form of an individual vein reflects its role in the production of the useful aerodynamic forces by the wing as a whole. On the leading edge of the wing, the longitudinal veins form a rigid spar supporting the wing as it moves through the air. Behind the leading edge, the wings are often longitudinally corrugated, thus providing of longitudinal bending resistance, while the elliptical cross-section of some veins confers further resistance to vertical bending [30]. In some groups, on the anterior margin of the wings appear a pigmented cell known as pterostigma, which mass is frequently greater than that of an equivalent area of adjacent wing and its inertia influences the movement of the whole wing movements. Without the pterostigma, the self-excitating vibrations would set in on the wings after a certain critical speed. According to Norberg [33], pterostigma acts as an inertial regulator of wing pitch. Even though the weight of single pterostigma was only 0.1% of a dragonfly weight, it raised the critical speed by 10-25% in some species.

3 AERODYNAMIC MECHANISMS

3.1 LEADING-EDGE VORTICES, ROTATIONAL LIFT, DELAY STALL & WAKE CAPTURE

Whereas the flow over a gliding wing remain attached to the wing´s surface (at low angles of attack – and becomes stalled at high angles of attack), the flow over a flapping wing typically separates at the leading edge and becomes entrained within a swirling vortex constantly present on the top of the wing; that ubiquitously indicates probably that such separated flow mechanism is the most important of all known mechanisms for the insect´s flight. The dynamics of vortex formation are governed by the adimensional Strouhal Number, which calculated the multiplication of the wingbeat frequency by the peak-to-peak wing tip excursion and divide this product by the air speed. The presence of the leading-edge vortices on top of the wings results in a local reduction in pressure, which causes an upwards-acting suction force known as vortex lift. Most recently smoke visualizations of free-flying bumblebees indicate the presence of independent leading-edge vortices on the root of each wing pair and its influence on the downwash distribution [34]. The aerodynamic forces acting on a wing, are increased as the angle of attack increases; so the expected effect of rotating the wing leading-edge upwards, as in supination, is to increase the aerodynamic forces; thus, rotational lift is created when the insect rotates the angle of attack of its wings, creating vortices; at is completion, such maneuver result in a powerful force propelling the insect forward. By rotating a wing leading-edge upwards delays the onset of stall and thereby extends the production of useful aerodynamics lift to higher angles of attack; such unsteady effect is known as the Kramer effect and may be responsible for the transient lift enhancement observed during the wing rotation in an insect flight. When any object moves quickly through a

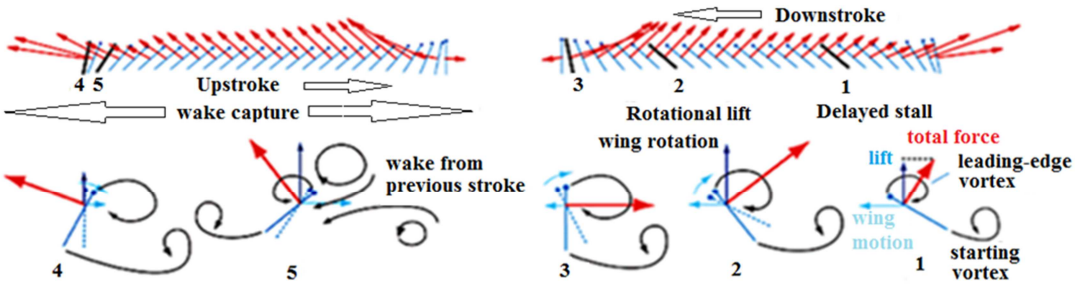

Figure 2: Schematic drawings of the aerodynamic mechanisms of: rotational lift (2), delay stall (1) and wake capture (5).

fluid, vortices are formed. In general these vortices (vortice wake - turbulence left behind the object) represent lost energy, as it takes energy to make them; and most flying insects push off of the vortices that they create, thus recapturing some of the wasted energy and adding power to each of their wingstrokes. A concluding remark of joint analysis of delay stall, rotational lift and wake capture, can infer that a comprehensive theory involving both rotational and translational mechanisms may explain the variety of wing´s patterns displayed by each different species of flying insects, essentially due to the fact that all insects enhanced aerodynamic performances results from the interaction of such three distinct yet interactive aerodynamic mechanisms.

3.2 CLAP AND FLING & CLAP AND PEEL

This kind of mechanism understood as an example of wing-wing interaction is used by some insects for a quick-start lift on the wings; the clap mechanism consists on both wings clapping together above the animal on the upstroke; prior to the dorsal stroke reversal, as the wings come together and join, they carry with them leading edge vortices (LEV) and trailing edge vortices (TEV) and wakes which attenuate each other due to their mutually opposite sense. And as they clap together, they squeeze out a jet of air between them, which the insects can use to augment thrust; and some insects may enhance their maneuverability by redirecting this jet of air [31]. The fling mechanism starts immediately when the wings peeled apart, by forcing the vorticity to start on the wings; air flows around the leading edge of each wing which creates a bound vortex on each wing acting as the starting vortex for the opposite wing which allows a rapid buildup of circulation as well as a handy low-pressure zone above their body (expelling air from between them), with the consequent increase in total lift production (when the wings then separate, air is quickly drawn in to fill the void); and as the wings are flung apart, the lift is immediately generated because the air is already moving in the correct way. The clap and fling mechanism has a variation mechanism - the clap and peel: instead of flinging apart more rigidly the wings peel apart due to fluid-structure interaction between the air and the flexible membrane wings: a peel mechanism with flexible wings might actually serve to augment lift forces relative to the rigid-fling case.

4 PROPERTY TYPE OF FLIGHT STAGES

4.1 HOVERING FLIGHT

Hovering flight is the most power-demanding type of locomotion in animals and is far more expensive than ordinary flapping flight because, relative to the undisturbed air, the

body has no accumulated kinetic energy. Davidovits [36] found that while in hovering flight, during the upwards movement of the insect´s wings, the gravitational force causes the insect to drop and during the downward, such movement produces an upwards force that restore the insect to its previous original position, this meaning a vertical position oscillation generated by the wingbeat frequency of the insect. High-speed video recorded [37] of free hovering flight of the dragonfly *Aeschna juncea* has shown that the animal body was held almost horizontal (~10º head-up) with both fore and hindwings beating at a frequency ~36-40 *Hz* in two almost parallel strokes planes tilted 60º relative to the horizontal. Other studies [38] revealed that the dragonflies hovering flight were performed with a 180º fore to hindwings difference phase (out of phase); angles ranging within 54-100º were used for forward flight and 0º, in-phase for the accelerating or to perform aggressive maneuvers. Dragonflies' often [39] take-off with in-phase flapping (0º) after what the forewings slows and the hindwings speeds up their beat for the normal antiphase (180º) pattern in one or two beats; they rarely flapped in phase for more than 5 or 6 wingbeats at a time, whether as on free or tethered flight; such pattern is used in situations that call for greater than normal force production: take-off, yaw turns and to reverse direction. Several studies confirmed that dragonflies and hoverflies use an inclined stroke plane for their hovering flights and these animals can remain hovering motionless in the air for a long time, a reputation that they compete as best flying hoverers. The stroke amplitude of hoverflies in flight stage range from 65 to 85º; the downstroke angle of attack (~50º) is much larger than the upstroke (~20º), unlike normal-hovering insects, whose downstroke and upstroke angles of attack are not very different. A mathematical model [40] predicted the flight of bumblebees at different speeds, indicate that their flight is unstable while hovering and fly slowly and becomes neutral or weakly stable at medium and high flight speeds, instability mainly caused by sideways wind on the movement of the wings - a "positive roll moment". As the bee flies faster, the wings bend towards the back of the body, reducing the effect of the sideways wind and increasing the stability of its flight. Altshuler *et al* [41], revealed that honeybees can hover at a relatively low strokes amplitude (~90º) and high wingbeat frequency (~230 *Hz*), producing multiple force peaks during each wingbeat. The authors submitted honeybees to air (1.21 kg/m^3) and to heliox (0.41 kg/m^3), which the animals accomplish by raising stroke amplitude (more ~50 degrees) while maintaining constant the wingbeat frequency. Under hover flight conditions, several [42, 43] authors showed numerically that left and right wings interaction (bees and flies) was negligible except during the "clap and fling" motion and several authors [43, 44] showed that the wing/body interaction was also negligibly small (less than 2 %). Ristroph *et al* [45], found that when the fruit flies are hovering or flying slowly, the average angle of their wings is near-vertical, with the wing tilted in opposite directions on the forward and backwards strokes. Inevitably, the drag forces of the air on the wing also push the insect back and forth, but the two cancel each other out. To fly faster, the fruit flies tilted their wings closer to the horizontal on the forward stroke to slice more cleanly through the air and then closer to the vertical on the backward stroke to maximize drag - paddling through the air. Hovering with extra weight - A well-laden honeybee can carry pollen and nectar as much as 80% of its own body weight. According to Feuerbacher *et al* [46], pollen foragers had hovering metabolic rates approximately 10% higher than nectar foragers, regardless of the amount of load carried; however, they found that honeybee foragers are able to carry significant loads without changing wingbeat frequency, stroke amplitude or inclination of stroke plane. Weis-Fogh [47] identified a normal hovering flight displayed by a *Drosophila* fruit fly, however performed on two different wing motion patterns: symmetrical and unsymmetrical; such patterns were in agreement with previous conclusive investigations on the fruit fly hovering flight have shown that the lift varies little with the angle of attack from 20º to 50º; another observation consisted on that the middle and outer wing-

sections produce more than 95 % of the lift and drag; flapping wings creates high force transients during the stroke cycle, even the slightest variation in the wing motion can rapidly alter the orientation of *Drosophila* fly and may lead to a hovering flight immediately followed by saccadic turning maneuvers, where the body of the animal may reach 2,000º s^{-1} within a few wing beats. High-speed videography recorded [48] sequences of individual *Manduca sexta* hawkmoths in free flight over a range of speeds from hovering to 5ms^{-1}; the stroke-plane angle on several individuals ranges between 10-30º and the body angle ranges between 30-40º, both relative to the horizontal plane; the stroke-plane increases as speed increases and indicates values of 50-60º at 5 ms^{-1}, while the body angle decreases as speed increases and indicates values of 15-20 at 5 ms^{-1}. In hovering flight, the trend for stroke amplitude rounded ~115-120º, with this amplitude referring to inner section of the wings; the outer sections peaked at over 150º (angle of more than 20º between inner/outer section of the wings); the wing pronated rapidly at the top of the stroke and a relatively sharp trough of rotation angle was reached early in the downstroke with the outer section at an angle of ~35-45º and the

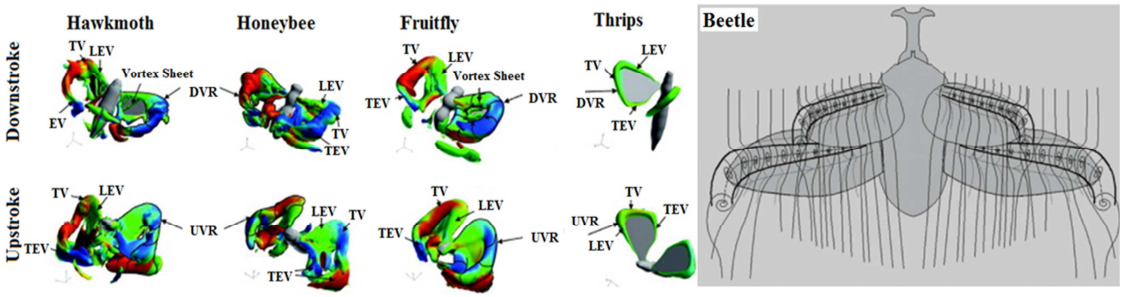

Figure 3: Different patterns of leading-edge vortices on hovering flight conditions: hawkmoth, honeybee, fruit fly and thrips – by integrated numerical framework consisting on the realistic wing-body morphology [52]; and a beetle – by visualization [51].

inner section at approximately ~5-10º steeper. Significant twisting along the wing´s length reappeared in translations phases as the inner section started to rotate in advance of the outer section. The mean angular velocities during the stroke reversals were respectively high as 10,000º s^{-1} for the outer section and > 5,000º s^{-1} for the inner sections of the wings, exposing a very clear difference between those sectors. The results provided a strong support for a decrease in stroke amplitude angle with the increasing of speed to values within $0 \leq ms^{-1} \leq 3$, suggesting that the amplitude is controlled through the minimum wing position. The results revealed also an asymmetry on the duration of downstroke/upstroke ratio (from 1.06 to 2.00 with a mean value of 1.42 - this values were particularly high, but the ratio on insects with asynchronous muscles generally tends to ratio values superior to 1.00). The wingbeat frequencies fell within the range of $24.8 \leq Hz \leq 26.5$ and decreased with the slightly increase of speed; the relationship between speed/wingbeat frequency figures a U-shape graphic, with the lowest frequencies at intermediate speeds. Research [49] on the hovering flight on butterflies, indicates a pattern in most species to maintains the body of ~15º related to the horizontal; normal hovering were observed in many flights and inclined stroke-plane were also observed exceptionally; the stroke amplitude varied in a range within 24º to 90º; the wingbeat frequency within $5.1 \leq Hz \leq 21$; and the mean angular velocity higher value reveals the 145 $rads^{-1}$ obtained by *Papilio rumanzovia*. The upstroke/downstroke relationship indicates an increasing on values, when compared with obtained results for another flight stages and revealed values within 0.8 to 0.92. During hovering flight, the wings of the chalcid wasp *Encarsia Formosa* [48] presents a normal hovering pattern (moved almost horizontally and the body kept almost in vertical); their wingstroke indicates three unusual phases: the clap, the fling and the flip; in the flip, which is a

supination at the beginning of the morphological upstroke, the wings are rapidly twisted through about 180º. Flow visualization on Rhinoceros Beetle (*Trypoxylus dichotomus*) [51] during the hovering flight, indicate the use of a reverse clap and fling mechanism, where the hindwings touch together at the end of the downstroke. During the flapping motion, both elytra and hindwings flap with the same frequency (37-40 *Hz*) however with very different stroke angles (elytra: 34º-38º; hindwings 160º-180º). The non-dimensional upstroke/downstroke ratio indicates ~1. The elytron generated relatively small vertical or horizontal forces, indicating no significant contribution to the aerodynamic force for hovering maintenance. LEVs appear on the hovering flight of the beetle on both elytron and hindwings, with its size constantly enlarged from the beginning to the end of the downstroke movement; the observed LEV on elytron may consequently produce a lift force in forward flight; such wings may have not the exclusive purpose of protecting the hindwings. A recent numerical research on Reynolds effects on several realistic wing-body morphology insects hovering aerodynamics - hawkmoth, honeybee, fruit fly and thrips - indicate an overview of scaling effects on vortex dynamics and wake structures. The hawkmoth model is based on the experimental data of an hovering flight of *Manduca sexta*, with a body angle of 39.8º, stroke angle of 15º relative to the horizontal, amplitude stroke of 114.6º and wingbeat frequency of 26.1 *Hz* – *Re* ~6,300 (hawkmoth hovering flight ↔ 4,000 ≤ *Re* ≤ 8,000). The honeybee model is based on the experimental data of an hovering flight of *Apis mellifera*, with a body angle of 45.0º, stroke angle of 0º relative to the horizontal, amplitude stroke of 90.5º and wingbeat frequency of 229.8 *Hz* – *Re* ~1,123 (honeybee hovering flight ↔ 1,000 ≤ Re ≤ 2,000). The fruit fly model is based on the experimental data of an hovering flight of *Drosophila melanogaster*, with a body angle of 45.0º, stroke angle of 0º relative to the horizontal, amplitude stroke of 139.8º and wingbeat frequency of 200 *Hz* – *Re* ~134 (fruit fly hovering flight ↔ 100 ≤ *Re* ≤ 500). The thrips wing-body model is based *Franklinella intonsa*; due to the lack of experimental data of an hovering flight on thrips, all of their kinematics observed were similar to the flapping of a small insect, like fruit fly: body angle of 45.0º, stroke angle of 0º relative to the horizontal, amplitude stroke of 139.8º and wingbeat frequency of 200 *Hz* – *Re* ~12 (thrips hovering flight ↔ 5 ≤ Re ≤ 20). All models are based on rigid wings. The results revealed how the leading-edge vortices (LEV) is related to the trailing-edge vortices (TEV) and the tip vortex (TV) as well as to a downstroke and upstroke vortex ring (DVR, UVR) and pointed to the importance of the vortex ring in stabilizing the LEV and hence in enhancing the force-generation [52]. Transitions from hovering to slow speed flight indicates [53]. on few changes: the horizontal forward or backward flight is achieved with a change in the mean stroke angle; the vertical climb or decent is achieved with stroke a change amplitude or an equal change in the down- and upstroke angles of attack, *i.e.*, a proper combination of mean stroke angle and stroke amplitude controls can give a flight of any (small) speed in any desired direction.

4.2 FLIGHT TURNS (SLOW, FAST AND SACCADES)

Observations [35] on turns sequences in dragonflies revealed two distinct types of turns, namelly the conventional (accomplished with roll - banking, analogous to a turning airplane) and the yaw (accomplished without roll); yaw turns were extremely fast (in free flight - 90º in 2 wingbeats and 180º in less than 3 wingbeats; in tethered flight - 90º in 4-6 strokes). In a conventional turn in order to roll into a bank, dragonflies produce unbalanced forces on one their sides, *i.e.*, left-right asymmetries in the wing stroke angle and consequently on the angle of attack; in sequences of conventional turns, one or both pairs of wings revealed left-right asymmetries in the stroke angle, being the

lower amplitude verified on the wings inside of the turn (inner wings) and in several cases with a clearly higher angle verified on the wings outsider the turn (outer wings). Dragonflies may change the inner and/or the outer wings on one or both sides, as well as the fore- and hindwings strokes can be changed to different degrees; in a moment, each one of the all four wings could present a different stroke angle. And once the desired bank angle is established, the animal return to its previous normal stroke pattern, some like as airplanes controls. The yaw kind of turning maneuver is initiate with forewings having similar amplitude and the fore- and hindwings not in phase, but reaching the in-phase almost immediately; at that time, the forewings begins to diverge their amplitudes: the outer wing reaching much larger amplitudes, presenting extreme swings of the forewings angle of attack, caused by the outer wing peak during the downstroke and the inner wing higher on the upstroke with a peak at the top of one stroke. Initially, the inner hindwings presented a higher vertical amplitude component that became similar when the fore- and hindwings reached the in-phase; posteriorly, the hindwings angles of attack increased during the turn and revealed no consistent patterns of asymmetry. As result, the first stroke revealed a strong asymmetry in horizontal stroke angle and yaw the insect ~10º; during the second upstroke the outer wing moved with much higher horizontal amplitude and the insect yawed its body ~15º. Dragonflies may also turn while gliding by the exclusive change on the angle of attack. The chosed turn is adjusted to fit the requirements and circumstances each time it is performed. Locusts could use differential changes in wing profile (camber) as a way to produce unbalanced lift and thus initiate a turn. Fruit flies can often fly via straight sequences of movement interspersed by rapid turns called *saccades* (also known as collision avoidance maneuvers), characterized by a rapid rotation of the body about the yaw axis (sharp and right angles turns). The fly starts the *saccade* with a path velocity (~0.19 ms^{-1}) and slows down to (~0.08 ms^{-1}) as it changes heading, and then accelerates forward at the end of the turn. The *saccade* is generated by two specific and remarkably subtle changes in wing motion strongly correlated with the yaw torque: a backward tilt of the stroke plane, that elevates flight force during the upstroke by increasing the aerodynamic angle of attack; and an increase in stroke amplitude that further augments force by elevating wing velocity, i.e. by inducing differences between the amplitude of the left and right wings of about 5º and shifting the stroke plane by ~2º. At the onset of a *saccade* the outside wing undergo these changes, thereby creating torque to rotate the

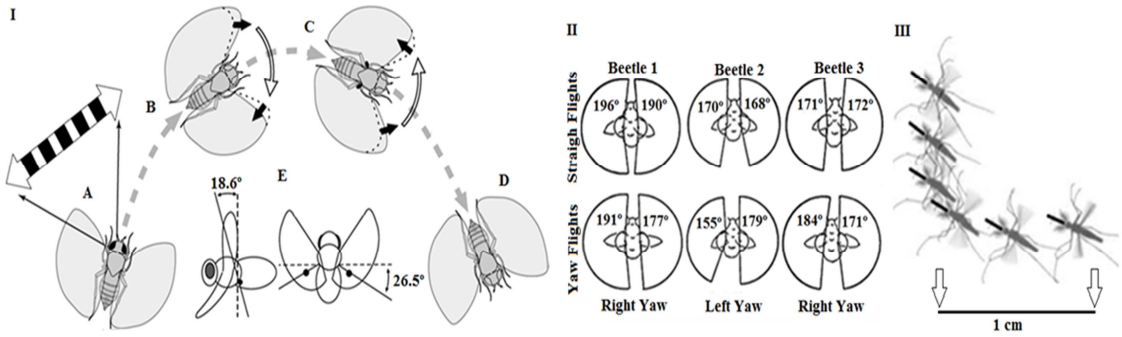

Figure 4: I) Saccade summary [67]: A) The visual expansion triggers the saccade; B) the insect produce small changes wingstroke changes; C) the halteres detect rotation and triggers counter-turn; D) the fly continues on new heading. - E) Detail of the angular orientation of the halteres stroke plane; II) Comparison of the horizontal amplitude wingstrokes on the straight flights and on the yawing turns on beetles [65]; and III) Snapshots of a mosquito turning maneuver at 30 ms intervals ~25 wingbeats; a rapid change in flight direction while the insect's heading evolves much more slowly and does not

body at the start of the turn; after about ~20 ms the inside wing exhibits similar changes, thereby generating counter-torque to terminate the *saccade*. A fly can change direction by 90º in less than 50 ms [21]. The maximal angular velocity [54] during a *saccade* turning is independent of the forward velocity of the fruit fly and is approximately 1,600º s^{-1}, while their continuous smoothly turns are well below 1,000º s^{-1}; such profile depends critically on at least three factors: time course of yaw torque, the moments of body inertia and the frictional damping on body and wing. *Drosophila* can perform a saccade during a vertical ascent. By increasing and decreasing the amount of haltere-mediated feedback (by increasing the haltere endknob mass on some flies and by ablated one haletere in others) decreases and increases *saccade* amplitude respectively [55]. During flight the halteres oscillate vertically (with a stroke angle ~180º) in antiphase with the wings; the haltere´s rotating mass tends to conserve its angular momentum and to oppose any change of its plane of oscillation. Halteres most important roles is to provide rapid feedback to wing-steering muscles to stabilize aerodynamic force moments and also to stabilize the head during flight, thus acting as a balancing and guiding system, helping these insects to perform their fast maneuvers. Beyond *saccades* [56], the repertoire of the horse-fly *Hybomitra hinei* has been recorded using a modified form of Immelmann turn (half-loop followed by half-roll) in rapid reversals of flight direction. Despite the lack of halteres, the flight behaviour of hoverflies repertoire (*Eristalis tenax*: mass ~100/125 mg) and honeybees (*Apis mellifera*, worker, mass ~90/100 mg) includes also saccades; both species flew in a 40x40x40 cage. Independent of vertical motion, the hoverfly is able to fly sideways and backwards and can perform saccadic-like turns; its head starts to perform the saccade ~10 ms later than the thorax and ends earlier and between the saccades typical interval (~200-300 ms) head and thorax are held stable; overall, the head mostly follows the thorax motion. Honeybees can also perform sideways and backwards flights with interspected hovering periods lasting ~200 ms once or twice a second (between 220-500 and 1,540-1,760 ms); they can also perform U-turns with no truly saccadic-like behaviour: the head shows saccade-like motion in the yaw direction every ~200 ms [57]; from 0 to 540 ms, the hoverflies performed a 360º sideway, circling and climbing flight followed by backward flight; the 540 to 840 ms interval show a leveled backward and sideway flight; from 840 to 1,040 ms show a descendent sideway flight with posterior new climbing. Stroboscopic photographs of tethered beetles executing yaw directional change revealed that such maneuvers were mainly achieved by a unilateral increase or decrease of the horizontal amplitude of the wingstrokes, essentially due to the increase or decrease on the frequency of the nervous input to all fibrillar flight muscles of the appropriate side; in forward flight, when the maximum horizontal wingstrokes amplitude is applied, the animal (beetle 1) in order to made a turn, reduces that angle on both sides, with a higher reduction applied on its inner wing (desired turn direction); while flying at a submaximal horizontal wingstrokes amplitude, the animal (beetle 2) increases the outer wing and decreases the inner wing horizontal amplitudes, or decreases the outer wing and maintain the inner wing (beetle 3) [58]. High speed video observations [59]; revealed that free flight of the "*Aedes aegypti*" mosquito reached a wingbeat frequency of ~850 *Hz*, with an unusual short and quick wingstrokes, subtending just 45º with their wings on each half stroke, compared with the -120º for the fruit fly. All freely initiate maneuvers videotaped a course of 4,000 wingbeats of flight data; authors observed sideslip based turns that envolved abrupt changes in flight direction; turns envolving large changes on body orientation and gradual U-turns. A frequently used pattern of flight on these turns revealed an unaligned body orientation related to the flight direction, exposing that sideways acceleration plays an important

role on part of their flight repertoire - mosquito flight direction changes more frequently and much more quickly than does body heading. These turning maneuvers, in which the flight direction of the insect changes by 50º up to 200º, involve a combination of deceleration along the direction aligned with the body axis and acceleration in a sideways direction. A mosquito can fly continuosly for up to twenty-four hours and are known to travel 150 km or more in nature [60].

4.3 GLIDING FLIGHT

Some insects possess the ability to glide and so far, they revealed three kinds of gliding flight: on the free gliding, an insect simply stops stroking its wings and glides slowly down for a few seconds; on the updraft gliding at hill crests, the insect adjusts its wing positioning to float in the air without the need to beat its wings; and gliding in towed females, where a female in the wheel position holds her wings out and glides while the male provides the motive force. Detailed investigations [61, 62, 63] has been made for the dragonfly remarkable gliding capability; very different wings from dragonflies species and in spite of this, when they are tested in similar conditions (*Re* = 7,000; angle of attack 5º) the results presents small differences in flow patterns and vortex trains generation process; the corrugation wings structures (as they possess very noticeable corrugation over the first quarter-chord) and cruciform configuration allow that air circulates in the cavities between pleats creating areas of very low drag that aid the lift-generating airflow across the wing. Such corrugated wings during acceleration do not change the form of the outer flow and revealed good stability in unsteady wind conditions, providing superior flying characteristics for MAVs fixed wings in low Re flight, enabling a continued stable flight at low Re. In addition, dragonfly configuration has additional merit in its compatibility with propellers or high lift devices; a combination that may suggest MAVs with much broader flight envelope and could provide simple solutions for Earth atmosphere and living things observation, as well as for a candidate for flight in the Mars atmosphere. *Megaloprepus coerulatus* can glide without any impulse from the wings for more than 20 meters at an angle of attack of 10º and with velocities up to 74 cm^{-1}, corresponding to a gliding ratio of 1:6, similar to that of some birds [64].

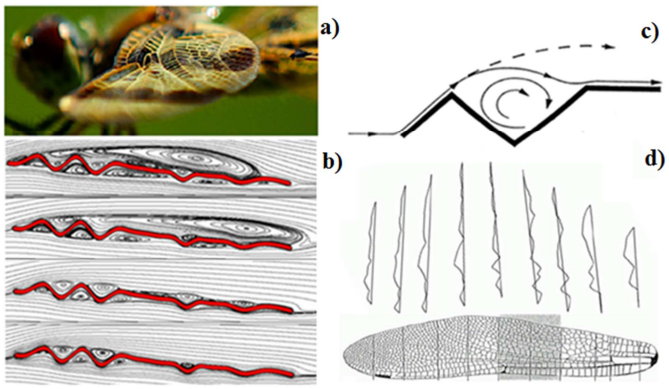

Figure 5: a, b) Dragonfly wing and several cross-sections revealing different corrugation patterns; right, top: pleated airfoil with 5º angle of attack and Re = 10,000, 5,000, 1,000 and 500 (respectively from top to bottom), where the flow looks as if it pertains to the airfoils; c): detail of a recirculation zone in a valley of the wing [64]; d) different corrugations along the wing.

4.4 SIDEWAYS FLIGHT AND SUDDEN ACCELERATION-DECELERATION

Drosophila melanogaster (fruit fly) feature the ability to generate sideways forces during some maneuvers on which they apply strong lateral acceleration associated with differences between the left and right wing angles of attack; such asymmetry can be induced by simply altering the relative timing of flips between the right and left wings -

fruit flies can employ timing differences as high as 10% of a wing beat period while accelerating sideways at 40% of gravitational acceleration. The sideway force is obtained by asymmetric rotation (flip) of both wings at the same time. During sideway flight, each snapshot reveal the areas of the right and left wings: small wing area means the wing meets the air at a high angle of attack and thus generates large drag forces; large area means the wing is cutting through the air at low angle attack and thus feels small drag. This difference in the angle of attack between wings generate asymmetric drag forces that causes sideway flight; the unbalanced drag points to the left because the wings flap in large-amplitude arcs [64]. Observations on the hoverfly *Syritta pipiens* [14] indicate the ability to perform sideways without changing its heading; such maneuver suggests that those animals possess independent control of roll and yaw, verified on research on the blowfly *Calliphora erythrocephala* flight, where roll and yaw often followed different time courses. Dragonflies and Damselflies are capable of fast flights and great acceleration and deceleration and can execute extremely rapid maneuvers in a very limited space. Experiences [65] on more than 20 species with different sizes (the wingbeat frequency is size-dependent and in all species vary between 4.7/59.5 *Hz*) the take-off acceleration (from 0 to 0,1 s) revealed the highest value of 25 ms^{-2} (*Sympetrum danae*); the highest acceleration from 01 to 0.2 s of flight revealed a value of 10 ms^{-2} (*Aeshna cyanea*); and the highest speed recorded in flight is 1,000 cms^{-1} (*Aeshna cyanea*). The highest flight distance / wingbeat are 25 cm (*Aeshna cyanea*). The maximal acceleration obtained in all flights is 36.5 ms^{-2} (*Orthetrum cancellatum*). Some can fly at speeds up to 54 km/h [39]. The body shape of dragonflies probably reflects a selection by requirements of rapid flight: four-wings with large áreas when compared to the body; large rounded eyes for a 360º visual acuity and an elongated abdomen for passive flight stability. During flight maneuvers involved marking acceleration, *Orthetrum cancellarum* increase the stroke amplitude from ~80-90º while hovering, to a 130º during vertical take-off from the water. *Leucorrhina rubicunda* pointed to 90º stroke amplitude while hovering to 150º during vertical take-off with a female in mating position. *Calopteryx splendens* and *Calopteryx virgo* indicate a noteworthy ability flight pattern: these dragonflies can fold their wings together over the abdomen after every or several wingbeats and hold them still, gliding like songbirds in ballistic flight, travelling relatively large distances per wingbeat. *Lestes viridis* during a simultaneous fore- and hindwings downstroke, increased the flight velocity by as much as 40%; this acceleration could be also managed in the upstroke, depending as larger the part of cycle in which wings beat in parallel - evidently extremely effective. By employing large angles of attack during the upstroke, the wings generated mainly thrust and the less steeply angled wings during the downstroke generated mainly lift. Large angles of attack were observed (57-75º) during a stroke away from the flight direction, and small (10-35º) during a stroke in the flight direction. In slow forward flight, the upstroke/downstroke ratio indicates 1/1.2 and in fast forward flight, the ratio indicates 1/1.9, with shorter upstroke. *Megaloprepus coerulatus* on a descended forward flight carrying a female on mating position reached an extremely short upstroke course time (upstroke/downstroke ratio 1/3). The upstroke/downstroke ratio of fore- and hindwings may also vary: in hovering and slow forward flight, the upstroke in hindwings indicate ~10% shorter than that of forewings (*Aeshna cyanea*, *Anax imperator* and *Calopteryx splendens*); ~35% shorter in *Lestes viridis*. The *Poecilobothrus nobilitatus* male fly, during his courtship behaviour perform a complex and notorious aerial performance: a D-shaped flight [66]: two arcs and one straight flight ; the display flight is initiate with a pair of rather flattened 180º arcs around the female (the male finish this pattern of flight where he began); then the fly perform a directly flight over the female, with an extremely fast (40ms) spin halfway (180º) which leaves the male flying backwards (completing the maneuver by decelerating backwards to a hovering stop. During these flights, the forward velocity

reaches 0.6 ms^{-1}; the acceleration 12 ms^{-2} (1.2 g); the angular velocity 4,500 ms^{-1} and the corresponding angular acceleration is at least 225,000 ms^{-2}; during such display, the inner wing is held out literally as an air-brake and the fly pivots around like a rower round as an oar. Previous results have shown that fruit flies mainly control force and moments by changing stroke amplitude of the two wings [67, pp.234]. The hoverfly *Syritta pipiens L.*, revealed four different sideway flights excerpts: angular orientation saccadic change without a change on the course direction; change of course direction resulting exclusively from an angular orientation change; change of course orientation resulting from sideway velocity increase and forward velocity decrease; and also a mixture of the two last flight excerpts. The fastest tracking flights made by hoverflies - rapes - culminates in a rapid dart towards another hoverfly: in a rape, the male very frequently display a continuosly acceleration (~500 cms^{-2}) and turning sideways (normally ~90º) before it lands; during the same rape, the forward acceleration is practically uniform and the sideways movements present much more variations.

4.5 BACKWARD FLIGHT

Changes [68] in the angle of attack have been observed to initiate low speed forward or backward flight acceleration; insects increase the angle of attack to a large upstroke or downstroke values and use the increased drag to initiate acceleration. The angles of attack on the drag-producing half-stroke often approach 90º and provide large horizontal acceleration. This "*paddling/rowing*" motion also rotates the body (and the stroke plane) in the correct direction because the drag force is applied above the centre of mass. As the stroke plane tilts, the increased drag would detract from weight support, and the insects revert to more normal angles of attack after only one or two wingbeats. The capacity of an insect to perform backwards flight it may be not displayed frequently, or if it is, it may very rapidly, lasting for several miliseconds, such as happens in the case of the Hoverfly *Syritta pipiens*; the hoverfly displayed a crusing flight (3s of flight with observed position every 20 ms) in which changed the angular position in a *saccade* performance, during which can fly forward, sideways and backward [14]. A 180º horizontal backward flight is reported to *Calopteryx splendens* (Zygoptera); the measured velocities of the wingtips in forward and backward flight on this insect were 180-310 cms^{-1}. A point halfway along the wing will move over half the distance and hence will have half that velocity, *i.e.*, 90-155 cms^{-1}. *Mercitogaster ornata* (Zygoptera) can change its wingbeat frequency from 15 *Hz* immediately after take-off to 20 *Hz* during rapid backward flight, and then to 15 and 13-5 *Hz* while hovering. *Lestes viridis* (Zygoptera), in tandem position beat its wings at 28,7 *Hz* during downward flight, compared with up to 35 *Hz* during straight forward flight and up to 37,5 *Hz* when flying steeply upwards and backwards. By employing a flight with parallel stroking (phase shifted by no more than 30º), *Mercitogaster ornata* is able to perform rapid backward flight and *Anisoptera* presented flight abilities requiring great force (rapid acceleration - backward upwards flight or carrying a female) in the range from straight up to horizontally backward flight, such flights in velocity conditions within 40 to 120 cms^{-1} and presenting mean and maximal acceleration values of 7 and 33.7 ms^{-1}, respectively. *Orthetrum cancellatum* displays a vertical backward take-off (flight direction approx. 100º) in parallel-stroking mode. A male *Calopteryx splendens* that had been slowly approaching a female in a counterstroking courting flight, advancing at a rate of 12,4 mm per wingbeat, can propel himself 46,5 mm backwards by only one parallel wingbeat. During take-off backward, *Megaloprepus coerulatus* (Zygoptera) the first forward stroke was executed with the wings at a steep angle (measured in the midregion of the downstroke), whereas in the first backward stroke the angle of attack was small; during the subsequent transition to straight forward flight, the wings were

inclined at small angles in the middle of the forward stroke and at large angles during the backward stroke [66].

4.6 FLIGHT ON COMPLEX WEATHER CONDITIONS

Free-flying mosquitoes not only can survive the high-impact of falling raindrops [69], as regardless of impact type (glancing – rotate the insect; direct – impact on insect body, pushing the animal for a considerable distance), they can recover quickly and resume flight. A raindrop could have a mass of 50 mosquitoes and a diameter < 8 mm, presenting falling velocities of ~5-9 ms^{-1}; a generic mosquito has a mass of ~0.002 g and their velocity could be up to ~1 ms^{-1}. Mosquitoes possess hairy wings; such hair, increase the wing surface area and so its energetic cost of wetting – the hair contributes a hydrophobic wings; low simply drops simply bounce off the insect. The mass of the insect determines the acceleration and speed after the impact; firstly mosquitoes survive by using their low mass relative to raindrops; due to differences of mosquito/drop mass, the mosquitoes slow raindrops by only ~1-17%; because of the impact, mosquitoes are accelerated by 30-300 G for 1 ms. The impact of 9 ms^{-1} accelerates the mosquito to a velocity of 2.1 ms^{-1} within duration of 1.5 ms; after tumbling a distance of 39 mm (13 body lengths) the mosquito separates laterally from the drop and land safely. The glancing impacts cause a pitch, yaw, or roll to insect depending on the impact point; the insect tends to recover its original position in 0.01 s.

4.7 LONGITUDINAL AND LATERAL CONTROL USING POSTURAL CHANGES

In addition to varying the wing kinematics, several insects could manage their longitudinal and lateral flight control by deflecting their own body while in-flight. *Drosophila melanogaster* could elevate their abdomen in response to nose-down disturbances, thus displacing the centre of gravity dorsal to the line of thrust, which therefore generates a restoring nose-up moment with the inertia of the fly´s body. Other similar postural changes have been observed in *Calliphora erythrocephala*. *Drosophila virilis* have also been observed to elevate their hindlegs following a nose-down disturbance, which should increase drag dorsally and generate a nose-up pitching moment; such hindlegs movement could have interference from the wake of the wings, and so enhance the fly´s turning effect. Locusts appear to regulate lift independent of thrust and have also been claimed to exhibit a “constant-lift reaction” in which the vertical component of the force is kept more or less constant following by imposed changes of body angle of up 20º. Related to lateral control using postural changes, such *Calliphora erythrocephala* and *Drosophila melanogaster* could manage a delayed supination on the inside wing and advanced supination on the outside wing have been observed during fictive turns. Lateral movements of hindlegs and abdomen have also been observed in response to visual roll stimuli in locusts (*Orthoptera*). Similar postural adjustments appear to be ubiquitous steering responses in insects and have been reported in mantids, heteropteran bugs, Strepsipterans, and moths [70].

5 CONCLUSIONS

The behavioral flight capacitance and ability of insects in flight in recent years, has been an active research that provided inspiration on their maneuverability and agile flight, for the design and control of man-made MAVs and NAVs, essentially by identifying and exploiting the basic principles of performance in-flight displayed by the insects. The

current investigation focus is on the achieving of a greater perception of flight performances held by several types of insects on displaying their abilities on flight maneuvers on resemblat flight stages; thus regarding to a bio inspired flapping wings robustness for MAVs and/or NAVs applications.

ACKNOWLEDGEMENTS

The authors express their gratitude to FCT for the funding of the research project: PTDC/EME-MFE/122849/2010: Nature – New-biomimetic Aerodynamic Technologies for Undersized Reynolds.

REFERENCES

[1] Nguyen, Q-V. Park, H. C., Goo, N. S., Byun D., Aerodynamic force generation of an insect-inspired flapper actuated by a compressed unimorph actuator, *Chinese Science Bulletin,* Vol. 54, No. 16, pp. 2871-2879, 2009.

[2] McMichael, J. M., Francis, M. S., Micro Air Vehicles - Toward a New Dimension in Flight, http://www.fas.org/irp/program/collect/docs/mav_auvsi.htm [cited 21.05.2014].

[3] Petricca, L, Ohlckers, P., Grinde, C., Micro- and Nano-Air Vehicles: State of the Art, *International Journal of Aerospace Engineering*, Vol. 2011, Article ID 214549, 17 pages.

[4] Hylton, T., Martin, C., Tun, R., Castelli, V., The DARPA Nano Air Vehicle Program, 50th AIAA Aerospace Sciences Meeting Including the New Horizons Forum and Aerospace Exposition, 09-12 January 2012, Nashville, Tennessee, USA.

[5] Borelli, G. A., *De Motu Animalium*, Rome: A. Bernabo, 1680.

[6] Lilienthal, O., *Der Vogelflug als Grundlage der Fliegekunst. Ein Beitrag zur Systematik der Flugtechnik*, Berlin, 1889.

[7] Marey, E-J., *Physiologie du Mouvement: Le Vol des Oiseaux,* G. Masson, Éditeur, Libraire de L'Academie de Médicine, 1890.

[8] Marey, E-J., Flight of Winged Animals, *Harper's New Monthly magazine*, Volume 41, Issue 245, Oct., 1870.

[9] Marey, E-J., Flight of Birds and Insects, Harper's *New Monthly magazine*, Volume 41, Issue 246, Nov., 1870.

[10] Marey, E-J., Marey's Apparatus for Recording the Flight of Birds, *Harper's New Monthly magazine,* Volume 43, Issue 255, Aug., 1871.

[11] Marey, E-J., The Velocity of Insects' Wings during Flight, *Scientific American, New Series*, Volume 20, Issue 16, Apr. 17, pp. 241-256, 1869.

[12] Pettigrew, J. B., *Animal Locomotion or Walking, Swimming and Flying with a Dissertation on Aeronautics,* 2nd Edition, Henry S. King & Co., London, 1874.

[13] Jensen, M., Biology and Physics of Locust Flight. III. The Aerodynamics of Locust Flight, *Philosophical Transactions, R. Soc. London,* B, Vol. 239 no. 667, pp. 511-552, 1956.

[14] Collett, T. S., Land, M. F., Visual control of flight behaviour in the hoverfly Syritta pipiens, *Journal of Comparative Physiology*, Volume 99, No. 1, pp 1-66, 1975.

[15] Ellington, C. P., The Aerodynamics of Hovering Insect Flight, *Philosophical Transactions of the Royal Society of London,* Series B, Biological Sciences, Vol. 305, pp. 1-181, 1984.

[16] Ellington, C. P., The Aerodynamics of Hovering Insect Flight. VI. Lift and Power, *Philosophical Transactions of the Royal Society of London*, Series B, Biological Sciences, Vol. 305, No.1122, pp. 145-181, 1984.
[17] Ennos, A. R., The kinematics and aerodynamics of the free flight of some Diptera, *Journal of Experimental Biology*, Cambridge, Vol. 142, pp. 49-85, 1989.
[18] Dudley, R., Biomechanics of flight in neotropical butterflies: morphometrics and kinematics, *Journal of Experimental Biology*, Cambridge, Vol. 150, pp. 37-53, 1990.
[19] Dudley, R., Biomechanics of flight in Neotropical butterflies: aerodynamics and mechanical power requirements", *Journal of Experimental Biology*, Vol. 159, pp. 335–357, 1991.
[20] Dudley, R., Ellington, C. P., Mechanics of forward flight in bumblebees. II. Quasi-steady lift and power requirements, *Journal of Experimental Biology*, Cambridge, Vol. 148, pp. 53-88, 1990.
[21] Fry, S. N., Sayaman, R., Dickinson, M. H., The aerodynamics of free-flight maneuvers in Drosophila, *Science*, Vol. 300, pp. 495-498, 2003.
[22] Fry, S. N., Sayaman, R., Dickinson, M. H., The aerodynamics of hovering flight in Drosophila, *Journal of Experimental Biology*, Vol. 208, pp. 2303-2318, 2005.
[23] Hedrick, T. L., Software techniques for two- and three-dimensional kinematic measurements of Biological and biomimetic systems, *Bioinspiration Biomimetics*, Vol. 3, 034001, 6 pages, 2008.
[24] Ramamurti, R., Sandberg, W. C**.,** A three-dimensional computational study of the aerodynamic mechanisms of insect flight, *Journal of Experimental Biology*, Vol. *205*, pp. *1507*-1518, 2002.
[25] Sun, M., Xiong, Y., Dynamic flight stability of a hovering bumblebee, *Journal of Experimental Biology*, Vol. 208, pp. 447-459, 2005.
[26] Dickinson, M. H., Lehmann, F-O., Sane, S, P., Wing Rotation and the Aerodynamic Basis of Insect Flight, *Science*, Vol. 284, pp. 1954-1960, 1999.
[27] Sane, S. P., Dickinson, M. H., The control of flight force by a flapping wing: lift and drag production, *Journal of Experimental Biology*, Vol. 204, pp. 2607-2626, 2001.
[28] Tanaka, H., Whitney, J. P., Wood, R. J., Effect of Flexural and Torsional Wing Flexibility on Lift Generation in Hoverfly Flight, *Integrative and Comparative Biology*, Vol. 51, No. 1, pp. 142-150, 2011.
[29] Ang, H-S., Xiao, T-H., Duan, W-B., Flight Mechanism and Design of Biomimetic Micro Air Vehicles, *Science in China Series E: Technological Sciences*, Vol. 52. No. 12, pp. 3722-3728, 2009.
[30] Knospe, C. R., Insect Flight Mechanisms: Anatomy and Kinematics, Mechanical and Aerospace Engineering, University of Virginia, 1988.
[31] Chapman, R. F., *The Insects, Structure and Function*, 5th Edition, Cambridge University Press 2013, pp, 194-232, ISBN 978-0-521-11389-2
[32] Wilson, D. M., Bifunctional Muscles in the Thorax of Grasshoppers, *Journal of Experimental Biology*, Vol. 39, pp. 669-677, 1962
[33] Norberg, R. A., The Pterostigma of Insect Wings an Inertial Regulator of Wing Pitch, *Journal of Comparative Physiology A*: Neuroethology, Sensory, Neural, and Behavioral Physiology, Vol. 81, No. 1 pp. 9-22, 1972, DOI:10.1007/BF00693547
[34] Bomphrey, R. J., Taylor, G. K., Thomas, A. L. R., Smoke visualization of free-flying bumblebees indicates independent leading-edge vortices on each wing pair, DOI: 10.1007/s00348-009-0631-8, *Experiments on Fluids*, Vol. 46, pp. 811-821, 2009.

[35] Sane, S. P., Steady or Unsteady? Uncovering the Aerodynamic Mechanisms of Insect Flight, DOI: 10.1242/jeb.048330, *Journal of Experimental Biology*, Vol. 214, pp. 349-351, 2011.
[36] Davidovits, P., *Physics in Biology and Medicine*, 3rd Edition, ISBN-13:978-0-12-369411-9, Printed in USA, Complementary Science Series, Elsevier, 2008.
[37] Norberg, R. A., Hovering flight of the Dragonfly Aeschna juncea L.: kinematics and aerodynamics. In *Swimming and Flying in Nature*, Vol. 2, (eds T. Y.-T. Wu, C. J. Brokaw & C. Brennen), pp. 763-781, New York, Plenum Press, 1975.
[38] Deng, X., Hu, Z., Wing-Wing Interaction in Dragonfly flight, *The Neuromorphic Engineer*, 10.2417/1200811.1269, http://www.ine-news.org/pdf/1269/1269.pdf [cited 26.07.2014]
[39] Alexander, D. E., Unusual Phase Relationships Between the Forewings and Hindwings in Flying Dragonflies, *Journal of Experimental Biology*, Vol. 109, pp 379-383, 1984.
[40] Xu, N., Sun, M., Lateral dynamic flight stability of a model bumblebee in hovering and forward flight, DOI: 10.1016/j.jtbi.2012.11.033, *Journal of Theoretical Biology*, Vol. 319, pp. 102-115, 2013.
[41] Altshuler, D. L., Dickson, W. B., Vance, J. T., Roberts, S. P., Dickinson, M. H., Short-amplitude high-frequency wingstrokes determine the aerodynamics of the honeybee flight, Proceedings of the National Academy of Sciences of the United States of America, Vol. 102, nº 50, pp. 18213-18218, December 13, 2005, DOI: 10.1073/pnas.0506590102
[42] Sun, M., Yu, X., Aerodynamic force generation in hovering flight in a tiny insect, *AIAA Journal*, Vol. 44, nº. 7, pp. 1532-1540, July 2006
[43] Yu, X., Sun, M., A computational Study of the wing-wing and wing-body interactions of a model insect, *Acta Mechanica Sinica*, Vol. 25, nº 4, pp. 421-431, 2009.
[44] Aono, H., Liang, F., Hao, Liu, H., Near- and far-field aerodynamics in insect hovering flight: an integrated computational study, doi: 10.1242/jeb.008649, *Journal of Experimental Biology*, Vol. 211, pp. 239-257, 2007.
[45] Ristroph L., Bergou, A. J., Guckenheimer, J., Wang, Z. J., Cohen, I., Paddling Mode of Forward Flight in Insects, *Phys. Rev. Lett.* 106, 178103, 2011.
[46] Feuerbacher, E., Fewell, J. H., Roberts, S. P., Elizabeth F. Smith, E. F., Jon F. Harrison , J. F., Effects of load type (pollen or nectar) and load mass on hovering metabolic rate and mechanical power output in the honey bee Apis mellifera, doi: 10.1242/jeb.00347, *Journal of Experimental Biology*, Vol. 206, 1855-1865, 2003.
[47] Weis-Fogh, T., Quick Estimates of Flight Fitness in Hovering Animals, Including Novel Mechanisms for Lift Production, *Journal of Experimental Biology*, Vol. 59, pp. 169-230, 1973.
[48] Willmott, A. P., Ellington, C. P., The Mechanics of the Flight in the Hawkmoth Manduca sexta, I. Kinematics of the Hovering and Forward Flight, *Journal of Experimental Biology*, Vol. 200, pp. 2705-2722, 1997
[49] Betts, C. R., Wootton, R. J., Wing Shape and Flight Behaviour in Butterflies (Lepidoptera; Papilionoidea and Hesperioidea): A Preliminary Analysis, *Journal of Experimental Biology*, Vol. 138, pp. 271-288, 1988.
[50] Grodnitsky, D. L., Dudley, R., Gilbert, L., Wing Decoupling in Hovering Flight of Swallowtail Butterflies (Lepidoptera: Papilionidae), *Tropical Lepidoptera*, Vol. 5, nº 2, pp. 85-86, 1994.
[51] Truong, T. V., Le, T. Q., Tran, H. T., Park, H. C., Yoon, K. J., Byun, D., Flow Visualization of Rhinoceros Beetle (Trypoxylus dichotomus) in Free Flight, *Journal of Bionic Engineering*, Vol. 9, pp. 304,314, 2012.
[52] Aono, H., Liu, H., Flapping wing aerodynamics of a Numerical Biological flyer model in hovering flight, *Computers & Fluids*, Vol. 85, pp. 85-92, 2013.

[53] Wu, J., Sun, M., Control for going from hovering to small speed flight of a model insect, *Acta Mechanica Sinica*, DOI 10.1007/s10409-009-0241-y, Vol. 25, pp. 295-302, 2009.

[54] Floreano, D., Zufferey, J-C., Srinivasan, M. V., Ellington, C., (Eds.*): Flying Insects and Robots*, Springer-Verlag Berlin Heidelberg 2009, ISBN: 978-3-540-89392-9, DOI 10.1007/978-3-540-89393-6, pp. 232

[55] Bender, J. A., Dickinson, M. H., A comparison of visual and haltere-mediated feedback in the control of body saccades in Drosophila melanogaster, *Journal of Experimental Biology*, Vol. 209, pp. 4597-4606, 2006.

[56] Wilkerson, R.C., Butler, J. F., The Immelmann turn, a pursuit maneuver used by hovering male Hybomitra hinei wrighti (Diptera: Tabanidae), *Annals of the Entomological Society of America*, Vol. 77, nº. 3, pp. 293-295, 1984.

[57] Stavenga, D. G., Hateren, J. H. van, *Insect Fight* , Eye movement, and Vision, Chapter 6, Flight behaviour and head movements of the hoverfly and honeybee: a preliminary analysis, ISBN 90-367-1090-1 pp. 77-86, 1999.

[58] Burton, A. J., Directional Change in a Flying Beetle, *Journal of Experimental Biology*, Vol. 54, pp. 575-585, 1971.

[59] Iams, S. M., Free flight of the mosquito Aedes, Cornell University Library, http://adsabs.harvard.edu/abs/2012arXiv1205.5260I, [cited 16.09.2014]

[60] Insect Flight, Chapter 5, Sounds of Insects in Flight, Proceedings of Life in Sciences, DOI: 10.1007/978-3-642-71155-8_5, Publisher Springer Berlin Heidelberg, 1986, pp. 60

[61] Obata, A., Shinohara, S, Akimoto, K., Suzuki, K., Seki, M., Aerodynamic Bio-Mimetics of Gliding Dragonflies for Ultra-Light Flying Robot, *Robotics*, Vol. 3, pp. 163-180, 2014, DOI: 10.3390/robotics3020163

[62] Vargas, A., Mittal, R., Dong, H., A computational study of the aerodynamic performance of a Dragonfly wing section in gliding flight, doi:10.1088/1748-3182/3/2/026004, *Bioinspiration & Biomimetics*, Vol. 3, 026004, (13pp), 2008.

[63] Deubel, T., Wanke, S., Weber, Ch.,Wedekind, F., Modelling and Manufacturing of a Dragonfly Wing as Basis for Bionic Research, International Design Conference - Design 2006, Dubrovnik - Croatia, May 15 - 18, 2006.

[64] http://cohengroup.lassp.cornell.edu/research.php?project=10008 [cited 12.09.2014]

[65] Rüppell, G., Kinematic Analysis of Symmetrical Flight Manoeuvres of Odonata, *Journal of Experimental Biology*, Vol. 144, pp. 13-42, 1989.

[66] Land, M. F., The visual control of courtship behaviour in the fly Poecilobothrus nobilitatus, *Journal of Comparative Physiology A*, Vol. 173, nº.5, pp. 595-603, 1993.

[67] Vigoreaux, J. O., *Nature's Versatile Engine: Insect Flight Muscle Inside and Out*, *Molecular Biology Intelligence Unit*, ISBN: 0-387-25798-5, Springer Science+Business Media, Landes Bioscience, 2006

[68] Ellington, C. P., The aerodynamics of hovering insect flight III. Kinematics, doi: 10.1098/rstb.1984.0054, *Philosophical Transactions of the Royal Society B*, London, Vol. 305, 41-78, 1984.

[69] Dickerson, A. K., Shankles, P. G., Madhavan, N. M., Hu, D. L., Mosquitoes survive a raindrop collision by virtue of their low mass, Proceedings of the National Academy of Sciences of the United States of America, Vol. 109, nº 25, pp. 9822-9827, 2012.

[70] Taylor, G. K., Mechanics and aerodynamics of insect flight control, DOI: 10.1017/S1464793101005759, *Biological Reviews*, Vol. 76, nº 4, pp. 449–471, 2001.

Propulsion for Biological Inspired Micro-Air Vehicles (MAVs)

1. Introduction

This paper is focused on the mechanisms involved with natural locomotion (thrust and/or lift). Commonalities between natural flying and swimming are analyzed together with flow control issues. The present study has been driven by the ability of living organisms to fit an ecological system in terms of their locomotion. Historically, it was envisaged that men would fly by flapping artificial wings like birds; their physiological and biomechanical flapping flight procedure have been explored by men since Giovanni Alphonso Borelli [1]. On the XIX Century, Étienne Jules Marey developed studies about the insects flapping flights and was the first to notice a complex horizontal 8 shape wing motion pattern on its trajectory during the flight. In 1874 Pettigrew Bell published a book [2] on which he drew attention to the fact that the birds while flying and during every cycle of wingbeat, run movements that could be represented with considerable accuracy with an 8-figure drawn vertically, while the insects run the same figure drawn horizontally displaced. In 1902, Pettigrew stated that in a way to confer on the insect´s wings the multiplicity of movements which they require, they are supplied with double hinge or compound joints, which enable them to move not only in an upward, downward, forward, and backward direction, but also on several intermediate degrees of obliquity – meaning this that insects wings are actually acting as helices, or twisted levers, and elevating weights much greater than the area of the wings would seem to warrant [3]. Similarly, by studying the fish's species, men found that most of them swim with lateral body undulations running from head to tail, in motion that also remind a 8-shape figure configuration, when viewed from the top.

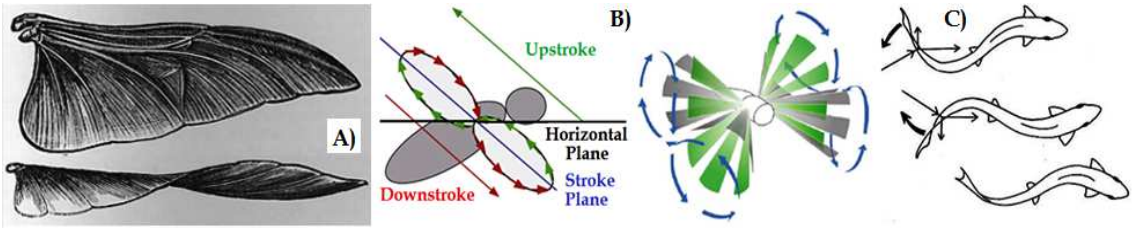

Figure 1 – A) Illustrative examples of the form and deformation of wings alluded to, those of the beetle, bee, and fly - Pettigrew Bell [3]; B) lateral and isometric view of a generic insect wingstroke plane revealing a horizontal 8-shape figure drawn; C) top view of fish's motion revealing an 8-shape figure drawn.

2. Background

Small Unmanned Aerial Vehicles (UAVs) have been receiving an increasingly interest in the last decades. This interest was fostered by the need of vehicles able to perform surveillance, communications relay links, ship decoys, and detection of biological, chemical, or nuclear materials [4]. Smaller and handy vehicles (micro air vehicles or MAVs) become even more challenging when DARPA launched in 1997 a pilot study into the design of portable (150mm) flying vehicles to operate in D^3- dull, dirty and dangerous – environments [5]. More recently DARPA launched a Nano Air Vehicle (NAV) program with the objective of developing and demonstrating small (<100mm) lightweight air vehicles (<10g) with the potential to perform indoor and outdoor missions [6]. All requirements of low altitude, long flight duration at low speeds (up to 100km/h), small wing spans and masses, together with demanding capabilities of takeoff, climb, loiter, hover, maneuver, cruise, stealth and gust response are further beyond today's fixed wing or rotorcraft vehicles. At the same time, MAVs fit in the general sizes, weights, and locomotion performance of natural flying or swimming animals [7].

Nevertheless, biomimetic engineered devices are still far from the living organisms and more research is needed [8]. There is a general agreement that an unsteady dynamics approach is required to capture the physical phenomena at this scale [9]. Additionally, propulsion and lift should not be considered independently. Flapping wing systems appeared in animals such as insects, birds, and fishes, which are known to exhibit remarkable aerodynamic and propulsive efficiencies. So, there have been several experimental and numerical studies of the biomimetic propulsive flapping [10, 11]. Most of these studies addressed the role of kinematic parameters such as flapping frequency, amplitude and phase difference on thrust generation and propulsive efficiency. At the same time, the effect of airfoil configuration has been considered far less and the published work is not always in agreement. For example, the results [12-14] show that thick airfoils can improve plunging airfoil performance, whereas [15-17] suggest than thin airfoils perform better, and the inviscid analysis [16] concludes no influence of airfoil thickness on plunging airfoil propulsion. Some authors attribute the superior efficiency of natural systems of thrust generation and propulsive efficiency to wing flexibility and focused their research on flexible wings with chord and span flexibilities [18, 19]. Has been reported [20] that flapping wings induce three rotational accelerations: angular, centripetal and Coriolis in the air near to the wing's surface, which diffuse into the boundary layer of the wing. Their results suggest that swimming and flying animals could control de predictability of vortex-wake interactions, and the corresponding propulsive forces with their fins and wings. Researchers [21] investigated dimensionless numbers to study swimming and flight, and their findings were disappointing since it became clear that different points of view exist in the biomechanics field on how to best define and use. So, successful biology-inspired or biomimetic concepts will depend on the understanding of the natural mechanisms especially when they do not agree with the present engineering design principles.

3. Some considerations related to fluid media (water and air)

Water and air are both regarded as fluid media, however, they are distinguished from each other: water is comparatively heavy (~1 ton/m^3) and incompressible; air, on the other hand, is comparatively light (~1.225 kg/m^3 at sea level, at 15ºC) and incompressible below Mach number M ~ 0.3 (the ratio of flow velocity/sound velocity must be greater than ~0.3 for a change fluid density of > 5%); for M > 0.3, significant compressibility occurs; - all insect´s fly in an incompressible air flow. When an animal swim through the water, the drag obtained is much greater when compared with the drag obtained from air similarly treated. Unsteady water flows are very common in nature, yet the swimming performance of fishes is typically evaluated by researchers, at constant, steady speeds at an appropriate facility. Similarly, most studies of insect flight are conducted in smooth flow or still air conditions. On both cases, it is still mostly unknown if unsteady water flows represent advantages and/or disadvantages to swimming fishes, and as well, if variable wind in nature affects flying insects as an advantage and/or disadvantage; however, in order to meet such peculiar requirements, all traveling organs of aquatic and flying animals (feet, fins, flippers, or wings) are not designed by nature as of rigid materials; instead, they are elastic materials.

4. Swimmer organisms: locomotion on fish: tail and fins – control surfaces

Most fish species swim with lateral body undulations running from head to tail, by exerting force against the surrounding water; these waves are slower than the waves of muscle activation; i.e, they contract muscles on either side of its body in order to generate flexion waves that travel the length of the body from head to tail. Fish's body is often fusiform, a streamlined body plan often found in fast-moving fish. They may also be filiform (eel-shaped) or vermiform (worm-shaped). Also, fish are often either laterally thin (compressed), or dorso-ventrally flat (depressed). Their muscle power is converted to thrust either directly by the bending body or almost exclusively by the tail, depending upon the body shape of the species and the swimming kinematics. Comparative scientists (physiologists and neurobiologists) have

long been interested to realize how locomotion mechanisms used by aquatic organisms, propel themselves through water. The main external features of the fish are fins, composed of bony spines protruding from the body with skin covering them and joining them together; and as they are located at different body´s places on the fish, they serve as well for different purposes, such as moving forward, turning, and keeping an upright position. Dorsal fins are located on the back: most fishes have one dorsal fin, but some fishes have two or three (as well as also could have finlets - small fins, generally between the dorsal and the caudal fins). The dorsal fins serve to protect the fish against rolling. The caudal fin (tail) is located at the end of the caudal peduncle and is used for propulsion. The tail fin can be: rounded at the end; truncated; forked; emarginate; or continuous. The anal fin is located on the ventral surface and is used to stabilize the fish while swimming. The pectoral fins are located on each side of the fish. A peculiar function of pectoral fins, highly developed in some fish, is the creation of the dynamic lifting force that assists sharks, in maintaining depth; they also enables the "flight" for flying fish and the "walking" in some anglerfish in the mud. The ventral fins assist the fish in going up or down through the water, turning sharply, and stopping quickly. Torsional angles changes on fish's fins can be produced by active control, via muscles force, or by passive control, via inertial hydrodynamic forces.

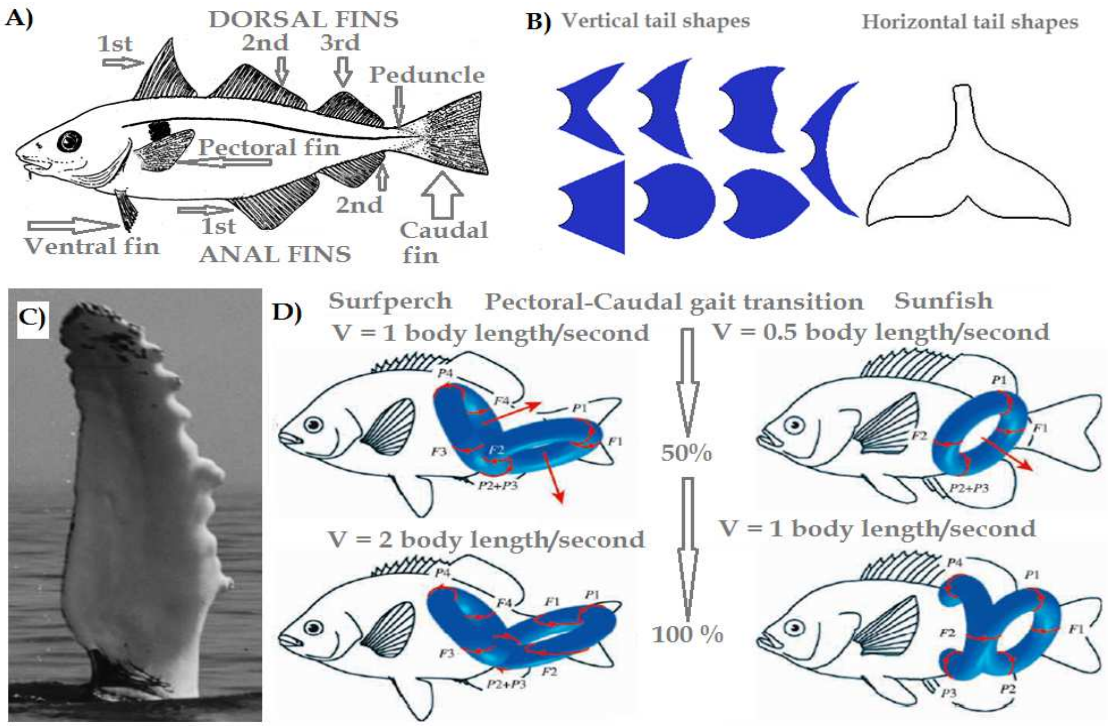

Figure 2 – A) Control surfaces on a generic fish; B) different types of fish fin tails known; C) Photo of a pectoral flipper of the humpback whale (*Megaptera novaeangliae*) show leading edge tubercles [23]; D) Black surfperch (*Embiotoca jacksoni*) and Bluegill sunfish (*Lepomis macrochirus*), revealing vortex rings at different speeds [25].

Extensive studies have been made on the Dolphins [22]; their fusiform and streamlined body shape, reduce the pressure component of the drag through maintenance of laminar flow; their maximum thickness (where transition to turbulent flow and boundary-layer separation is likely to develop) it is nearly at 45% of a body length from the beak, meaning that at list 45% of dolphins body may have laminar flow, due to a favorable pressure gradient up to the maximum thickness. The dolphins fineness ratio (FR = body length/maximum diameter) is $3.85 \leq FR \leq 5.55$ approach the optimum value of lowest drag (FR = 4.5). Their propulsive movements are confined to the vertical plane in the posterior 1/3 of the body, with greatest amplitude at the caudal peduncle; the anterior body part acts as an inertial mass, minimizing energy loss from body oscillations. Dolphins could perform maximum speed up tom 9.3 ms^{-1}.

Orcinus orca could perform maximum speed up to 15.5 ms^{-1} during 20 minutes. The pectoral flippers of the humpback whale (*Megaptera novaeangliae*) show leading edge tubercles [23]. Comparisons of wing sections with and without tubercles using CFD models, showed a 4.8% increase in lift; 10.9% reduction in induced drag; 17.6% increase in lift to drag ratio for wing section with tubercles at 10^{o} angle of attack. Enhanced maneuverability by the addition of leading edge tubercles has potential application in the development of modern vehicles operating in air or water. Experimental flow visualization [24] compared with numerical simulations on both velocity and vorticity fields, revealed a good agreement; those results also revealed that fish can control body-generated vorticity, through body flexure and active manipulation by the caudal fin. Other researchers [25], using DPIV, approach the question of why some fishes are able to swim faster than others, from a hydrodynamic perspective; they investigate the structure and strength of the 3D wake to determine how hydrodynamic forces varies on Black surfperch (*Embiotoca jacksoni*) and Bluegill sunfish (*Lepomis macrochirus*). Both species (similar in size) swim at low speed using pectoral fins exclusively and both species at high speed, switch to pectoral-caudal fin locomotion; the surfperch can swim twice fast. It was found that surfperch presented a pair of linked vortex rings for all velocities, while the sunfish for low speed, presented only one vortex ring per fin and a pair of linked vortex rings with one ring only partially complete and attached to the body, at maximum speed. One of the most striking aspects of fish diversity is the presence of multiple locomotor control surfaces playing hydrodynamic roles during steady swimming and unsteady maneuvering locomotion, as well as the vortex wake interactions among all fins, a subject to be fully understood in the future. The skin of fast-swimming sharks (mako sharks) [26] is composed by a tooth-like scales (denticles) that generated vortexes on the front edge of the skin, *i.e.*, eddies that essentially would help to pull the shark forward; this kind of skin composition is not found on slow-swimming sharks. Many researchers study this skin, by direct mimicking in its 3D shape or in a simplified grooved surface (riblets). Upon close examination of a dolphin's skin revealed micro dermal ridges that delay the transition to turbulent, by trap water molecules at the surface of the skin. Thus, the molecules of trapped water on the skin surface allows the animal to pass through the water more easily than if the same animal had a dry skin surface. The sailfish (that has V-shaped protrusions on skin) is known as fastest sea animal, reaching maximum speeds exceeding 110km/h. His fin on the back which grows along the back can be spread and folded at will. Since sailfish is the fastest-swimming animal, researchers expected that sailfish's skin textures might produce skin-friction reduction; however, directly measures and numerical investigation showed increases or negligible reduction (~1%) on skin-friction. Yet, scientists advanced other explanations; the role of sailfish skin knowledge is to be confirmed.

5. Insects: a Biological Flight Machine and their wing's kinematics

Every insect´s wings when in motion are deformed by either the aerodynamic forces from the surrounding air flow, or by the inertial acceleration; the overall wing deformation is a combination of both and is in a continuously and constantly changing. The power product of the flight´s muscles is transmitted to the wings which unlike an aircraft wings are neither streamlined nor smooth: the shape, corrugation and performance of the wings and the complex flapping motion during each stroke cycle will determine the ability of an animal to fulfil successfully every stunning maneuver. Each wingstroke cycle is typically divided into two translational phases: upstroke and downstroke; and two rotational phases: pronation and supination. In the forward-downstroke movement - main power stroke - the wing initiate the downward loop with a high angle of attack until the leading edge tilts downwards, where the wing momentarily becomes horizontal in the middle of the stroke, minimizing the angle of attack; stalling is prevented due to the fastest moving of the wing at this point. During the recovery stroke, when the wing moves upwards and backwards, the leading edge tips backwards. The wing is rotated again at the top of the recovery stroke, restoring the maximum angle of attack immediately before the next downstroke movement initiation. Every motion streamed to the wing lies in a composition of rotational, horizontal, vertical and

torsional movements. Torsional angles changes on insect's wings can be produced by active control, via muscles force, or by passive control, via inertial aerodynamic forces. Insect's flight maneuverability is remarkable and by far, superior to every maneuverability of any man-made flying vehicle. Dickinson *et al*. [27], stated that the aerodynamic performance of insects results from an interaction of three distinct, yet, interactive flight mechanisms: delayed stall, meaning that the wing sweep through the air with large angle of attack, during the translational portions of the stroke; rotational lift, meaning an augment in angle of attack at the end of the stroke, providing extra lift; and wake capture, meaning that the wing will capture some energy, left behind on the air by the previous wingstroke, providing extra power. Dragonfly wings possess great stability and high load-bearing capacity during flapping flight, gliding and hovering, despite the fact that their mass is less than 2% of the insect's total mass; such wings (forewings – front wings; and hindwings – rear wings) are composed by a thin cuticular membrane, supported by a vein system (venation) [28]. This venation structure consists on a net of veins (of different sections) that forms rectangular frames at the leading edge and hexagons or polygons with more than four sides at the trailing edge, allowing the requirements for different wing zones bearing different loads. Adding to this, their wings are highly corrugated (more corrugated at first ¼ at the leading edge), which increases significantly the stiffness and strength of the wings and results in a lightweight structure with very good aerodynamic performance. The flow induced by the motion of insect's wings is highly unsteady and vortical. In fact, insect´s generate enough force to keep themselves in the air, because they flap their wings at a very high angle of attack that creates a structure at the leading edge of the wing, (a tornado-like structure) called leading edge vortex (LEV). Large LEV's are formed at the beginning of each half stroke and remains attached to the wing until the beginning of the next half stroke. It was found on some small insects, an unsteady inviscid high lift mechanism (*clap-and-fling*), consisting on the use of interaction between wings, as they press each other together (like a '*clap*') at the extreme ends of the stroke, providing a total vertical flapping angle of ~180º. At the end of the '*clap*', leading edges began to separate as the trailing edge remains connected initially (V-shape at ~120º); after that, the trailing edge separates as well ('*fling*'); such movement leads that air to rush into low pressure widening gap and produce high strength vortices of equal and opposite sign [29]. The current state of the art of micro-CT scanners (X-ray Microtomography) is nowadays limited to large insect's wings [30]; since the resolution of micro-CT scanners is increasing every year, in near future, any insect wing could be successfully scanned.

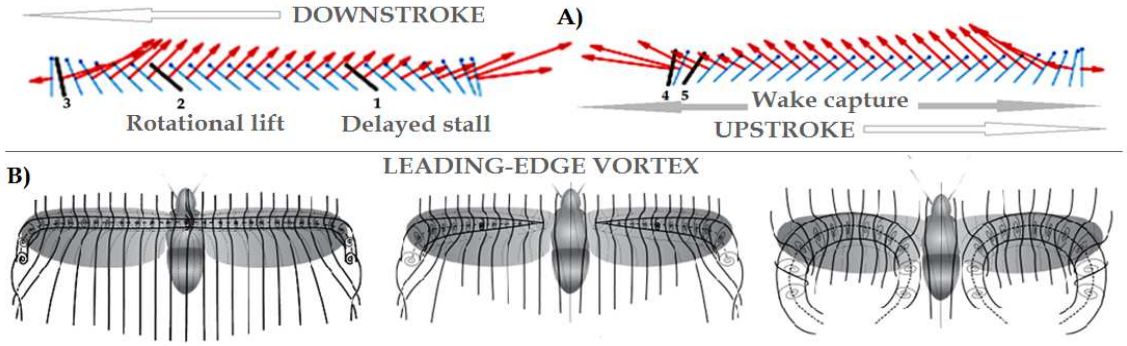

Figure 3 – A) Illustration a of complete insect wingstroke showing the delayed stall and rotational lift on the downstroke movement and the wake capture during all course of the upstroke; blue colour - wing position, with leading edge always on top; red colour - representing the total force [31]; B) Illustration of 3 different leading-edge vortex: extends across thorax; attached at the base of the wing and horseshoe-shaped vortex on both wings.

The main challenge for accurately digitizing the wings 3D architecture is minimizing the deformation due to drying of the wing needed to reduce scatter and noise in the scan due to evaporation. Researchers used this technology to scan a dragonfly "*Sympetrum vulgatum*" forewing and hindwings; they found that both vein and membrane thickness increases from tip to root on both wings, which allows the wing to effectively bear both inertial and

aerodynamic loads. On their model, they discover that the inertial loads along the wingspan were approximately 1.5 to 3 times higher than the aerodynamic loads – wings deformation were dominated by inertial loads. Based on computations, they also found that wing deformation was smaller during the downstroke, due to structural asymmetry. By the analyses on the work on several researchers, In fact generically, both inertial and aerodynamic force can be the primary cause of wing deformation: in contrast with above statement, and referring also to dragonfly's natural wings, a study concluded that their deformation was mainly due to the aerodynamic forces. Insects have no active control over the wing configuration during flight. The architecture of the wing and the material properties of its element determine how the wing changes their shape in response momentarily to external forces changing, since the wing movement is very complex. It is nowadays a great challenge to researchers, how to build a model with similar properties; of course, another challenge is how to incorporate the wing flexibility into the theoretical model predicting the aerodynamic force during insect flight – both, remains an ongoing challenge to the researchers [32].

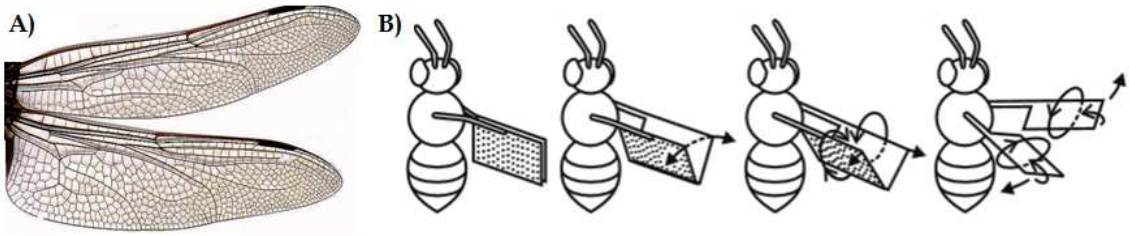

Figure 4 – A) illustration of forewings and hindwings of a dragonfly and their venation structure as referred on [27] and also a pigmented cell known as pterostigma which mass is frequently greater than that of an equivalent area of adjacent wing and its inertia influences the movement of the whole wing movements. Without the pterostigma, the self-excitating vibrations would set in on the wings after a certain critical speed - pterostigma acts as an inertial regulator of wing pitch; B) Illustration of the '*clap-and-fling*' flight mechanism: at a certain moment, the wings press together each other (clap); then wing separate as shown (V-shape), generating a low pressure zone between them.

As previously referred, leading-edge vortex is the main flight mechanism that allows insects to be able to fly; studies on the unsteady aerodynamics on the flapping wing of a *Manduca sexta* hawkmoth robotic model (while hovering) were made by the use of computational fluid dynamic (CFD) modelling [33]; CFD computations revealed a large leading-edge vortex (LEV1) presence during most of the downstroke movement (from the base at ~60/75% of the wing length); as the wing moves towards horizontal position, this structure becomes larger spiralling vortex with strong axial flow at the core, towards the wing tip. Immediately after the middle of the dowsntroke, the LEV breaks down at 75% of the wing length, creating this, a second LEV (LEV2 - also revealing a spiral axual flow towards the wing base) between the wing tip and the broken-down position of the first LEV. At the initial supination rotation, LEV2 is pushed off the leading edge due to wing deceleration and the breakdown point of LEV1 moves into half of wing length. During the upstroke a very-small leading-edge vortex (quite 2D struture) appeared at the wing tip and by the time the wing reaches the middle position, this structure extends from wing tip to the wing base. After the upstroke's middle course, the LEV grows rapidelly (comparable in size with the dowstroke LEV1) and hence enlarges the negative pressure region. At the later part of downstroke, the LEV breaks don at ~60/70% if the wing length without shedding the tip vortex. During the pronation, the upstroke LEV remained attached to the leading edge of the lower wing surface and a trailing-edge vortex (TEV) was also detected (larger than LEV, lies below it and run from the base to the tip), probably due to wing rotation. Lentink & Dickinson [34] suggested that LEV could be an efficient high-lift nechanism for small and big hovering insects; this suggestion is reenforcing the idea that insect while hovering, more easily might capture the energy left behind in air, by the previous stroke; even more, the insects with four separated wings (part of them as two pairs coupling wings) might benefit their rear pair on the work of forewing's wake flow. A challenge on build insect's wing models approaching the natural wings morphology was made by Tanaka & Wood [35]. They described the fabrication of an artificial insect (hoverfly) wing

with a rich set of topological features by micro molding a thermosetting resin; the venation system diameter varied between 50–125 *μm* heights and the corrugation of the wing measured 100 *μm*. Both solid veins and membrane were simultaneously formed and integrated by a single molding process, by the use of a layered laser ablation technique; each 3D mold were created with 5 *μm* resolution in height. The replicated wing matched at-scale high precision surface profiles of the natural one, thus enabling parametric experiments of the functional morphology of insect wings. Authors referred that stiffness measured along the natural and model wings on identical values of magnitude. However, nature had adapted insects with wings were stiffness varies ad varies the location region on the wings. Later, on another investigation [36] on the subject of flexural and torsional wing flexibility, they were able to create a rigid wing model (hoverfly) that could produce more lift than the natural one's, thus, in prejudice of maneuverability, a requirement that insects had at their disposal (at their will), at almost 350 million years: the experience to fly in the skies of the Earth. After filming a beetle tethered flight [37] with a high-speed camera, researchers build a model of wing system of identical size of natural wings, on a way to follow the natural performance of: flapping frequency, stroke plane, wing tip path, wing rotation angles and flapping angles; however, their experience demonstrated to them that flapping frequency and wing rotation need an improvement to satisfy the natural mimic, since the positive vertical force achieved was only ~1/5 of the total weight of the system. From all bibliographic revision on birds, bats and insects, all researchers invoked that those fliyng animals may benefit aerodinamically from the flexibility of their wings – a general idea stating that temporal wing deformation is the basis of force generation. From the design aspect, flexibility may benefit MAVs as well, from several points of view: aerodynamically and lightness of structures. Since insect's flight maneuverability far higher superior to every maneuverability achieved by any man-made flying vehicle, thus, Barata *et al* [38], made an extensive comparative bibliographyc research on the wings motion patterns on several types of insects on resemblant flights, regarding the expoliting of their in-flight basic principes for the acquired performance. They found that the same insect uses their wings in very differently manners, depending, thus, on the maneuver they intend to carry. Every single movement of their wings generates lift (downstroke or upstroke) and the time rate downstroke/upstroke could easily vary at their will. Some of them possess the ability to use the wings in independent ways (differences on wingstroke, wings with different torsions at the same instant, or even one wing used as aerodynamic brake). Despite the flight mechanisms used by insects are not yet fully understood by humans, their replication for use in MAVs will be even more far from being achieved.

Conclusions

The current investigation is focused on the mechanisms involved with natural locomotion (thrust and/or lift). Biological systems with interesting applications to Micro Air-Vehicles (MAVs) are generally inspired on flying insects or birds; however, similarly to the aerodynamics of flight, powered swimming requires animals to overcome drag by producing thrust. Commonalities between natural flying and swimming are analyzed together with flow control issues. As it was shown by several researchers on this bibliography work review, the perception of flight performances held by insects and swimming performances held by fishes are not completely understood. All control surfaces present on living aquatic and flying animals (feet, fins, flippers, or wings) are not design by nature as of rigid materials; instead, they are elastic materials. Insect's wings are morphological wonder (elastic material: every wing motion is a sum of horizontal, vertical and torsional movement), however, what really enables the wings to make enough force for the animal to stay in the air, is the way insects flaps them: at a very high angle of attack, creating a structure at the leading edge of the wing, (tornado-like structure) called leading-edge vortex. Researchers investigated dimensionless numbers to study swimming and flight, and their findings were disappointing since it became clear that different points of view exist in the biomechanics field on how to best define and use. So, successful biology-inspired or biomimetic concepts will depend on the understanding of the natural mechanisms especially when they do not agree with the

present engineering design principles. An additional difficulty (and a very important one) is the fact that state of art on elastic materials with identical or similar elastic properties of natural insect's wing, does not exist yet.

Acknowledgements

The authors express their gratitude to FCT for the funding of the research project: PTDC/EME-MFE/122849/2010: Nature – New-biomimetic Aerodynamic Technologies for Undersized Reynolds

Bibliography

[1] G. A. Borelli. *De Motu Animalium*. Rome, A. Bernabo, 1680.
[2] J. B. Pettigrew. *Animal Locomotion or Walking, Swimming and Flying with a Dissertation on Aeronautics*. New York, D. Appleton & Company, 1874.
[3] http://www.1902encyclopedia.com/F/FLI/flight-flying-machines.html (16/06/2015).
[4] Mueller, T. J.; DeLaurier, J. D.: "Aerodynamics of Small Vehicles", *Annual Review of Fluid Mechanics*, Vol. 35, (2003), ISSN 0066-4189, pp. 89-111.
[5] McMichael J. M.; Francis M. S.: *Micro air vehicles - Toward a new dimension in flight*, Defense Advanced Research Projects Agency, 10 January 2005, Online Internet available from http://www.darpa.mil/tto/MAV/mav_auvsi.htm, August 1997 (29/05/2014).
[6] Hylton, T., Martin, C., Tun, R., Castelli, V. The DARPA Nano Air Vehicle Program. *Proceedings of 50th AIAA Aerospace Sciences Meeting Including the New Horizons Forum and Aerospace Exposition*, Nashville, Tennessee, USA, 09-12 January, 2012.
[7] von Ellenrieder, K. D.; Parker, K.; Soria, J.: "Fluid mechanics of flapping wings", *Experimental Thermal and Fluid Science*, Vol. 32, No. 8, (2008), ISSN 0894-1777, pp. 1578-1589.
[8] Evers, J. H. Biological Inspiration for Agile Autonomous Air Vehicles. *Platform Innovations and System Integration for Unmanned Air, Land and Sea Vehicles (AVT-SCI Joint Symposium)*, Meeting Proceedings RTO-MP-AVT-146, Paper 15: 1-14, Neuilly-sur-Seine, France.
[9] Ho, S.; Nassef, H.; Pornsinsirirak, N.; Tai, Y.; Ho, C.: "Unsteady aerodynamics and flow control for flapping wing flyers", *Progress in Aerospace Sciences*, Vol. 39, No. 8, (2003), ISSN 0376-0421, pp. 635-681.
[10] DeLaurier J. D.; Harris J. M.: "Experimental study of oscillating-wing propulsion", *Journal of Aircraft*, Vol. 19, (1982), ISSN 0021-8669, pp. 368–373.
[11] Tuncer, I. H.; Platzer M.F.: "Computational study of flapping airfoil aerodynamics", *Journal of Aircraft*, Vol. 37, (2000), ISSN 0021-8669, pp. 514–520.
[12] Rozhdestvensky, K.V.; Ryzhov, V.A.: "Aerohydrodynamics of flapping-wing propulsors", *Progress in Aerospace Sciences*, Vol. 39, No. 8, (2003), ISSN 0376-0421, pp. 585–633.
[13] Lentink, D., Gerritsma, M. Influence of airfoil shape on performance in insecto flight. *Proceedings of the 33rd AIAA Fluid Dynamics Conference and Exhibit*, Orlando, Florida, June 23–26, 2003.
[14] An, S.; Maeng, J.; Han, C.: "Thickness effect on the thrust generation of heaving airfoils", *Journal of Aircraft*, Vol. 46, No. 1, (2009), ISSN 0021-8669, pp. 216–222.
[15] Vandenberghe, N.; Childress, S.; Zhang, J.: "On unidirectional flight of a free flapping wing", *Physics of Fluids*, Vol. 18, No. 1, (2006), ISSN 1070-6631, pp. 014102–14108.
[16] Wang, Z. J.: "Vortex shedding and frequency selection in flapping flight", *Journal of Fluid Mechanics*, Vol. 410, (2000), ISSN 1469-7645, pp. 323–341.
[17] T. Cebeci. M. Platzer. H. Chen. K-C. Chang. J. P. Shao. *Analysis of Low-Speed Unsteady Airfoil Flows*. Horizons Publishing Inc., Long Beach, 2004.
[18] Le, T. Q.; Ko, J. H.; Byun, D.; Park, S. H; Park, H. C.: "Effect of Chord Flexure on Aerodynamic Performance of a Flapping Wing", *Journal of Bionic Engineering*, Vol. 7, No. 1, (2010), ISSN 1672-6529, pp. 87-94.

[19] Heathcote, S.; Wang, Z.; Gursul, I.: "Effect of spanwise flexibility on flapping wing propulsion", *Journal of Fluid and Structures*, Vol. 24, No. 2, (2008), ISSN 0889-9746, pp. 183-199.
[20] Lentink, D.; Van Heijst, G. F.; Muijres, F. T.; Van Leeuwen, J. L.: "Vortex interactions with flapping wings and fins can be unpredictable", *Biology Letters*, Vol. 6, No. 3, (2010), ISSN 1744-9561, pp. 394-397.
[21] Lentink, D.; Dickinson, M. H.: "Biofluiddynamic scaling of flapping, spinning and translating fins and wings", *Journal of Experimental Biology*, Vol. 212, No. 16, (2009), ISSN 0022-0949, pp. 2691-2704.
[22] Fish, F. E.; Hui, C. A.: "Dolphin swimming – a review", *Mammal Review*, Vol. 21, No. 4, (1991), ISSN 1365-2907, pp. 181-195.
[23] Fish, F. E.; Howle, L. E.; Murray, M. M.: "Hydrodynamic flow control in marine mammals", Integrative *and Comparative Biology*, Vol. 48, No. 6, (2008), ISSN 1557-7023, pp. 788-800.
[24] Wolfgang, M. J.; Anderson, J. M.; Grosenbaugh, M. A.; Yue, D. K.; Triantafyllou, M. S.: "Near-body flow dynamics in swimming fish", *Journal of Experimental Biology*, Vol. 202, (1999), ISSN 0022-0949, pp. 2303-2327.
[25] Drucker, E. G.; Lauder, G. V.: "A Hydrodynamic analysis of fish swimming speed: wake structure and locomotor force in slow and fast labriform swimmers", *Journal of Experimental Biology*, Vol. 203, (2000), ISSN 0022-0949, pp. 2379-2393.
[26] Choi, H.; Park, H.; Sagong, W; Lee, S: "Biomimetic flow control based on morphological features of living creatures", *Physics of Fluids*, Vol. 24, (2012), ISSN 1070-6631, pp. 121302-1/ 121302-20.
[27] Dickinson, M. H.; Lehman, F-O.; Sane, S. P.: "Wing rotation and the aerodynamic basis of insect flight", *Science*, Vol. 284 no. 5422, (1999), ISSN 0036-8075, pp. 1954-1960.
[28] Sun, J.; Bushan, B.: "The structure and mechanical properties of dragonfly wings and their role on flyability", *Comptes Rendus Mécanique*, Vol. 340, No. 1-2, (2012), ISSN 1631-0721, pp. 3–17.
[29] Ho, S.; Nassef, H.; Pornsinsirirak, N.; Tai, Y-C.; Ho, C-M.: "Unsteady aerodynamics and flow control for flapping wing flyers", *Progress in Aerospace Sciences*, Vol. 39, No. 8, (2003), ISSN 0376-0421, pp. 635-681.
[30] Jongerius, S. R.; Lentink, D.: "Structural Analysis of a Dragonfly Wing", *Experimental Mechanics*, Vol. 50, (2010), ISSN 0014-4851, pp. 1323-1334.
[31] http://www.scientificamerican.com/article/catching-the-wake/ (07/07/2015).
[32] Yin, B.; Luo, H.: "Effect of wing inertia on hovering performance flapping wings", *Physics of Fluids*, ISSN 1070-6631, Vol. 22, (2010), pp. 111902-1/111902-10.
[33] Liu, H.; Ellington, C. P.; Kawachi, K.; van den Berg, C.; Willmott, A. P.: "A computational fluid dynamic study of hawkmoth hovering", *Journal of Experimental Biology*, Vol. 21, (1998), ISSN 0022-0949, pp. 461-477.
[34] Lentink, D.; Dickinson, M. H.: "Rotatioanl accelerations stabilize leading edge vortices on revolving fly wings", *Journal of Experimental Biology*, Vol. 212, (2009), ISSN 0022-0949, pp. 2705-2719.
[35] Tanaka, H.; Wood, R. J.: "*Fabrication of Corrugated Artificial Insect Wings Using Laser Micromachined Molds*", *Journal of Micromechanics and Microengineering*, (2010), ISSN 1361-6439, Vol. 20, pp. 075008-1/075008-8.
[36] Tanaka, H.; Whitney, J. P.; Wood, R. J.: "Effect of Flexural and Torsional Wing Flexibility on Lift Generation in Hoverfly Flight", *Integrative and Comparative Biology*, Vol. 51, No. 1, ISSN 1557-7023, p. 142–150.
[37] Nguyen, Q. V.; Park, H. C.; Goo, N. S.; Byun. D.: "Characteristics of a Beetle's Free Flight and a Flapping-Wing System that Mimics Beetle Flight", *Journal of Bionic Engineering*, Vol. 7, No. 1. (2010), ISSN 1672-6529, pp. 77-86.
[38] Barata, J. M. M.; Neves, F. M. S. P.; Manquinho, P. A. R.: "*Comparative Study of Wing's Motion Patterns on Various Types of Insects on Resemblant Flight Stages*", *Proceedings of the AIAA Atmospheric Flight Mechanics Conference*, SciTech 2015, Kissimmee, Florida, USA, 5/9 January 2015.

Open Journal of Applied Sciences, 2016, 6, 7-15
Published Online January 2016 in SciRes. http://www.scirp.org/journal/ojapps
http://dx.doi.org/10.4236/ojapps.2016.61002

Propulsion for Biological Inspired Micro-Air Vehicles (MAVs)

Jorge M. M. Barata, Fernando M. S. P. Neves, Pedro A. R. Manquinho, Telmo A. J. Silva

Aerospace Sciences Department, Universidade da Beira Interior, Covilhã, Portugal
Email: fernandomneves@gmail.com

Received 21 December 2015; accepted 18 January 2016; published 21 January 2016

Abstract

Small Unmanned Aerial Vehicles have been receiving an increasingly interest in the last decades, fostered by the need of vehicles able to perform surveillance, communications relay links, ship decoys, and detection of biological, chemical, or nuclear materials. Smaller and handy vehicles Micro Air vehicles (MAVs) become even more challenging when DARPA launched in 1997 a pilot study into the design of portable (150 mm) flying vehicles to operate in D^3—dull, dirty and dangerous—environments. More recently DARPA launched a Nano Air Vehicle (NAV) program with the objective of developing and demonstrating small (<100 mm; <10 g) lightweight air vehicles with the potential to perform indoor and outdoor missions. The current investigation is focused on the mechanisms involved with natural locomotion (propulsion and lift should not be considered independently). Biological systems with interesting applications to MAVs are generally inspired on flying insects or birds; however, similarly to the aerodynamics of flight, powered swimming requires animals to overcome drag by producing thrust. Commonalities between natural flying and swimming are analyzed together with flow control issues as a purpose of improvement on biology-inspired or biomimetic concepts for Micro Air Vehicles implementation.

Keywords

Biomimetics, Flapping Wings, Insect Flight, Adaptive Biology

1. Introduction

This paper is focused on the mechanisms involved with natural locomotion (thrust and/or lift). Commonalities between natural flying and swimming are analyzed together with flow control issues. The present study has been driven by the ability of living organisms to fit an ecological system in terms of their locomotion. Historically, it was envisaged that men would fly by flapping artificial wings like birds; their physiological and biomechanical

How to cite this paper: Barata, J.M.M., Neves, F.M.S.P., Manquinho, P.A.R. and Silva, T.A.J. (2016) Propulsion for Biological Inspired Micro-Air Vehicles (MAVs). *Open Journal of Applied Sciences*, **6**, 7-15.
http://dx.doi.org/10.4236/ojapps.2016.61002

flapping flight procedures have been explored by men since Giovanni Alphonso Borelli [1]. On the XIX Century, Étienne Jules Marey developed studies about the insects flapping flights and was the first to notice a complex horizontal 8 shape wing motion pattern on its trajectory during the flight. In 1874 Pettigrew Bell published a book [2] on which he drew attention to the fact that the birds while flying and during every cycle of wingbeat, run movements that could be represented with considerable accuracy with an 8-figure drawn vertically, while the insects run the same figure drawn horizontally displaced. In 1902, Pettigrew stated that in a way to confer on the insect's wings the multiplicity of movements which they require, they are supplied with double hinge or compound joints, which enable them to move not only in an upward, downward, forward, and backward direction, but also on several intermediate degrees of obliquity—meaning this that insects wings are actually acting as helices, or twisted levers, and elevating weights much greater than the area of the wings would seem to warrant [3]. Similarly, by studying the fish's species, men found that most of them swim with lateral body undulations running from head to tail, in motion that also remind a 8-shape figure configuration, when viewed from the top (see **Figure 1**).

2. Background

Small Unmanned Aerial Vehicles (UAVs) have been receiving an increasingly interest in the last decades. This interest was fostered by the need of vehicles able to perform surveillance, communications relay links, ship decoys, and detection of biological, chemical, or nuclear materials [4]. Smaller and handy vehicles (Micro Air Vehicles or MAVs) become even more challenging when DARPA launched in 1997 a pilot study into the design of portable (150 mm) flying vehicles to operate in D^3—dull, dirty and dangerous—environments [5]. More recently DARPA launched a Nano Air Vehicle (NAV) program with the objective of developing and demonstrating small (<100 mm) lightweight air vehicles (<10 g) with the potential to perform indoor and outdoor missions [6]. All requirements of low altitude, long flight duration at low speeds (up to 100 km/h), small wing spans and masses, together with demanding capabilities of takeoff, climb, loiter, hover, maneuver, cruise, stealth and gust response are further beyond today's fixed wing or rotorcraft vehicles. At the same time, MAVs fit in the general sizes, weights, and locomotion performance of natural flying or swimming animals [7]. Nevertheless, biomimetic engineered devices are still far from the living organisms and more research is needed [8]. There is a general agreement that an unsteady dynamics approach is required to capture the physical phenomena at this scale [9]. Additionally, propulsion and lift should not be considered independently. Flapping wing systems appeared in animals such as insects, bats, birds, and fishes, which are known to exhibit remarkable aerodynamic and propulsive efficiencies. So, there have been several experimental and numerical studies of the biomimetic propulsive flapping [10] [11]. Most of these studies addressed the role of kinematic parameters such as flapping frequency, amplitude and phase difference on thrust generation and propulsive efficiency. At the same time, the effect of airfoil configuration has been considered far less and the published work is not always in agreement. For example, the results [12]-[14] show that thick airfoils can improve plunging airfoil performance, whereas [15]-[17] suggest than thin airfoils perform better, and the inviscid analysis [16] concludes no influence of airfoil thickness on plunging airfoil propulsion. Some authors attribute the superior efficiency of natural systems of thrust generation and propulsive efficiency to wing flexibility and focused their research on flexible wings with chord and span flexibilities [18] [19]. Has been reported [20] that flapping wings induce three rotational accelerations: angular, centripetal and Coriolis in the air near to the wing's surface, which diffuse into the boundary layer of the wing. Their results suggest that swimming and flying animals could control de predictability of vortex-

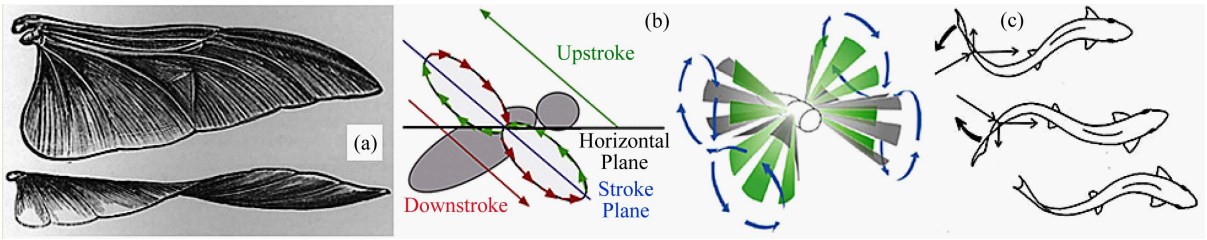

Figure 1. (a) Illustrative examples of the form and deformation of wings alluded to those of the beetle, bee, and fly—Pettigrew Bell [3]; (b) lateral and isometric view of a generic insect wingstroke plane revealing a horizontal 8-shape figure drawn; (c) top view of fish's motion revealing an 8-shape figure drawn.

wake interactions, and the corresponding propulsive forces with their fins and wings. Researchers [21] investigated dimensionless numbers to study swimming and flight, and their findings were disappointing since it became clear that different points of view exist in the biomechanics field on how to best define and use. So, successful biology-inspired or biomimetic concepts will depend on the understanding of the natural mechanisms especially when they do not agree with the present engineering design principles.

3. Some Consideration Related to Fluid Media (Water and Air)

Water and air are both regarded as fluid media, however, they are distinguished from each other: water is comparatively heavy (~1 ton/m^3) and incompressible; air, on the other hand, is comparatively light (~1.225 kg/m^3 at sea level, at 15˚C) and incompressible below Mach number M ~ 0.3 (the ratio of flow velocity/sound velocity must be greater than ~0.3 for a change fluid density of >5%); for M > 0.3, significant compressibility occurs; all insect's fly in an incompressible air flow. When an animal swim through the water, the drag obtained is much greater when compared with the drag obtained from air similarly treated. Unsteady water flows are very common in nature, yet the swimming performance of fishes is typically evaluated by researchers, at constant, steady speeds at an appropriate facility. Similarly, most studies of insect flight are conducted in smooth flow or still air conditions. On both cases, it is still mostly unknown if unsteady water flows represent advantages and/or disadvantages to swimming fishes, and as well, if variable wind in nature affects flying insects as an advantage and/or disadvantage; however, in order to meet such peculiar requirements, all traveling organs of aquatic and flying animals (feet, fins, flippers, or wings) are not designed by nature as of rigid materials; instead, they are elastic materials.

4. Swimmer Organisms: Locomotion on Fish: Tail and Fins—Control Surfaces

Most fish species swim with lateral body undulations running from head to tail, by exerting force against the surrounding water; these waves are slower than the waves of muscle activation; *i.e*., they contract muscles on either side of its body in order to generate flexion waves that travel the length of the body from head to tail. Fish's body is often fusiform, a streamlined body plan often found in fast-moving fish. They may also be filiform (eel-shaped) or vermiform (worm-shaped). Also, fish are often either laterally thin (compressed), or dorsoventrally flat (depressed). Their muscle power is converted to thrust either directly by the bending body or almost exclusively by the tail, depending upon the body shape of the species and the swimming kinematics. Comparative scientists (physiologists and neurobiologists) have long been interested to realize how locomotion mechanisms used by aquatic organisms, propel themselves through water. The main external features of the fish are fins, composed of bony spines protruding from the body with skin covering them and joining them together; and as they are located at different body's places on the fish, they serve as well for different purposes, such as moving forward, turning, and keeping an upright position. Dorsal fins are located on the back: most fishes have one dorsal fin, but some fishes have two or three (as well as also could have finlets—small fins, generally between the dorsal and the caudal fins). The dorsal fins serve to protect the fish against rolling. The caudal fin (tail) is located at the end of the caudal peduncle and is used for propulsion. The tail fin can be: rounded at the end; truncated; forked; emarginated; or continuous. The anal fin is located on the ventral surface and is used to stabilize the fish while swimming. The pectoral fins are located on each side of the fish. A peculiar function of pectoral fins, highly developed in some fish, is the creation of the dynamic lifting force that assists sharks, in maintaining depth; they also enables the "flight" for flying fish and the "walking" in some anglerfish in the mud. The ventral fins assist the fish in going up or down through the water, turning sharply, and stopping quickly. Torsional angles changes on fish's fins can be produced by active control, via muscles force, or by passive control, via inertial hydrodynamic forces (**Figure 2(a)** and **Figure 2(b)**). Extensive studies have been made on the Dolphins [22]; their fusiform and streamlined body shape, reduce the pressure component of the drag through maintenance of laminar flow; their maximum thickness (where transition to turbulent flow and boundary-layer separation is likely to develop) it is nearly at 45% of a body length from the beak, meaning that at least 45% of dolphins body may have laminar flow, due to a favorable pressure gradient up to the maximum thickness. The dolphins fineness ratio (FR = body length/maximum diameter) may range among the values $3.85 \leq FR \leq 5.55$ close to the optimum value of lowest drag of FR = 4.5 (e.g. [22]). Their propulsive movements are confined to the vertical plane in the posterior 1/3 of the body, with greatest amplitude at the caudal peduncle; the anterior body part acts as an inertial mass, minimizing energy loss from body oscillations. Dolphins could perform maxi-

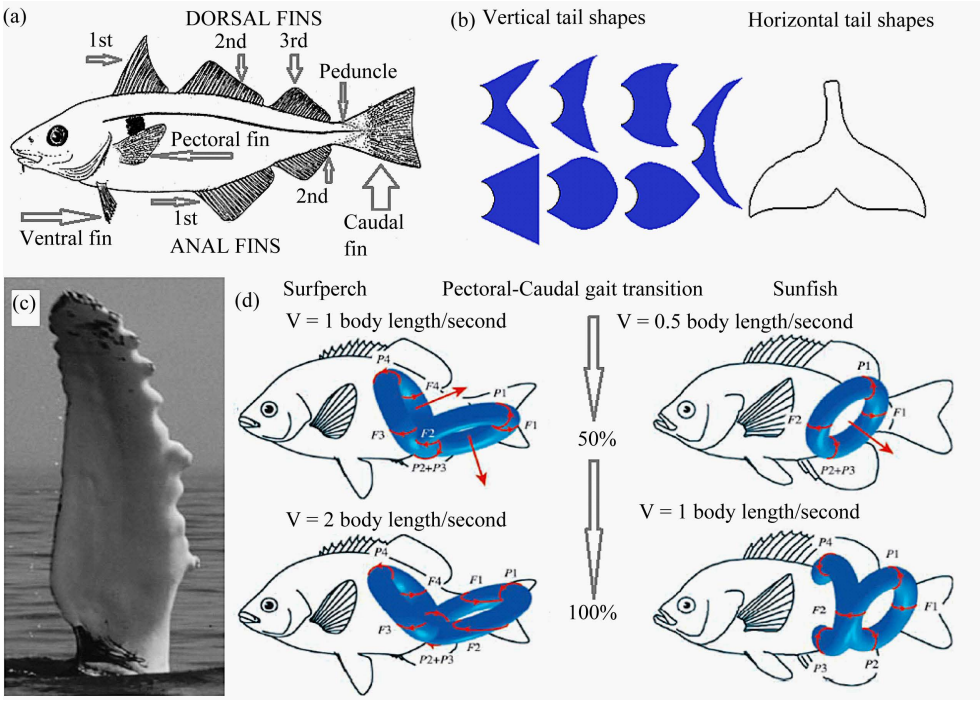

Figure 2. (a) Control surfaces on a generic fish; (b) Different types of fish fin tails known; (c) Photo of a pectoral flipper of the humpback whale (*Megaptera novaeangliae*) show leading edge tubercles [23]; (d) Black surfperch (*Embiotoca jacksoni*) and Bluegill sunfish (*Lepomis macrochirus*), revealing vortex rings at different speeds [25].

mum speed up tom 9.3 ms^{-1}. *Orcinus orca* could perform maximum speed up to 15.5 ms^{-1} during 20 minutes. The pectoral flippers of the humpback whale (*Megaptera novaeangliae*) show leading edge tubercles [23] as illustrates **Figure 2(c)**. Comparisons of wing sections with and without tubercles using CFD models, showed a 4.8% increase in lift; 10.9% reduction in induced drag; 17.6% increase in lift to drag ratio for wing section with tubercles at 10˚ angle of attack. Enhanced maneuverability by the addition of leading edge tubercles has potential application in the development of modern vehicles operating in air or water. Experimental flow visualization [24] compared with numerical simulations on both velocity and vorticity fields, revealed a good agreement; those results also revealed that fish can control body-generated vorticity, through body flexure and active manipulation by the caudal fin. Other researchers [25], using DPIV, approach the question of why some fishes are able to swim faster than others, from a hydrodynamic perspective (**Figure 2(d)**); they investigate the structure and strength of the 3D wake to determine how hydrodynamic forces varies on Black surfperch (*Embiotoca jacksoni*) and Bluegill sunfish (*Lepomis macrochirus*). Both species (similar in size) swim at low speed using pectoral fins exclusively and both species at high speed, switch to pectoral-caudal fin locomotion; the surfperch can swim twice fast. It was found that surfperch presented a pair of linked vortex rings for all velocities, while the sunfish for low speed, presented only one vortex ring per fin and a pair of linked vortex rings with one ring only partially complete and attached to the body, at maximum speed. One of the most striking aspects of fish diversity is the presence of multiple locomotor control surfaces playing hydrodynamic roles during steady swimming and unsteady maneuvering locomotion, as well as the vortex wake interactions among all fins, a subject to be fully understood in the future. The skin of fast-swimming sharks (mako sharks) [26] is composed by a tooth-like scales (denticles) that generated vortexes on the front edge of the skin, *i.e.*, eddies that essentially would help to pull the shark forward; this kind of skin composition is not found on slow-swimming sharks. Many researchers study this skin, by direct mimicking in its 3D shape or in a simplified grooved surface (riblets). Upon close examination of a dolphin's skin revealed micro dermal ridges that delay the transition to turbulent, by trap water molecules at the surface of the skin. Thus, the molecules of trapped water on the skin surface allows the animal to pass through the water more easily than if the same animal had a dry skin surface. The sailfish (that has V-shaped protrusions on skin) is known as fastest sea animal, reaching maximum speeds exceeding

110 km/h. His fin on the back which grows along the back can be spread and folded at will. Since sailfish is the fastest-swimming animal, researchers expected that sailfish's skin textures might produce skin-friction reduction; however, directly measures and numerical investigation showed increases or negligible reduction (~1%) on skin-friction. Yet, scientists advanced other explanations; the role of sailfish skin knowledge is to be confirmed.

5. Insect: A Biological Flight Machine and Their Wing's Kinematics

Every insect's wings when in motion are deformed by either the aerodynamic forces from the surrounding air flow, or by the inertial acceleration; the overall wing deformation is a combination of both and is in a continuously and constantly changing. The power product of the flight's muscles is transmitted to the wings which unlike an aircraft wings are neither streamlined nor smooth: the shape, corrugation and performance of the wings and the complex flapping motion during each stroke cycle will determine the ability of an animal to fulfil successfully every stunning maneuver. Each wingstroke cycle is typically divided into two translational phases: upstroke and downstroke; and two rotational phases: pronation and supination. In the forward-downstroke movement—main power stroke—the wing initiate the downward loop with a high angle of attack until the leading edge tilts downwards, where the wing momentarily becomes horizontal in the middle of the stroke, minimizing the angle of attack; stalling is prevented due to the fastest moving of the wing at this point. During the recovery stroke, when the wing moves upwards and backwards, the leading edge tips backwards. The wing is rotated again at the top of the recovery stroke, restoring the maximum angle of attack immediately before the next downstroke movement initiation. Every motion streamed to the wing lies in a composition of rotational, horizontal, vertical and torsional movements. Torsional angles changes on insect's wings can be produced by active control, via muscles force, or by passive control, via inertial aerodynamic forces. Insect's flight maneuverability is remarkable and by far, superior to every maneuverability of any man-made flying vehicle. Dickinson *et al*. [27], stated that the aerodynamic performance of insects results from an interaction of three distinct, yet, interactive flight mechanisms: delayed stall, meaning that the wing sweep through the air with large angle of attack, during the translational portions of the stroke; rotational lift, meaning an augment in angle of attack at the end of the stroke, providing extra lift; and wake capture, meaning that the wing will capture some energy, left behind on the air by the previous wingstroke, providing extra power. Dragonfly wings possess great stability and high load-bearing capacity during flapping flight, gliding and hovering, despite the fact that their mass is less than 2% of the insect's total mass; such wings (forewings—front wings; and hindwings—rear wings) are composed by a thin cuticular membrane, supported by a vein system (venation) [28]. This venation structure consists on a net of veins (of different sections) that forms rectangular frames at the leading edge and hexagons or polygons with more than four sides at the trailing edge, allowing the requirements for different wing zones bearing different loads. Adding to this, their wings are highly corrugated (more corrugated at first 1/4 at the leading edge), which increases significantly the stiffness and strength of the wings and results in a lightweight structure with very good aerodynamic performance. The flow induced by the motion of insect's wings is highly unsteady and vortical. The aerodynamics between flapping and gliding flight differ substantially in two important ways: in a gliding wing, the air tends to remain attached and flowing smoothly over the surface of any airfoil; by contrast, the air over a flapping wing tends to become entrained in a swirling vortex bound to the upper surface of the wing—separated flow. And whereas the attached flow over a gliding wing look approximately similar from one moment to next, the separate flow over a flapping wing varies constantly—unsteady flow. Nowadays it is widely accepted that the insects make an extensive use of unsteady separated flow mechanisms in order to generate far greater aerodynamic forces that for them, would be impossible to achieve with steady, or quasi-steady, attached flow. In fact, insect's generate enough force to keep themselves in the air, because they flap their wings at a very high angle of attack that creates a structure at the leading edge of the wing, (a tornado-like structure) called leading edge vortex (LEV—see **Figure 3**). Large LEV's are formed at the beginning of each half stroke and remains attached to the wing until the beginning of the next half stroke. It was found on some small insects, an unsteady inviscid high lift mechanism (*clap-and-fling*—see **Figure 4**), consisting on the use of interaction between wings, as they press each other together (like a "*clap*") at the extreme ends of the stroke, providing a total vertical flapping angle of ~180˚.

At the end of the "*clap*", leading edges began to separate as the trailing edge remains connected initially (V-shape at ~120˚); after that, the trailing edge separates as well ("*fling*"); such movement leads that air to rush into low pressure widening gap and produce high strength vortices of equal and opposite sign [29]. The current

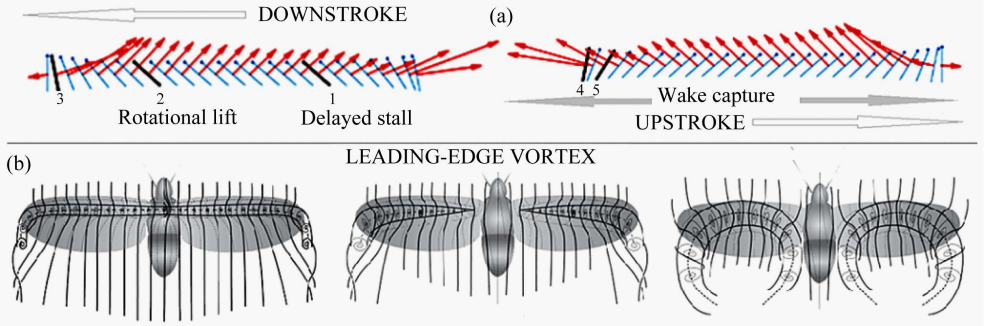

Figure 3. (a) Illustration of a complete insect wingstroke showing the delayed stall and rotational lift on the downstroke movement and the wake capture during all course of the upstroke; blue colour-wing position, with leading edge always on top; red colour-representing the total force [31]; (b) Illustration of 3 different leading-edge vortex: extends across thorax; attached at the base of the wing and horse-shoe-shaped vortex on both wings.

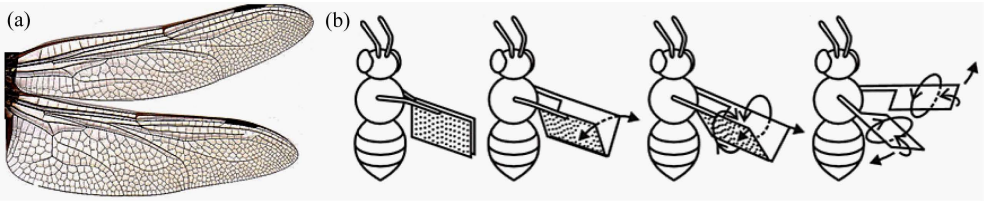

Figure 4. (a) Illustration of forewings and hind wings of a dragonfly and their venation structure as referred on [27] and also a pigmented cell known as pterostigma which mass is frequently greater than that of an equivalent area of adjacent wing and its inertia influences the movement of the whole wing movements. Without the pterostigma, the self-excitating vibrations would set in on the wings after a certain critical speed—pterostigma acts as an inertial regulator of wing pitch; (b) Illustration of the "*clap-and-fling*" flight mechanism: at a certain moment, the wings press together each other (clap); then wing separate as shown (V-shape), generating a low pressure zone between them.

state of the art of micro-CT scanners (X-ray Microtomography) is nowadays limited to large insect's wings [30]; since the resolution of micro-CT scanners is increasing every year, in near future, any insect wing could be successfully scanned. The main challenge for accurately digitizing the wings 3D architecture is minimizing the deformation due to drying of the wing needed to reduce scatter and noise in the scan due to evaporation. Researchers used this technology to scan a dragonfly "*Sympetrum vulgatum*" forewing and hindwings; they found that both vein and membrane thickness increases from tip to root on both wings, which allows the wing to effectively bear both inertial and aerodynamic loads. On their model, they discover that the inertial loads along the wingspan were approximately 1.5 to 3 times higher than the aerodynamic loads—wings deformation were dominated by inertial loads. Based on computations, they also found that wing deformation was smaller during the downstroke, due to structural asymmetry. By the analyses on the work on several researchers, In fact generically, both inertial and aerodynamic force can be the primary cause of wing deformation: in contrast with above statement, and referring also to dragonfly's natural wings, a study concluded that their deformation was mainly due to the aerodynamic forces. Insects have no active control over the wing configuration during flight. The architecture of the wing and the material properties of its element determine how the wing changes their shape in response momentarily to external forces changing, since the wing movement is very complex. It is nowadays a great challenge to researchers, how to build a model with similar properties; of course, another challenge is how to incorporate the wing flexibility into the theoretical model predicting the aerodynamic force during insect flight—both, remains an ongoing challenge to the researchers [32]. As previously referred, leading-edge vortex is the main flight mechanism that allows insects to be able to fly; studies on the unsteady aerodynamics on the flapping wing of a *Manduca sexta* hawkmoth robotic model (while hovering) were made by the use of computational fluid dynamic (CFD) modelling [33]; CFD computations revealed a large leading-edge vortex (LEV1) presence during most of the downstroke movement (from the base at ~60/75% of the wing length); as the wing moves towards horizontal position, this structure becomes larger spiralling vortex with strong axial flow at the

core, towards the wing tip. Immediately after the middle of the dowsntroke, the LEV breaks down at 75% of the wing length, creating this, a second LEV (LEV2—also revealing a spiral axual flow towards the wing base) between the wing tip and the broken-down position of the first LEV. At the initial supination rotation, LEV2 is pushed off the leading edge due to wing deceleration and the breakdown point of LEV1 moves into half of wing length. During the upstroke a very-small leading-edge vortex (quite 2D structure) appeared at the wing tip and by the time the wing reaches the middle position, this structure extends from wing tip to the wing base. After the upstroke's middle course, the LEV grows rapidly (comparable in size with the dowstroke LEV1) and hence enlarges the negative pressure region. At the later part of downstroke, the LEV breaks don at ~60/70% if the wing length without shedding the tip vortex. During the pronation, the upstroke LEV remained attached to the leading edge of the lower wing surface and a trailing-edge vortex (TEV) was also detected (larger than LEV, lies below it and run from the base to the tip), probably due to wing rotation. Lentink & Dickinson [34] suggested that LEV could be an efficient high-lift mechanism for small and big hovering insects; this suggestion is reenforcing the idea that insect while hovering, more easily might capture the energy left behind in air, by the previous stroke; even more, the insects with four separated wings (part of them as two pairs coupling wings) might benefit their rear pair on the work of forewing's wake flow. A challenge on build insect's wing models approaching the natural wings morphology was made by Tanaka & Wood [35]. They described the fabrication of an artificial insect (hoverfly) wing with a rich set of topological features by micro molding a thermosetting resin; the venation system diameter varied between 50 - 125 μm heights and the corrugation of the wing measured 100 μm. Both solid veins and membrane were simultaneously formed and integrated by a single molding process, by the use of a layered laser ablation technique; each 3D mold were created with 5 μm resolution in height. The replicated wing matched at-scale high precision surface profiles of the natural one, thus enabling parametric experiments of the functional morphology of insect wings. Authors referred that stiffness measured along the natural and model wings on identical values of magnitude. However, nature had adapted insects with wings were stiffness varies ad varies the location region on the wings. Later, on another investigation [36] on the subject of flexural and torsional wing flexibility, they were able to create a rigid wing model (hoverfly) that could produce more lift than the natural one's, thus, in prejudice of maneuverability, a requirement that insects had at their disposal (at their will), at almost 350 million years: the experience to fly in the skies of the Earth. After filming a beetle tethered flight [37] with a high-speed camera, researchers build a model of wing system of identical size of natural wings, on a way to follow the natural performance of: flapping frequency, stroke plane, wing tip path, wing rotation angles and flapping angles; however, their experience demonstrated to them that flapping frequency and wing rotation need an improvement to satisfy the natural mimic, since the positive vertical force achieved was only ~1/5 of the total weight of the system. From all bibliographic revision on birds, bats and insects, all researchers invoked that those flying animals may benefit aerodynamically from the flexibility of their wings—a general idea stating that temporal wing deformation is the basis of force generation. From the design aspect, flexibility may benefit MAVs as well, from several points of view: aerodynamically and lightness of structures. Since insect's flight maneuverability far higher superior to every maneuverability achieved by any man-made flying vehicle, thus, Barata *et al.* [38], made an extensive comparative bibliographyc research on the wings motion patterns on several types of insects on resemblant flights, regarding the expoliting of their in-flight basic principles for the acquired performance. They found that the same insect uses their wings in very differently manners, depending, thus, on the maneuver they intend to carry. Every single movement of their wings generates lift (downstroke or upstroke) and the time rate downstroke/upstroke could easily vary at their will. Some of them possess the ability to use the wings in independent ways (differences on wing stroke, wings with different torsions at the same instant, or even one wing used as aerodynamic brake). Despite the flight mechanisms used by insects are not yet fully understood by humans, their replication for use in MAVs will be even more far from being achieved.

6. Conclusion

The current investigation is focused on the mechanisms involved with natural locomotion (thrust and/or lift). Biological systems with interesting applications to Micro Air-Vehicles (MAVs) are generally inspired on flying insects or birds; however, similarly to the aerodynamics of flight, powered swimming requires animals to overcome drag by producing thrust. Commonalities between natural flying and swimming are analyzed together with flow control issues. As it was shown by several researchers on this bibliography work review, the perception of

flight performances held by insects and swimming performances held by fishes are not completely understood. All control surfaces present on living aquatic and flying animals (feet, fins, flippers, or wings) are not designed by nature as of rigid materials; instead, they are elastic materials. Insect's wings are morphological wonder (elastic material: every wing motion is a sum of horizontal, vertical and torsional movement), however, what really enables the wings to make enough force for the animal to stay in the air, is the way insects flap them: at a very high angle of attack, creating a structure at the leading edge of the wing, (tornado-like structure) called leading-edge vortex. Researchers investigated dimensionless numbers to study swimming and flight, and their findings were disappointing since it became clear that different points of view exist in the biomechanics field on how to best define and use. So, successful biology-inspired or biomimetic concepts will depend on the understanding of the natural mechanisms especially when they do not agree with the present engineering design principles. An additional difficulty (and a very important one) is the fact that state of art on elastic materials with identical or similar elastic properties of natural insect's wing, does not exist yet.

Acknowledgements

The authors express their gratitude to FCT for the funding of the research project: PTDC/EME-MFE/122849/2010: Nature—New-biomimetic Aerodynamic Technologies for Undersized Reynolds.

References

[1] Borelli, G.A. (1680) De Motu Animalium. A. Bernabo, Rome.

[2] Pettigrew, J.B. (1874) Animal Locomotion or Walking, Swimming and Flying with a Dissertation on Aeronautics. D. Appleton & Company, New York.

[3] Flight, Flying Machines. http://www.1902encyclopedia.com/F/FLI/flight-flying-machines.html

[4] Mueller, T.J. and DeLaurier, J.D. (2003) Aerodynamics of Small Vehicles. *Annual Review of Fluid Mechanics*, **35**, 89-111. http://dx.doi.org/10.1146/annurev.fluid.35.101101.161102

[5] McMichael, J.M. and Francis, M.S. (1997) Micro Air Vehicles—Toward a New Dimension in Flight. http://fas.org/irp/program/collect/docs/mav_auvsi.htm

[6] Hylton, T., Martin, C., Tun, R. and Castelli, V. (2012) The DARPA Nano Air Vehicle Program. *Proceedings of* 50*th AIAA Aerospace Sciences Meeting Including the New Horizons Forum and Aerospace Exposition*, Nashville, Tennessee, 9-12 January 2012, 8549-8557. http://dx.doi.org/10.2514/6.2012-583

[7] von Ellenrieder, K.D., Parker, K. and Soria, J. (2008) Fluid mechanics of flapping wings. *Experimental Thermal and Fluid Science*, **32**, 1578-1589. http://dx.doi.org/10.1016/j.expthermflusci.2008.05.003

[8] Evers, J.H. (2007) Biological Inspiration for Agile Autonomous Air Vehicles. In *Platform Innovations and System Integration for Unmanned Air, Land and Sea Vehicles* (*AVT-SCI Joint Symposium*). Meeting Proceedings RTO-MP-AVT-146, Paper 15, RTO, Neuilly-sur-Seine, France, 15-1-15-14.

[9] Ho, S., Nassef, H., Pornsinsirirak, N., Tai, Y. and Ho, C. (2003) Unsteady Aerodynamics and Flow Control for Flapping Wing Flyers. *Progress in Aerospace Sciences*, **39**, 635-681. http://dx.doi.org/10.1016/j.paerosci.2003.04.001

[10] DeLaurier, J.D. and Harris, J.M. (1982) Experimental Study of Oscillating-Wing Propulsion. *Journal of Aircraft*, **19**, 368-373. http://dx.doi.org/10.2514/3.44760

[11] Tuncer, I.H. and Platzer, M.F. (2000) Computational Study of Flapping Airfoil Aerodynamics. *Journal of Aircraft*, **37**, 514-520. http://dx.doi.org/10.2514/2.2628

[12] Rozhdestvensky, K.V. and Ryzhov, V.A. (2003) Aerohydrodynamics of Flapping-Wing Propulsors. *Progress in Aerospace Sciences*, **39**, 585-633. http://dx.doi.org/10.1016/S0376-0421(03)00077-0

[13] Lentink, D. and Gerritsma, M. (2003) Influence of Airfoil Shape on Performance in Insect Flight. *Proceedings of the* 33*rd AIAA Fluid Dynamics Conference and Exhibit*, Orlando, 23-26 June 2003.

[14] An, S., Maeng, J. and Han, C. (2009) Thickness Effect on the Thrust Generation of Heaving Airfoils. *Journal of Aircraft*, **46**, 216-222. http://dx.doi.org/10.2514/1.37903

[15] Vandenberghe, N., Childress, S. and Zhang, J. (2006) On Unidirectional Flight of a Free Flapping Wing. *Physics of Fluids*, **18**, 014102-1-14102-8. http://dx.doi.org/10.1063/1.2148989

[16] Wang, Z.J. (2000) Vortex Shedding and Frequency Selection in Flapping Flight. *Journal of Fluid Mechanics*, **410**, 323-341. http://dx.doi.org/10.1017/S0022112099008071

[17] Cebeci. T., Platzer. M., Chen. H., Chang, K.C. and Shao, J.P. (2005) Analysis of Low-Speed Unsteady Airfoil Flows. Edition 2005, Horizons Publishing Inc., Long Beach.

[18] Le, T.Q., Ko, J.H., Byun, D., Park, S.H. and Park, H.C. (2010) Effect of Chord Flexure on Aerodynamic Performance of a Flapping Wing. *Journal of Bionic Engineering*, **7**, 87-94. http://dx.doi.org/10.1016/S1672-6529(09)60196-7

[19] Heathcote, S., Wang, Z. and Gursul, I. (2008) Effect of Spanwise Flexibility on Flapping Wing Propulsion. *Journal of Fluid and Structures*, **24**, 183-199. http://dx.doi.org/10.1016/j.jfluidstructs.2007.08.003

[20] Lentink, D., Van Heijst, G.F., Muijres, F.T. and Van Leeuwen, J.L. (2010) Vortex Interactions with Flapping Wings and Fins Can Be Unpredictable. *Biology Letters*, **6**, 394-397. http://dx.doi.org/10.1098/rsbl.2009.0806

[21] Lentink, D. and Dickinson, M.H. (2009) Biofluiddynamic Scaling of Flapping, Spinning and Translating Fins and Wings. *Journal of Experimental Biology*, **212**, 2691-2704. Http://Dx.Doi.Org/10.1242/Jeb.022251

[22] Fish, F.E. and Hui, C.A. (1991) Dolphin Swimming—A Review. *Mammal Review*, **21**, 181-195. http://dx.doi.org/10.1111/j.1365-2907.1991.tb00292.x

[23] Fish, F.E., Howle, L.E. and Murray, M.M. (2008) Hydrodynamic Flow Control in Marine Mammals. *Integrative and Comparative Biology*, **48**, 788-800. http://dx.doi.org/10.1093/icb/icn029

[24] Wolfgang, M.J., Anderson, J.M., Grosenbaugh, M.A., Yue, D.K. and Triantafyllou, M.S. (1999) Near-Body Flow Dynamics in Swimming Fish. *Journal of Experimental Biology*, **202**, 2303-2327.

[25] Drucker, E.G. and Lauder, G.V. (2000) A Hydrodynamic Analysis of Fish Swimming Speed: Wake Structure and Locomotor Force in Slow and Fast Labriform Swimmers. *Journal of Experimental Biology*, **203**, 2379-2393.

[26] Choi, H., Park, H., Sagong, W. and Lee, S. (2012) Biomimetic Flow Control Based on Morphological Features of Living Creatures. *Physics of Fluids*, **24**, Article ID: 121302. http://dx.doi.org/10.1063/1.4772063

[27] Dickinson, M.H., Lehman, F.-O. and Sane, S.P. (1999) Wing Rotation and the Aerodynamic Basis of Insect Flight. *Science*, **284**, 1954-1960. http://dx.doi.org/10.1126/science.284.5422.1954

[28] Sun, J. and Bushan, B. (2012) The Structure and Mechanical Properties of Dragonfly Wings and Their Role on Flyability. *Comptes Rendus Mécanique*, **340**, 3-17. http://dx.doi.org/10.1016/j.crme.2011.11.003

[29] Ho, S., Nassef, H., Pornsinsirirak, N., Tai, Y.C. and Ho, C.M. (2003) Unsteady Aerodynamics and Flow Control for Flapping Wing Flyers. *Progress in Aerospace Sciences*, **39**, 635-681. http://dx.doi.org/10.1016/j.paerosci.2003.04.001

[30] Jongerius, S.R. and Lentink, D. (2010) Structural Analysis of a Dragonfly Wing. *Experimental Mechanics*, **50**, 1323-1334. http://dx.doi.org/10.1007/s11340-010-9411-x

[31] Scientific American, The Sciences, Catching the Wake. http://www.scientificamerican.com/article/catching-the-wake/

[32] Yin, B. and Luo, H. (2010) Effect of Wing Inertia on Hovering Performance Flapping Wings. *Physics of Fluids*, **22**, Article ID: 111902. http://dx.doi.org/10.1063/1.3499739

[33] Liu, H., Ellington, C.P., Kawachi, K., van den Berg, C. and Willmott, A.P. (1998) A Computational Fluid Dynamic Study of Hawkmoth Hovering. *Journal of Experimental Biology*, **21**, 461-477.

[34] Lentink, D. and Dickinson, M.H. (2009) Rotational Accelerations Stabilize Leading Edge Vortices on Revolving Fly Wings. *Journal of Experimental Biology*, **212**, 2705-2719. http://dx.doi.org/10.1242/jeb.022269

[35] Tanaka, H. and Wood, R.J. (2010) Fabrication of Corrugated Artificial Insect Wings Using Laser Micromachined Molds. *Journal of Micromechanics and Microengineering*, **20**, Article ID: 075008. http://dx.doi.org/10.1088/0960-1317/20/7/075008

[36] Tanaka, H., Whitney, J.P. and Wood, R.J. (2011) Effect of Flexural and Torsional Wing Flexibility on Lift Generation in Hoverfly Flight. *Integrative and Comparative Biology*, **51**, 142-150. http://dx.doi.org/10.1093/icb/icr051

[37] Nguyen, Q.V., Park, H.C., Goo, N.S. and Byun. D. (2010) Characteristics of a Beetle's Free Flight and a Flapping-Wing System that Mimics Beetle Flight. *Journal of Bionic Engineering*, **7**, 77-86. http://dx.doi.org/10.1016/S1672-6529(09)60195-5

[38] Barata, J.M.M., Neves, F.M.S.P. and Manquinho, P.A.R. (2015) Comparative Study of Wing's Motion Patterns on Various Types of Insects on Resemblant Flight Stages. *Proceedings of the AIAA Atmospheric Flight Mechanics Conference*, *SciTech* 2015, Kissimmee, 5-9 January 2015, 828-848.